ACTA UNIVERSITATIS SZEGEDIENSIS

ACTA MINERALOGICA-PETROGRAPHICA

Tomus XXIX

SZEGED, HUNGARIA
1987—1988

NOTE TO CONTRIBUTORS

General

The Acta Mineralogica—Petrographica publishes original studies on the field of geochemistry mineralogy and petrology, first of all studies of Hungarian researchers, papers resulted in by co-operation of Hungarian researchers and those of other countries and, in a limited volume, papers from aboad on topics of global interest.

Manuscripts schould be written in English and submitted to the Editor-in-chief, Institute of Mineralogy, Geochemistry and Petrography, Attila József University, H-6701 Szeged, Pf. 651 Hungary.

The authors are responsible for the accuracy of their data, references and quotations from other sources.

Manuscript

Manuscripts should be typewritten with double spacing, 25 lines on a page and space for 50 letter, in a line. Each new paragraph should begin with an indented line. Underline only words that should be typed in italics.

Manuscripts should generally be organized in the following order:

Title
Name(s) of author(s) and their affiliations, in foot-note the address of the author to whom the correspondence should be sent.
Abstract
Introduction
Methods, techniques, material studied, description of the area investigated, etc.
Results
Discussion or conclusions
Acknowledgement
Explanation of plates (if any)
Tables
Captions of figures (drawings, photomicrographs, etc.)

Abstract

The abstract cannot be longer than 500 words.

Tables

The tables should be typewritten on separate sheets and numbered according to their sequence in the text, which refers to all tables.

The title of the table as well as the column headings must be brief, but sufficiently explanatory.

The tables generally should not exceed the type-area of the journal, i.e. 12.5×18.5 cm. Fold-outs can only exceptionally be accepted

ACTA UNIVERSITATIS SZEGEDIENSIS

ACTA MINERALOGICA-PETROGRAPHICA

Tomus XXIX

SZEGED, HUNGARIA
1987—1988

HU ISSN 0365—8066
HU ISSN 0324—6523

Redigit

TIBOR SZEDERKÉNYI

Edit

Institutum Mineralogicum, Geochimicum et Petrographicum
Universitatis Szegediensis de Attila József nominatae

Nota

Acta Miner. Petr., Szeged

Szerkeszti

SZEDERKÉNYI TIBOR

a szerkesztőbizottság tagjai:

KUBOVICS IMRE
EGERER FRIGYES
SZÖŐR GYULA
KLEB GYULA

Kiadja

a József Attila Tudományegyetem Ásványtani, Geokémiai és
Kőzettani Tanszéke
H—6722 Szeged, Egyetem u. 2—6.

Kiadványunk címének rövidítése
Acta Miner. Petr., Szeged

CONTENTS

Acta Mineralogica-Petrographica, Szeged, XXIX, 5—12, 1987—1988

QUASICRYSTALS AND THEIR SPONTANEOUS FORMATION POSSIBILITIES IN THE NATURE

G. GÉVAY, T. SZEDERKÉNYI

Department of Mineralogy, Geochemistry and Petrography
Attila József University

ABSTRACT

Quasicrystals are a recently (1984) discovered family of structures producing X-ray diffraction diagrams with five-fold symmetry. This non-crystallographic symmetry can be explained by supposing that the strict periodic order is replaced here by a weaker order, called quasiperiodicity. Some of their properties as well as the possibility of formation in natural geological processes are discussed briefly in the paper.

A BRIEF INTRODUCTION TO QUASICRYSTALS

Quasicrystals were discovered by SHECHTMAN *et al.* (1984). A puzzling aspect of this discovery is that the BRAGG diffraction diagram of quasicrystals consists of sharp spots that indicates long-range order, however, it exhibits *five-fold* rotational symmetry. It is well known that this kind of symmetry is forbidden by the fundamental laws of classical crystallography (BARLOW's theorem, COXETER, 1961). Thus it is supposed that we are facing a new type of order, called quasiperiodicity (ROMERIO, 1971). Indeed, as it turned out, the mathematics of diffraction does not require strict periodicity in order to produce sharp peaks, but quasiperiodicity is sufficient (LEVINE and STEINHARDT, 1984). This latter means, in a descriptive sense, that a quasiperiodic structure is built of two (or more) different unit cells instead of one, such that the ratio of their corresponding geometric parameters (e.g. volume) is irrational number (and so is their relative frequency, i.e. occurrence in at least in principle, an infinite structure). Thus, the translational order is lacking here. On the other hand, the long-range rational order is replaced by a long-range "orientational" order. This means that the characteristic bonding directions fit to some straight lines of different orientation.

A two-dimensional model of such a quasiperiodic structure is visualized in *Fig. 1.* It is directly seen that picking out any lattice point and considering the densest packed straight lines passing through it, these lines succeed one after the other by an angle $360/5 = 72°$. "Thus, the symmetry of this "quasilattice" reveals itself in such an indirect way (or, as mentioned above, through the symmetry of its diffraction pattern).

In three dimensions, taking another such pentagyre through the same point, further five-fold axes are induced, thus we have altogether six pentagyres. Actually, ten three-fold axes and fifteen two-fold axes will be generated at the same time. This configuration of symmetry elements corresponds just to the point group consist-

H—6701 Szeged, P.O.Box: 651, Hungary.

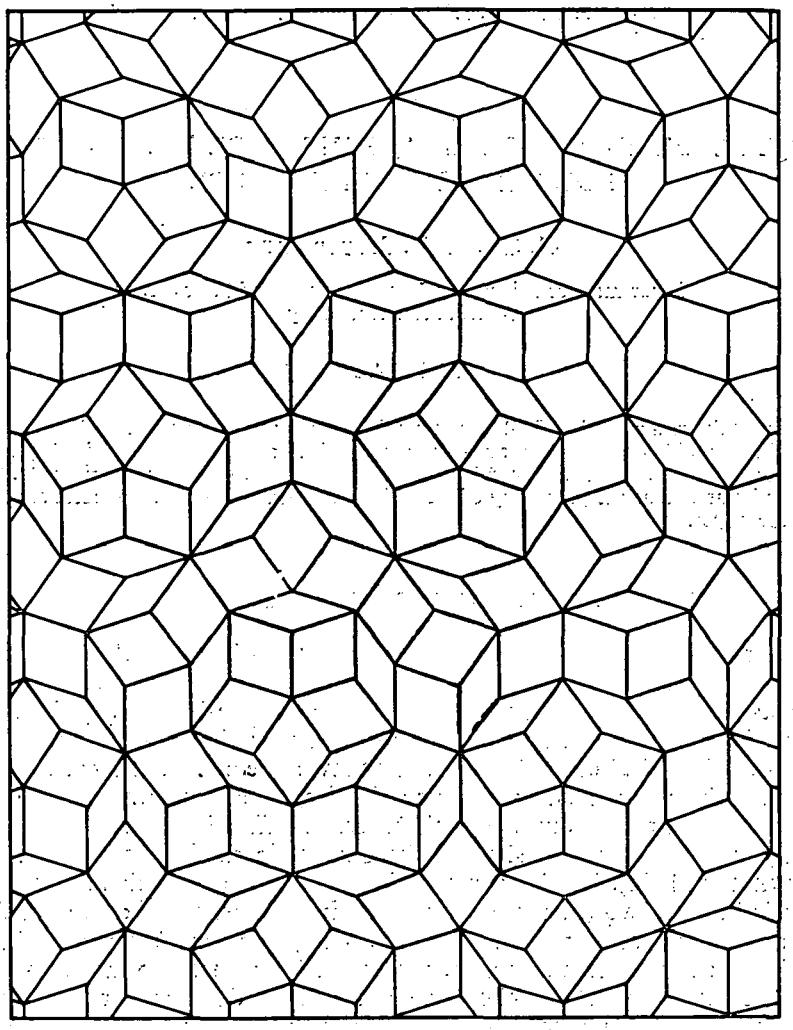

Fig. 1. A two-dimensional quasiperiodic structure: the Penrose pattern

ing of all rotations of an icosahedron *(Fig. 2)*, or of a regular pentagonal dodecahedron *(Fig. 3)*. So, these two regular polyhedra (Platonic solids), exorcised from the classical crystallography, appear in the geometry of quasicrystals. The symmetric axes listed before can be more easily perceived on a combination of these two Platonic solids *(Fig. 4)*, which is an intermediate form recalling the cuboctahedron of the classical crystals. The stereographic projection of the point group I—235 considered is shown in *Fig. 5*. This may be regarded as a hemihedral "quasicrystal class" and, as it contains only rotational axes, an enantiomorphic one. Adding inversion centre to it, fifteen additional mirror planes are induced and the holohedral class I_h — $m\bar{3}\bar{5}$ is obtained *(Fig. 6)*, which is the full symmetry group of the icosahedron. The corresponding general (i.e. having faces of maximal number) "quasicrystal form" consists of 120 faces ("hecatonicosahedron", *Fig. 7*). This form is obtained from a single face

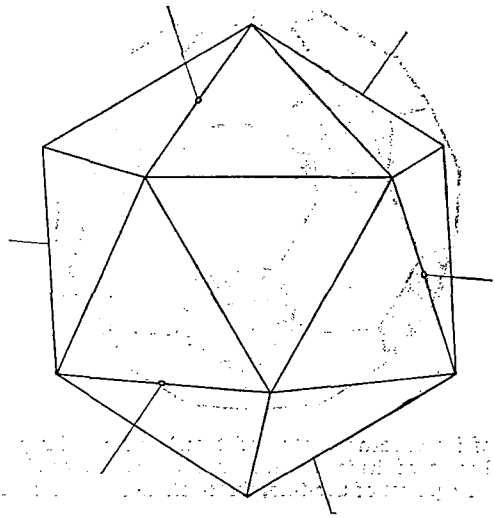

Fig. 2. Icosahedron, representing quasicrystalline symmetry

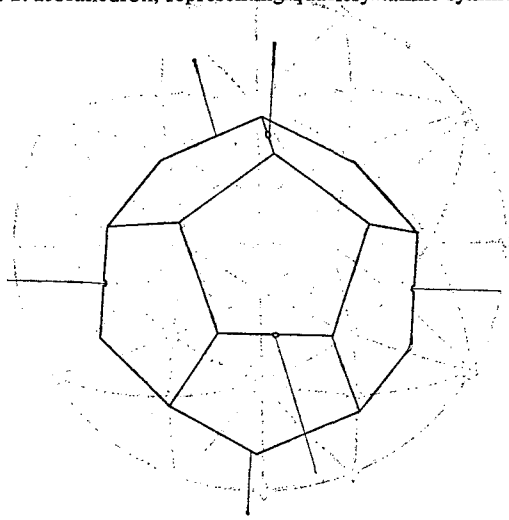

Fig. 3. The regular pentagonal dodecahedron

situated so that it is orthogonal to none of the symmetry elements of I_h: in this case each element of the point group will multiply it.). For completeness, we note that the 3-dimensional quasilattice of icosahedral symmetry is built also of two unit cells, acute and obtuse rhombohedra with edges of equal length (just as the two-dimensional pentagonal quasilattice is built of acute and obtuse rhombuses, cf. *Fig. 1*). Moreover, any section through a lattice point and orthogonal to a five-fold axis provides just the PENROSE pattern (for further details of this quasilattice see e.g. GINGL, 1988).

As a matter of fact, the "shechtmanite" $Al_{0.86}Mn_{0.14}$ described by SHECHTMAN *et al.* (1984) exhibits this icosahedral symmetry and phases like that have been called

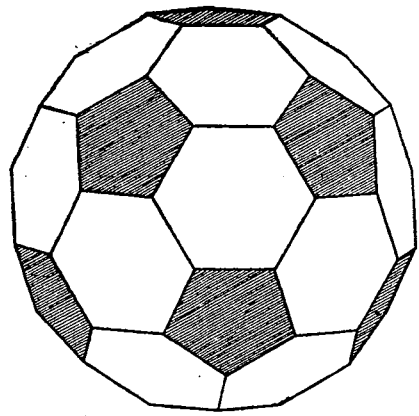

Fig 4. A combination of icosahedron (unshaded faces) and regular pentagonal dodecahedron (shaded faces). The central points of shaded faces, unshaded faces and of edges between two unshaded faces are the emergence points of five-fold, three-fold and two-fold axes, respectively

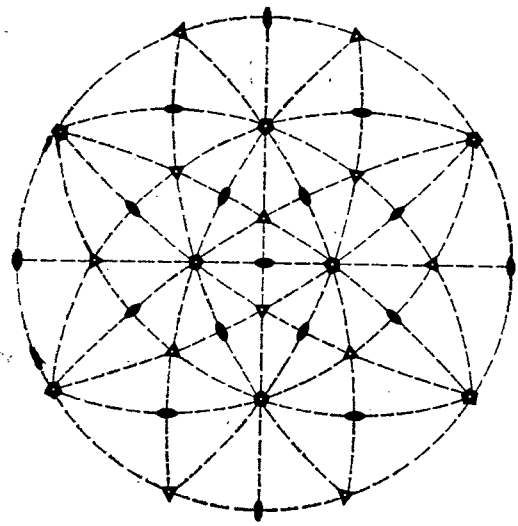

Fig. 5. Stereographic projection of the point group I—235.

since then icosahedral phase (IP). One should note, however, that this is not a unique type of quasicrystals: there are other phases which are characterized by ten-fold (BENDERSKY, 1985), moreover, by twelwefold (ISHIMASHA *et al.* 1985) rotational axis.

CONSIDERATIONS ON THE FORMATION OF QUASICRYSTALS

The first publications on quasicrystals described preparations produced in laboratory conditions. Naturally arises the question, in what circumstances can quasicrystals be expected to form spontaneously in Nature. Such a possibility cannot

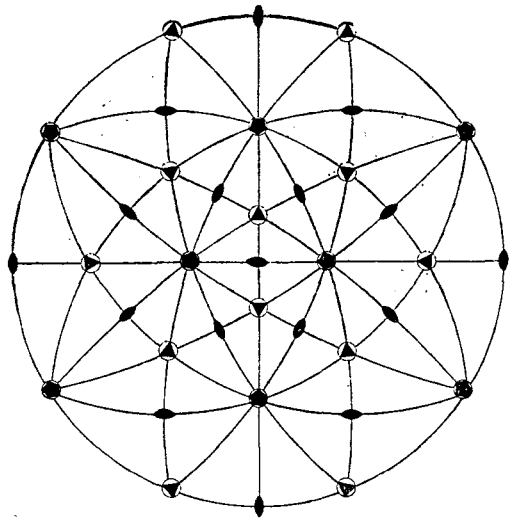

Fig. 6. Stereographic projection of the point group I_h—m$\bar{3}\bar{5}$.

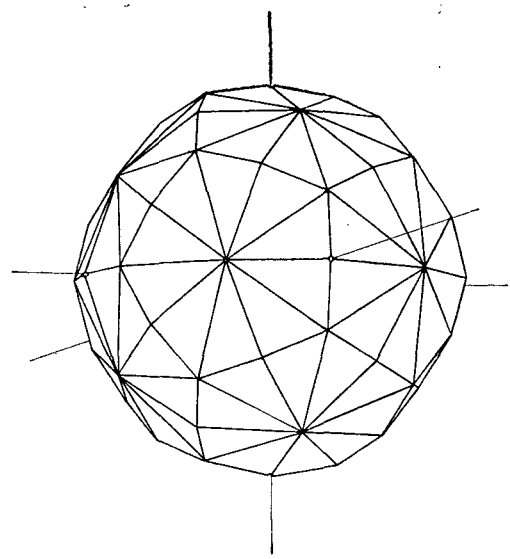

Fig. 7. Hecatonicosahedron, the form of maximal face number corresponding to the point group I_h—m$\bar{3}\bar{5}$. It has 120 faces, 180 edges and 62 vertices. It is an icosahedral anal ogueof the hexakis octahedron of cubic symmetry

be excluded *ab ovo,* as it is indicated by some analogies in connection with other "exotic" structures, as follows.

In a sense, silicon atoms in octahedral position can be considered strange enough. However, stishovite, a high pressure modification of SiO_2 known from the Arizona meteor crater (STRUNZ, 1966) contains [SiO_6] octahedra (type rutil). In extreme conditions, silicon atoms are forced into such a coordination (formation at 1200—

1400 °C, > 160,000 atm), though, here is no indication of violating the strict periodicity.

A real deviation from strict periodicity can be observed in a continuously broadening group of structures which are called modulated structures. Modulation means that a periodic perturbation occurs in the lattice (GUGGENHEIM and EGGLETON, 1987). These phases were discovered in the sixties on the basis of the observation that in their diffraction diagram extra (satellite) reflections could be found. The satellite reflections cannot be indexed in the usual way, actually, they often have irrational indices, violating the classical law of rationality (DE WOLFF, 1974). The irrationality is considered as a consequence of incommensurability between the translational and modulation period (i.e. their ratio cannot be represented as a ratio of two integer numbers). Since the discovery, a number of modulated crystals have been found and described (see e.g. the review by GUGGENHEIM and EGGLETON. 1987), indicating that the world of minerals is more abundant than one might imagine merely on the basis of classical crystallography.

The relation of modulated (incommensurate) crystals and quasicrystals is still a debated problem. However, it is worth pondering on the possibility of proper quasicrystals among minerals. For example, BOISEN JR. and GIBBS (1985) speculate on a possible quasicrystalline form of skutterudite. In the skutterudite (Co_4As_{12}), there are icosahedral units As_{12} which, combining with interstitial Co atoms, form a lattice of cubic (m3) symmetry. The authors cited refer to the fact that the dominant crystal form of skutterudite, the pyritohedron, closely resembles the regular pentagonal dodecahedron. Their supposition that this mineral may have passed through a quasicrystalline state prior to its final crystallization, is in accordance with OSTWALD'S rule. By this rule, a stable modification often does not form directly, but the action progresses through successive steps in which intermediate phases appear. Its application here is justified by the observation that formation of quasicrystals is a non-equilibrium process and they are generally in metastable state. It is also worth mentioning that skutterudite has a metalloid structure and the quasicrystalline substances (according to our present knowledge) are generally alloys. Thus the crystal chemical resemblance also supports the idea due to the above authors.

Let us see now the laboratory formation circumstances of quasicrystals. By now a series of methods is known, see RONCHETTI (1987). From our point of view. the most important methods are those in which rapid melt cooling (quenching) is applied (with often a simultaneous spinning of melt). A common and important feature of these and other methods is the high nucleation rate in comparison with growth rate. This seems to be a rather characteristic condition for the formation of quasicrystals.

In what follows we try to give some geological examples where physico-chemical conditions mentioned just above might be expected to favour formation of natural quasicrystals.

A. *Rapid cooling* resulting in highly supercooled melt in which crystallization is characterized by high nucleation rate is a typical feature of magma intrusion. An additional parameter intensifying nucleation is the strong convective motion of the melt: the intruding magma is forced in the magma chamber into an intense motion controlled by several interconnected thermodynamical parameters. Actually, at least three types of convection are distinguished (MORSE, 1988) thermal convection (due to thermal gradient, especially that between floor and roof of the chamber), two-phase convection (involving crystal+liquid suspensions that can move much faster than small individual crystals can settle), and compositional convection (due

to rejection of solute by growing cumulates). Study of layered intrusions show that competition between nucleation, growth, and cooling rates (THY *et al.* 1988) can often lead to an oscillatory behaviour of the multisaturated liquid, which is reflected in the rhyhtmic layering (MAALØE, 1978) of the product phases. Though nucleation theories aiming at explaining rhythmic layering are, at least partly, in controversy with each other, they admit that abrupt changes in parameters controlling nucleation can occur, giving rise to burst of nucleation. This is the very point which is important to our discussion: the magmatic dynamic patterns may create appropriate physicochemical conditions for the formation of quasicrystals.

B. *Shock-hardened meteorites:* in these substances a number of specific transformations can be traced. Hardening, multiple twinning and polymorphic transition are typical alterations induced by terrestrial or preterrestrial shock.

From the point of view of solid state physics, hardening is due to blocking the motion of dislocations (KITTEL, 1978). This can be achieved, for example, by homogenizing the dislocation density, a transformation which results e.g. from explosive deformation. A related process that also blocks the motion of dislocations is the formation of short-range order. As quasiperiodicity is an intermediate case between long-range (periodic) order and total disorder, a factor of hardening may be such partial disordering, i.e. formation of quasicrystalline domains. In this respect, a phenomenon called "preferred disorder" respectively "preferred orientation" (JAIN and LIPSCHUTZ, 1970) may be worthy of attention. This roughly means that disordering is confined to certain directions and it is revealed by radial streaks in X-ray diffraction photographs, which is called asterism. In a more recent work by HORZ *et al.* (1986), Debye—Scherrer patterns of experimentally shocked augite and naturally shocked pyroxenes from the Shergotty meteorite are shown. As it is noted there, substantial disturbance of long-range order and preferred orientation are indicated, the latter by discontinuous and streaky reflections. Moreover, what is mainly essential from our point of view, the asterism exhibits nearly 14-fold symmetry (*Fig. 1* in the paper referred to; the relevant photographs cannot be adequately reproduced here because of their small dimension). These figures originate from discrete grains of 220—250 μm diameter and are said to be hybrids between single crystals and fine-grained powders, and the lattice is considered as mechanically disaggregated by shock. It is stressed by the authors that "crystallographic control becomes impractical for such highly fragmented samples". However, despite of the difficulties. such and similar phenomena perhaps would be worthy to be subjected to further investigation, in our opinion.

As for the other two phenomena, viz. multiple twinning and polymorphism in meteorites, here we only refer to the fact that there exists an alternative notion of quasicrystals emphasized by LINUS PAULING (1987), according to which the properties of quasicrystals can be satisfactorily explained by supposing certain multiple twinning structures. The debate has not been concluded yet (WOLNY *et al.*, 1988).

CONCLUDING REMARKS

Of course, the train of thought in A and B is a tentative one and even does not pretend to be anything more. This is because the knowledge on quasicrystals is in an accumulation period and theoretical (e.g. geometric) description of their structure is not completed yet, in contrast to classical crystals for which at least the geometric point lattice theory essentially was completed at the beginning of the century. On the other hand, actually in *any* geological sample having more or less

peculiarity in its formation circumstances one may find (at least small domains of) quasicrystals. Perhaps a number of researchers have already met without recognizing them: surely all of us are more or less confined to scientific "dogmas", like for example the strict crystallographic prohibition of five-fold symmetry.

ACKNOWLEDGEMENT

One of the authors (G. G.) is grateful to Prof. J. MEZŐSI for inspiring discussions.

REFERENCES

BENDERSKY, L. (1985): Quasicrystal with one-dimensional translational symmetry and a tenfold rotation axis. Phys. Rev. Lett. **55**, 1461—1463.

BOISEN Jr., M. B. and GIBBS, G. V. (1985): Mathematical Crystallography. In: Reviews in Mineralogy (Ed. P. H. Ribbe). Vol. **15**.

COXETER, H. S. M. (1961): Introduction to Geometry. Wiley, New York.

GINGL, Z. (1988): Local structure of quasicrystals. Degree Work. JATE Institute of Mineralogy, Geochemistry and Petrography, Szeged (in Hungarian).

GUGGENHEIM, S. and EGGLETON, R. A. (1987): Moduled 2:1 layer silicates: Review, systematics and predictions, Amer. Mineral., **72**, 724—738.

HORZ, F., HANSS, R. and SERNA, C. (1986): X-ray investigations related to the shock history of the Shergotty achondrite. Geochim. Cosmochim. Acta **50**, 905—908.

ISHIMASHA, T., NISSEN, H. U. and FUKANO, Y. (1985): New ordered state between crystalline and amorphous in Ni-Cr particles. Phys. Rev. Lett. **55**, 511—513.

JAIN, A. V. and LIPSCHUTZ, M. E. (1970): On preferred disorder and the shock history of chemical group IVA meteorites. Geochim. Cosmochim. Acta **34**, 883—892.

KITTEL, C. (1978): Introduction to Solid State Physics, Wiley, New York.

LEVINE, D. and STEINHARDT, P. J. (1984): Quasicrystals: a new class of ordered structures. Phys. Rev. Lett. **53**, 2477—2480.

MAALOE, S. (1978): The origin of rhythmic layering. Mineral. Mag. **42**, 337—345.

MORSE, S. A. (1988): Motion of crystals, solute and heat in layered intrusions. Can. Mineral. **26**, 209—224.

PAULING, L. (1987): So-called icosahedral and decagonal quasicrystals are twins of an 820-atom cubic crystal. Phys. Rev. Lett. **58**, 365.

ROMERIO, M. W. (1971): Almost periodic functions and the theory of disordered systems. J. Math. Phys. **12** (3), 552—562.

RONCHETTI, M. (1987): Quasicrystals. An introductory overview. Phil. Mag. B. **56** (2), 237—249.

SHECHTMAN, D., BLECH, I., GRATIAS, D. and CAHN, J. W. (1984): Metallic phase with long-range orientational order and no translational symmetry. Phys. Rev. Lett. **53**, 1951—1953.

STRUNZ, H. (1966): Mineralogische Tabellen. Akademische Verlagsgesellschaft Geest und Portig K.-G. Leipzig.

THY, P., JAKOBSEN, N. N. and WILSON, J. R. (1988): Fine-scale graded layers in the Fongen—Hyllingen gabbroic complex. Norway. Can. Mineral. **26**, 235—243.

DE WOLFF, P. M. (1974): The pseudo-symmetry of modulated crystal structures. Acta Cryst. A**30** 777—785.

WOLNY, J., PYTLIK, L. and LEBECH, B. (1988): Quasi-crystals-random structures on twins? J. Phys. C.: Solid State Phys. **21**, 2267—2277.

Manuscript received, 5 September, 1988

Acta Mineralogica-Petrographica, Szeged, XXIX, 13—26, 1987—1988

DETERMINATION OF ANCIENT EROSION BY ZIRCON MORPHOLOGY AND INVESTIGATIONS ON ZONED TOURMALINE IN KŐSZEG-RECHNITZ WINDOW (WESTERN HUNAGRY)

A. DEMÉNY

Department of Petrology and Geochemistry, Loránd Eötvös University

ABSTRACT

The rocks exposed in the Kőszeg-Rechnitz Window in Western Hungary and Austria belong to the Penninic unit of the Alps. The investigated rocks are of sedimentary origin, mostly graphitic chlorite-muscovite phyllites and quartzphyllites. The latter contains significant amounts of detrital zircon and tourmaline. Morphology of zircon grains has been preserved during metamorphism and indicates alkaline granite, plagiogranite, monzogranite and garnodiorite source rocks. Electron microprobe investigation on tourmaline grains indicates formation in Ca-poor metapelites and metapsammites without Al-saturated phases. These rocks have shed part of the sediments deposited in the Penninic ocean.

Keywords: low-grade metamorphism, Penninic unit, Kőszeg-Rechnitz Window, zircon morphology, tourmaline compositions.

INTRODUCTION

The Kőszeg-Rechnitz sequence is formed of a lower and an upper tectonic unit. Both of them contain metamorphic rocks of igneous and sedimentary origin (JUGOVICS, 1917, BANDAT, 1928, 1932, VARRÓK, 1963, KOTSIS, 1965. NAGY, 1972, KISHÁZI and IVANCSICS, 1976, 1984, KOLLER and PAHR, 1980, KUBOVICS, 1983, KOLLER, 1985). The sedimentary sequence of the upper scale studied in the present work is made of rocks of psephitic-psammitic origin, turning more and more pelitic upwards. The gradual increase of the carbonate content is indicated by calcereous phyllite and calc-schist at the top. This trend is similar to that described by SZEBÉNYI *et al.* (1948).

SCHMIDT, (1956) was the first among the Austrian authors to suggest a Penninic position and the Mesozoic age of the Kőszeg-Rechnitz series. SCHÖNLAUB, (1973) recognised Middle Cretaceous sponge spicules in the calcareous phyllites.

We intended to study the composition of tourmaline and the morphology of zircon grains by electron microprobe and optical investigations, respectively.

The investigated samples have been collected from a quartzphyllite portion of the Velem Calcareous Phyllite Formation of the Kőszeg Hills.

RESULTS

1. *Tourmaline*

Tourmaline is one of the heavy minerals in the most significant quantities in the samples collected from the Kőszeg Hills. Some quartzphyllite samples from the Terv Road profile at Velem contain up to 0.5% tourmaline. The largest specimens

H—1088 Budapest, Múzeum krt. 4/A Hungary.

can be found here in this series up to 0.2 mm in diameter. The average diameter of the grains along the profile is about 0.02—0.03 mm.

Three tourmaline types have been recognised: an uncoloured, a brownish yellow and another with greenish blue pleochroism.

The uncoloured tourmaline is a rare type, forming the core of large (0.1—0.2 mm) grains with compound zonality (see *Fig. 2*). The uncoloured core is anhedral. Rarely a continuous transition can be observed between the brownish yellow zone and the core *(Fig. 2)*.

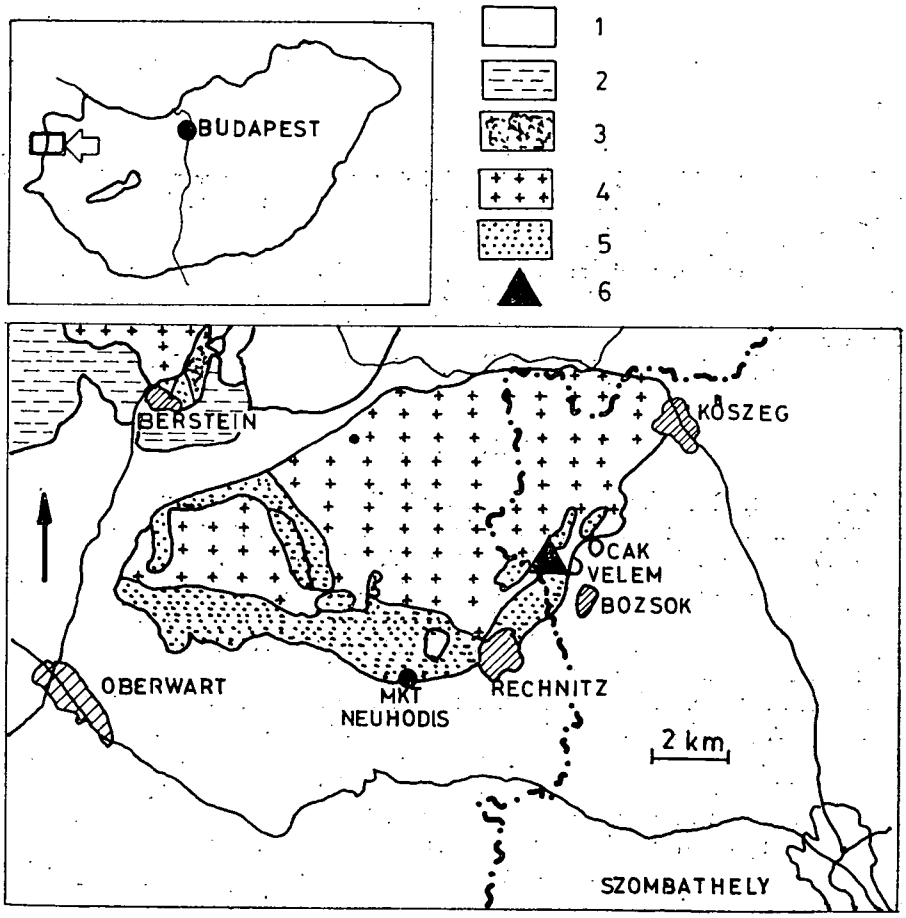

Fig. 1. The map of the Kőszeg Hills (Western Hungary—Eastern Austria). 1. Tercier, 2. Lower East-Alpine, 3. Serpentinite, 4. Metasediment, 5. Greenschist-metagabbro, 6. Samples

Most of the brownish yellow tourmaline grains are anhedral, rarely strongly resorbed *(Fig. 3)*. Oriented graphite inclusions were found in a grain *(Fig. 4)*, unparallel with the cleavage of the host rock. It indicates the detrital origin of the grain.

Some tiny (0.01 mm) euhedral yellow grains occur, too; these might have been formed after the main, syntectonic metamorphism of the rock (see later).

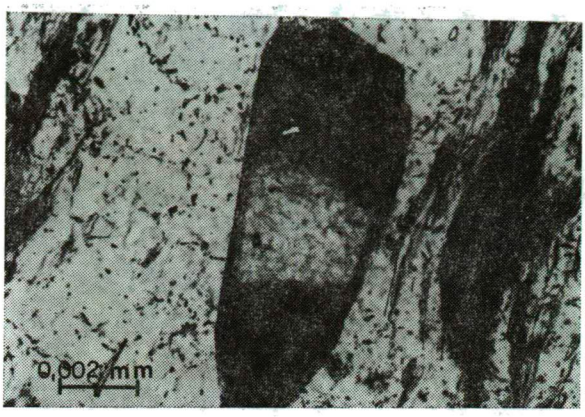

Fig. 2. Tourmaline grain with complex zonation (whitebrownish yellow-greenish blue). 1N

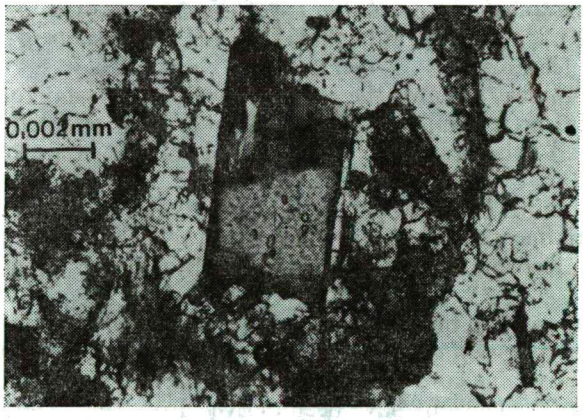

Fig. 3. Tourmaline grain with resorbed brownish yellow core and greenish blue overgrowth. 1N

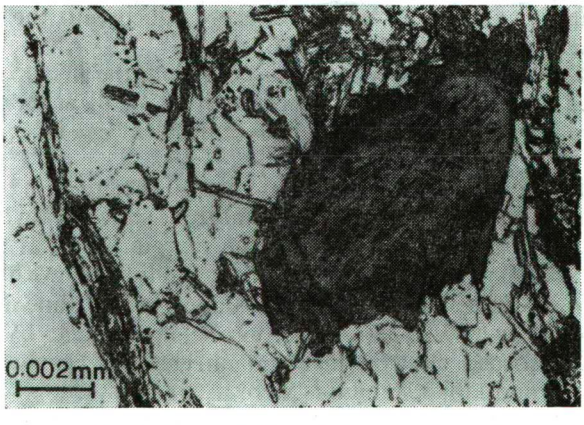

Fig. 4. Zoned tourmaline grain in quartzphyllite. Notice the oriented inclusions in the brownish yellow core. 1N

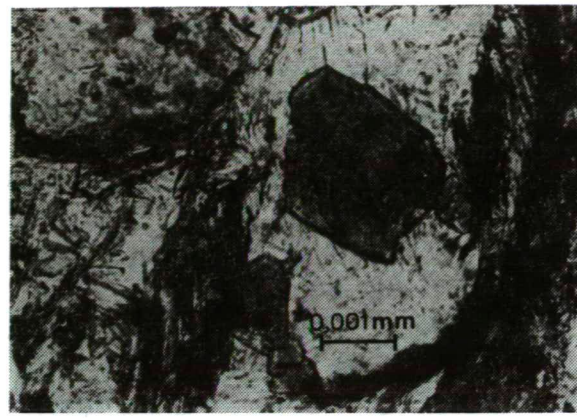

Fig. 5. Tourmaline grain with reverse zonation in quartzphyllite. 1N

Greenish blue tourmaline occurs in two forms: overgrowth on brownish yellow grains or a group of tiny (0.01 mm) euhedral grains. The overgrowth is characterized by the following features:

a) Sharp boundary towards the brownish yellow core and zone.

b) It contains great number of inclusions, mostly in oriented positions parallel with the cleavage of the host rock *(Fig. 3)*. The inclusions are mostly quartz and muscovite.

c) Rarely terminal forms of the crystalls can be observed *(Fig. 2);* the presence of intact prismatic faces characterize euhedral forms *(Fig. 3)*.

d) Frequent resorption phenomena can be observed on the greenish blue overgrowth.

The euhedral greenish blue grains bear no inclusions and rarely show resoprtion. Sometimes a thin yellowish green zone surrounds the grain *(Fig. 5)*. The difference between the greenish blue core and the yellowish green margins is less conspicuous.

The following conclusions have been derived from the results of the investigations:

— Brownish yellow tourmaline grains, rarely with uncoloured cores, originating from graphitic metamorphic rocks, have been shed into the sediments of the Velem Calcareous Phyllite Formation.

— Part of these grains has been dissolved during the first metamorphic phase and recrystallized as a greenish blue overgrowth or small euhedral crystalls. This process happened during the folding that caused the cleavage, i.e. it was a syntectonic process.

— During the second, posttectonic phase part of the greenish blue and brownish yellow tourmalines was dissolved and recrystallized, showing reverse zonality. The colour of the above mentioned yellowish green margin indicates the mixing of the two substances and that the margin wasn't in equilibrium with its environment.

Composition of the zones of three tourmaline grains shown on *Figs. 2, 3, 4* has been determined by a JXA—50 A microprobe, applying 15 kV acceleration voltage, 3×10^{-8} Å absorbed electron flux and an electron beam 1 μm is diameter. Biotite, barkevikite and albite standards were used.

Tables 1a and 1b show concentration values, cation numbers and end-member ratios. Boron data were calculated postulating three boron atoms. The zonality of

TABLE 1A

Concentration values for zones of tourmaline grains shown on Figs. 2, 3, 4

	Fig. 3		*Fig. 4*		*Fig. 2*		
	core	rim	core	rim	core	zone	rim
B_2O_3	10.98	10.54	10.75	10.53	10.94	10.73	10.45
SiO_2	37.40	37,30	37.50	37.60	37.40	36.40	37.00
Al_2O_3	32.90	30.90	33.30	30.20	32.00	33.10	29.10
TiO_2	0.53	0.25	0.60	0.38	0.50	0.80	1.20
Cr_2O_3	nd	nd	nd	nd	—	—	—
FeO_t	3.20	10.00	6.00	9.90	0.30	3.90	9.30
MgO	10.10	5.40	6.31	5.57	12.00	8.00	6.20
CaO	1.02	nd	0.31	nd	1.70	1.60	0.10
Na_2O	2.40	2.80	2.24	2.94	2.30	2.10	3.10
K_2O	nd	nd	nd	nd	nd	nd	nd
Total:	98.53	97.19	97.01	97.12	97.14	96.63	96.45

nd = non detectable

TABLE 1B

Cation numbers and end-member ratios for zones of tourmaline grains shown on Figs. 2, 3, 4

	Fig. 3		*Fig. 4*		*Fig. 2*		
	core	rim	core	rim	core	zone	rim
B	3	3	3	3	3	3	3
Si	5.9144	6.1440	6.0650	6.1989	5.9394	5.8897	6.1527
Al	6.1341	6.000	6.3396	5.8697	5.9858	6.3092	5.6999
Ti	0.0627	0.0307	0.0728	0.0470	0.0590	0.0972	0.1498
Fe	0.4229	1.3777	0.8103	1.3652	0.0400	0.5269	1.2908
Mg	2.3806	1.3253	1.5187	1.3681	2.8409	1.9297	1.5365
Ca	0.1720	—	0.0533	—	0.2890	0.2770	0.0179
Na	0.7355	0.4474	0.3503	0.4696	0.7059	0.6572	0.9990
sörl	15.25	54.95	36.68	49.95	1.34	18.80	42.31
dravite	62.30	45.05	56.08	50.02	56.46	29.32	48.02
uvite	18.90	—	7.24	—	29.03	29.65	1.76
elbaite	3.55	—	—	—	13.17	22.23	7.90

the grain shown on *Fig. 3* easily recognisable by the optical microscope, is clearly indicated by analytical data and by the linear measurement of element compositions *(Figs. 6, 7)*. The zonality is caused by concentration variations of FeO_{tot} and MgO. The discontinuous boundary indicates that the grains weren't produced by a single, progressive metamorphic phase, also shown by thin section investigations (see above).

The end-member calculations resulted Al and Si in surplus. Since we had no possibility to determine the concentrations of all elements (i.e. Li) constituting the tourmaline, it is supposed that the surplus is due to compositional causes, to be cleared during subsequent investigations.

Analytical data were plotted in Al-Fe_{tot}-Mg and Ca-Fe_{tot}-Mg diagrams *(Figs. 8. 9)*. These plots illustrate the interrelationships among rock types and compositions of tourmalines formed in them. Arrows show the core to margin trends.

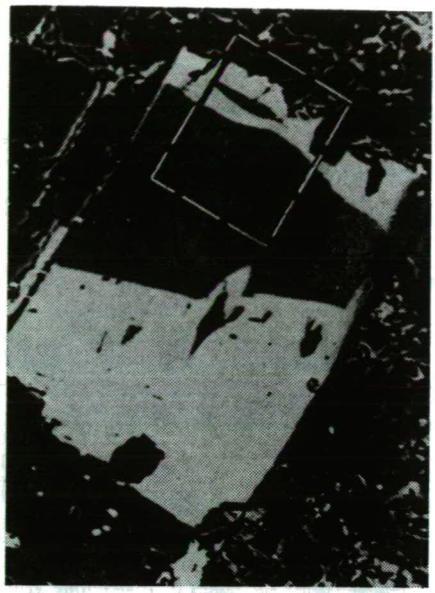

Fig. 6. Back scattered electron image of the tourmaline grain of *Fig. 3.* The marked area is shown on *Fig. 7.*

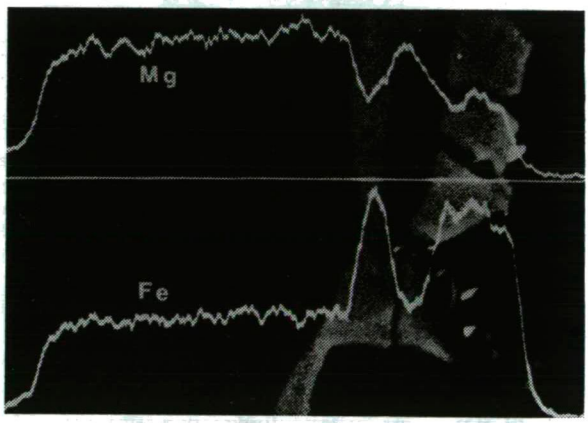

Fig. 7. A microprobe traverse in the area shown on *Fig. 6.*

One analysis has been made on the uncoloured core found in the thin-sections. The dot representing the composition of this core lies in the 5th or 7th field of the Al-Fe_{tot}-Mg diagram *(Fig. 8)*, due to the overlap of the two fields.

If the 7th field is correct, we have to decide, that the uncoloured tourmaline cores have been formed in a Cr, V-rich metasediment or in an ultramafic rock (*Fig. 8,* legend). To make the choice easier, point of a typical Cr, V-rich metasediment (FOIT and ROSENBERG, 1979) has been plotted. The two points lie in the same field of the diagram, but relatively far from each other. This divergence may indicate differences in the conditions of formation. The high Mg-content is characteristic for

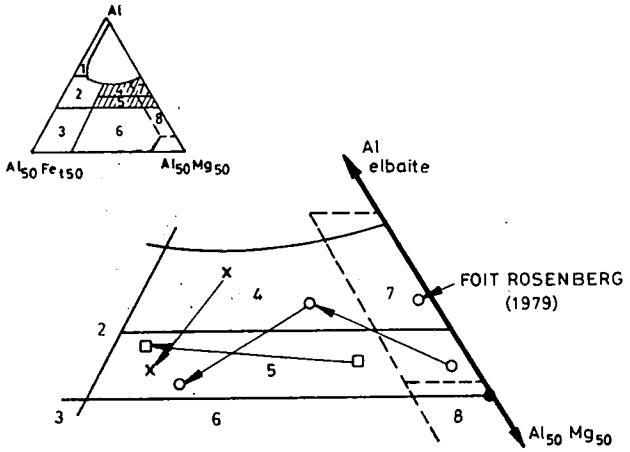

Fig. 8. Al-Fe_{tot}-Mg diagram (in molecular proportions) for tourmalines from various rock types. Fe_{tot} total Fe in the tourmaline; the rock types *represented* are:

(1) Li-rich granitoid pegmatites and aplites
(2) Li-poor granitoids and associated pegmatites and aplites
(3) Fe^{3+}-rich quartz-tourmaline rocks
(4) Metapelites and metapsammites coexisting with an Al-saturated phase
(5) Metapelites and metapsammites not coexisting with an Al-saturated phase
(6) Fe^{3+}-rich quartz-tourmaline rocks, calcsilicate rocks and metapelites
(7) Low Ca metaultramafics and Cr, V-rich metasediments
(8) Metacarbonates and metapyroxenites (after HENRY and GUIDOTTI, 1985)

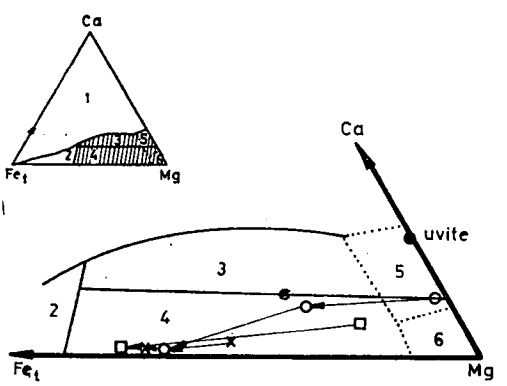

Fig. 9. Ca-Fe_{tot}Mg diagram (in molecular proportions) for tourmalines from various rock types. The fields are:

(1) Li-rich granitoid pegmatites and aplites
(2) Li-poor granitoids and their associated pegmatites and aplites
(3) Ca-rich metapsammites and metapelites; calcsilicate rocks.
(4) Ca-poor metapelites and metapsammites and quartz-tourmaline rocks.
(5) Metacarbonates
(6) Metaultramafics
(after HENRY and GUIDOTTI, 1985)

ultramafic rocks. Having a point in the Mg-rich part of the field indicates ultramafic origin. Accepting this result, the continuos transition from the uncoloured core to the yellow margin may be effect of metamorphic homogeneization, being characteristic for high-grade metamorphic rocks.

We cannot exclude the possibility that the uncoloured core belongs to the 5th field. Then it has been formed in a metapelite or metapsammite lacking an Al-saturated phase. Since the point lies in the Mg-rich part of this field, the source rock may have been a Mg-rich one.

Plotting the data in a Ca-Fe_{tot}-Mg diagram, interpretation of the uncoloured core leads to more problems. Here the point lies on the common boundary of three fields *(Fig. 9)*. Tourmaline of metacarbonates lies close to uvite, while analytical data of HENRY and GUIDOTTI (1985) from metaultramafites show higher dispersion. It means that the latter field is more close to the source rock. Overlap of the 4th and 6th fields means, that we cannot exclude from the source rocks a Ca-poor metapelite or metapsammite.

The three analytical results of the brownish yellow tourmaline show high dispersion in both kind of plots. It means different source rocks. Two points fall in the field of metapelites-metapsammites with Al-saturated phases, while one falls in the field without Al-saturated phases *(Fig. 8)*. This fact indicates the former origin; however, more analytical data are needed.

All three points fall in the field of the Ca-poor metapelites-metapsammites of the Ca-Fe_{tot}-Mg plot, with high dispersion. The three analytical data of the greenish blue margin fall almost to the same place in both plots. It means formation in the same rock under the same processes. These grains derived from quartzphyllite samples. It fulfils the requirements of metapelites-metapsammites without Al-saturated phases and it is Ca-poor (see *Figs. 8, 9*).

By these measurements we have calibrated the method for our rock, proving that tourmalines formed in a known rock fall in the field of the respective rock in the plots of HENRY and GUIDOTTI, (1985).

2. *Morphology of zircon grains*

Thin-section investigations show that while the zircon grains are of detrital origin, these are bordered by intact faces and edges, preserving the original morphology during transportation and metamorphism.

Zircon grains were separated by grinding of the rock, then applying bromophorme heavy liquid and magnetic separator.

Three hundred zircon grains from quartzphyllite have been analysed for morphological features following the method of PUPIN, (1980, 1985). The material was selected under binocular microscope.

Morphological types were determined after the diagram of PUPIN, (1980) *(Fig. 14)* and under binocular microscope, because usually the grains are slightly rounded. The results are shown on *Fig. 15*. The rock contains a large variety of zircons, with some types showing extramely large values (types G_1, D, Q_3, S_{25}, *Fig. 14*). The dominant forms are shown on *Figs. 10, 11, 12, 13*. The results are shown in a suggestive graphic form on *Fig. 16*.

Uncoloured, clear zircon grains dominate the investigated material; it is present in all kinds of morphological groups. Light pink, translucent crystalls are present among forms belonging to the S_{16}-S_{20} fields. However, this group also contains uncoloured grains. A third group is formed by uncolured crystalls with much inclu-

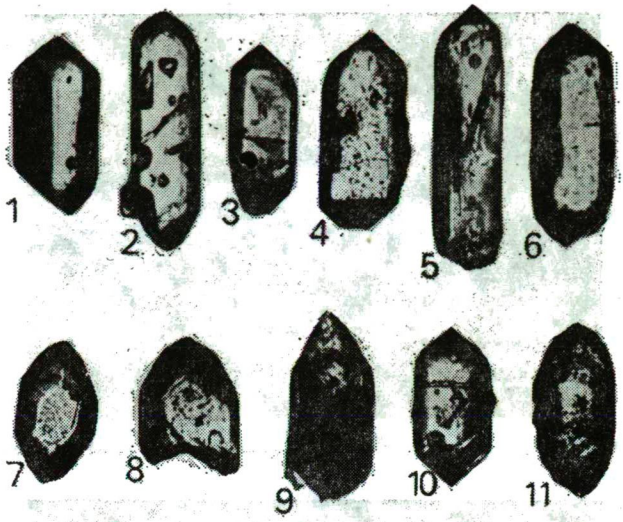

Fig. 10. Optical microscope pictures of the dominant types derived from quartzphyllite of the Kőszeg-Rechnitz series. 1. G_1, 2. P_2, 3. P_4, 4. P_5, 5. D, 6. D, 7. S_2, 8. S_7, 9. S_{11}, 10. S_{24}, 11. rounded grain with complex zonation. Some of the represented grains (4, 5, 8, 9) are cracked.

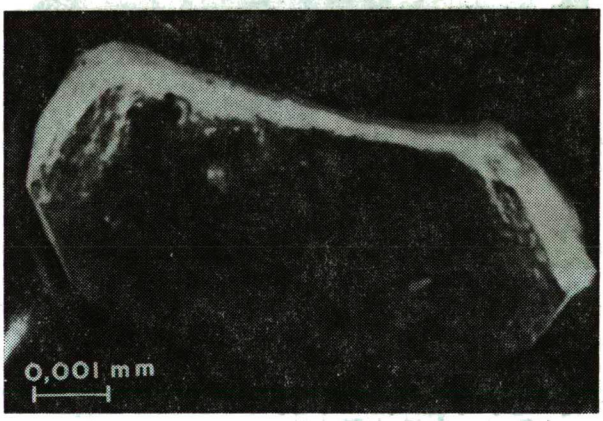

Fig. 11. Elongated S_4-type zircon grain from quartzphyllite. SEM picture.

sions. The inclusions are probably ore minerals, although lots of grains have obviously fluid inclusions *(Fig. 10—2.5)*. The high inclusion content makes some crystalls opaque. This type is characteristic for the group positioned along the J_4-S_{14}-P_1 line.

It may be important for subsequent studies that VOGGENREITER, (1986) also mentions similar types of inclusions found in zircon in Penninic quartzphyllites of Tauern Window.

Appearence of these groups with different colours indicates different source rocks.

The distribution curve shown on *Fig. 17* has been drawn from the data *Figs. 15* and *16*.

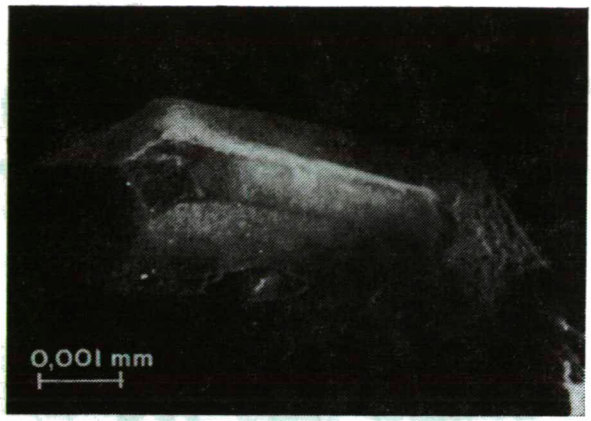

Fig. 12. S_{19}-type zircon grain from quartzphyllite. SEM picture.

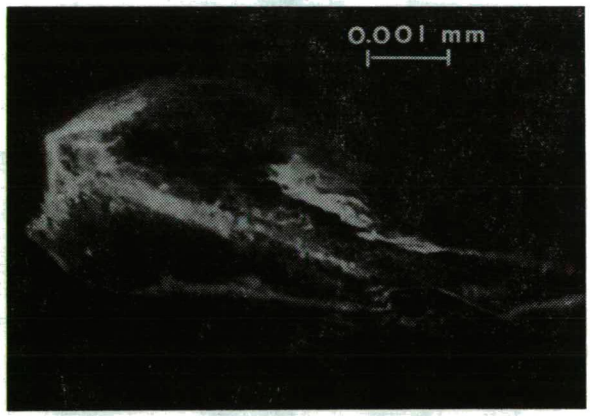

Fig. 13. D-type zircon grain from quartzphyllite, SEM picture.

Following the method of PUPIN, (1980), field I means alkaline granites and alkaline basalts. The large number of zircon grains in the investigated quartzphyllite makes derivation from the latter improbable.

Field II means porphiroidic granodiorite-monzogranite of anatectic origin, but the distribution maximum has moved towards form Q_3. This kind of shift hasn't been mentioned by PUPIN, (1980, 1985).

Field III, indicating type D grains on *Fig. 14*, corresponds to plagiogranites of tholeiitic suites and alkaline rhyolite. A conspicuously high distribution maximum has been found here, indicating either the erosion of a very large amount of alkaline rhyolite or a significant amount of plagiogranite.

From the above mentioned data we can conclude that the source rocks might have belonged to two different series. One of them was of crustal origin (field II), while the other derived from the mantle T (fields I and III).

Similar detrital material has been discussed by WEISSERT and BERNOULLI, (1985), proving a common erosion process of ophiolite and granite bodies for the formation of breccias between radiolarite beds of Tethian sedimentary sequences. POLINO and

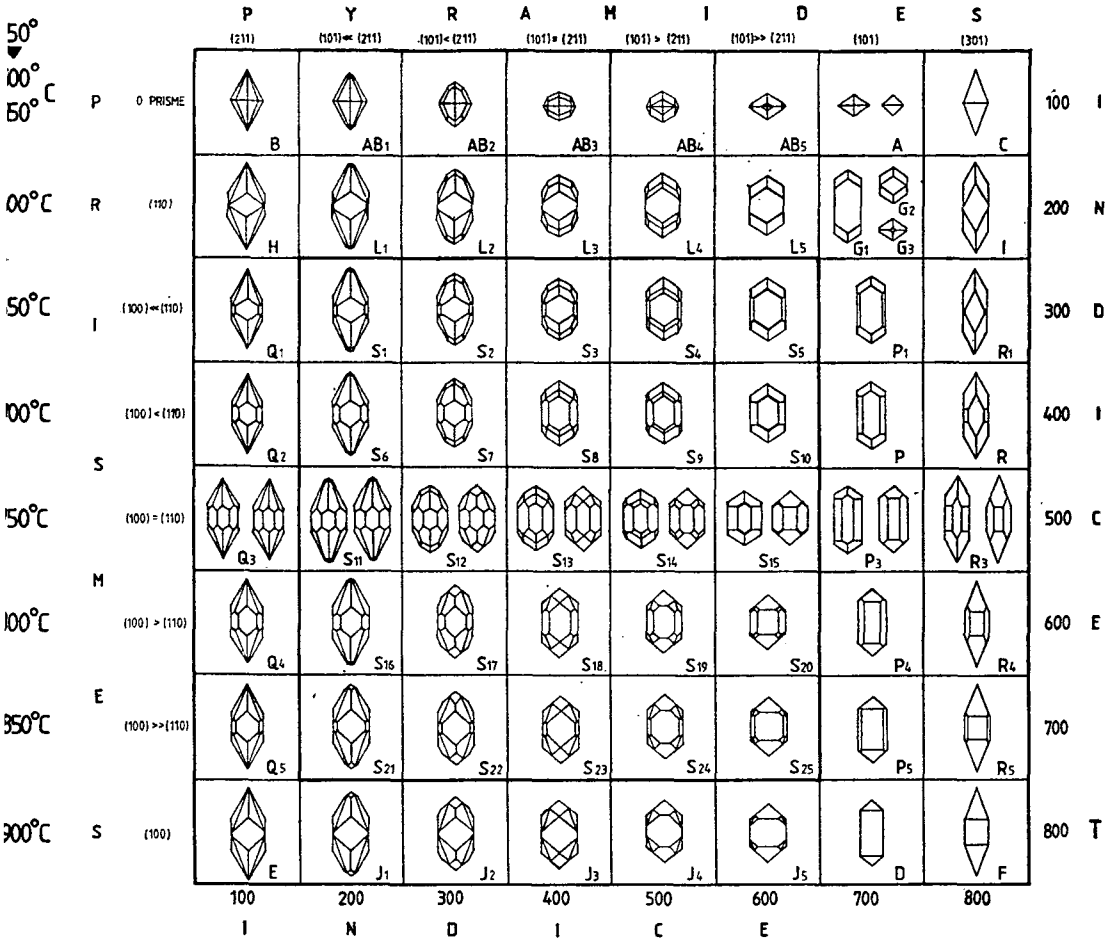

Fig. 14. Morphological types of zircon (by PUPIN, 1980).

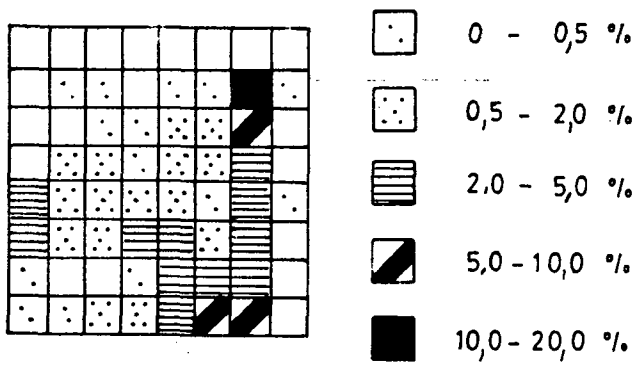

Fig. 15. **Percentage** of types shown on *Fig. 14* in our samples.

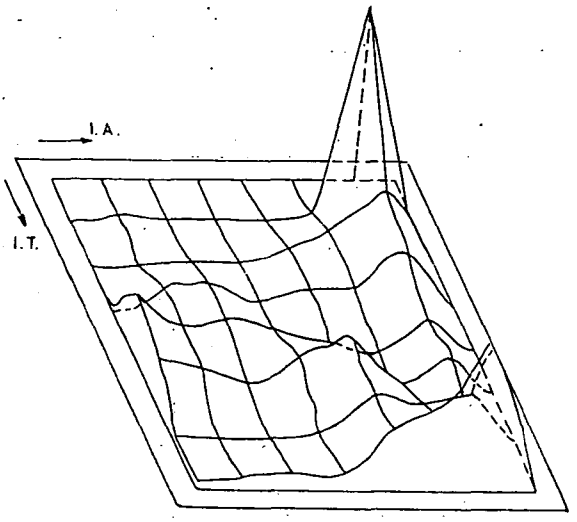

Fig. 16. Distribution of morphological types of zircon grains. Crossing points of the lines indicate the morphological forms, while distance from the base level is proportional with the quantity of the grains.

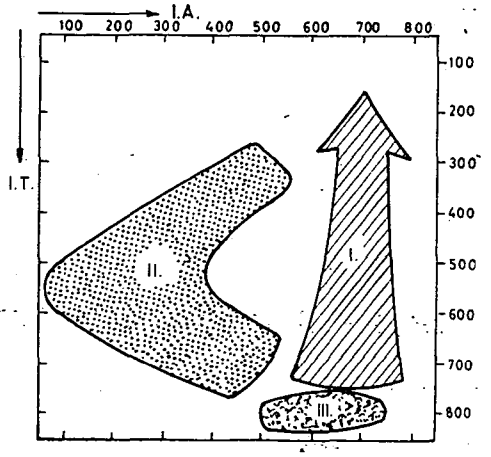

Fig. 17. Distribution fields of zircon grains in the quartzphyllite samples.

LEMOINE, (1984) described the mixing of continental and ophiolitic detritus in the Penninic sediments of the Lago Nero seies of the Western Alps. Among others the material of continental origin contains biotite granite.

Plagiogranite as source rocks has been mentioned by PUPIN (1980) for the Inzecca ophiolitic suite of Corsica. Also, CARON and DELCEY, (1979) have proven significant amount of rhyolite material shed into the East Corsican "schistes lustres" (a similar problem has been discussed in connection with field III of *Fig. 17*).

We can conclude, that in several Penninic regions the erosion of this kind of rock suites has occured.

In the Austrian part of the Kőszeg and Rechnitz window there are radiolarites (KOLLER PAHR, 1980), but these authors don't mention such detrital material.

CONCLUSIONS

Sedimentary rocks of the Kőszeg-Rechnitz series have been deposited in the Tethys ocean during the Jurassic and Cretaceous. Several kinds of metamorphic rocks and granites have been eroded contemporaneously with the sedimentation.

The former rocks might have belonged to medium or high metamorphic grade, and were Ca-poor metapelites-metapsammites with Al-saturated phases. These rocks contained a relatively large amount of tourmaline. Beside the parametamorphic rocks large amount of monzogranite-granodiorite (derived from the crust), alkaline granite and mantle-derived plagiogranite have been eroded. The metamorphic rocks belonging to an older tectogenesis indicate continental erosion, therefore the granitoids might be considered as relatively old, probably Variscan ones.

Literature data and our results indicate, that the sedimentation might have been fairly uniform in the Tethys ocean. Mostly zircon investigation results lead to this statement, since these ones agree well with data obtained from other parts of the Alps.

Similarly of detrital material in Tethyan rocks of different Alpine areas indicate, that the rocks affected by subaerial erosion were similar in large areas.

REFERENCES

BANDAT, H. (1928): Geological conditions of the Western of Kőszeg-Rechnitz Hills. Földtani Szemle **I, 3.** 1—24.(In Hungarian)

BANDAT, H. (1932): Die geologische Verhaltnisse des Kőszeg-Rechnitzer Schiefergebirge. Földtani Szemle **I, 2.** 140—186.

CARON, J. M., DELCEY, R. (1979): Lithostratigraphie des lustres corses: diversute des series post-ophiolitiques. C. R. Acad. Sci. Paris. Ser. D. **288,** 1525—1528.

FOIT, F., ROSENBERG, P. (1979): The structure of vanadium-bearing tourmaline and its implications regarding tourmaline solid solutions. American Mineralogist **64,** 788—798.

HENRY, D., GUIDOTTI, C. (1985): Tourmaline as a petrogenetic indicator mineral: an example from. the staurolitgrade metapelites of NW Maine. American Mineralogist. **70,** 1—15.

JUGOVICS, J. (1917): Geology and petrography of the Borostyánkő Hills. Annual Report Hung. Geol. Survey for 1916. 77—97. (In Hungarian)

KISHÁZI, P., IVANCSICS, J. (1976): Standardized investigations on metamorphic rocks in Western Hungary. II. The Rechnitz Metamorphic Complex. Hung. Geol. Survey., internal report. Manuscript. (In Hungarian)

KISHÁZI, P., IVANCSICS, J. (1984): Guide-book to the geology of the Kőszeg schist series. Hung. Geol. Survey, internal report. Manuscript. (In Hungarian)

KOLLER, F. (1985): Petrologie und Geochemie der Ophiolite des Penninikums am Alpenostrand. Jb. Geol. Bundesanst. **128,** 83—150.

KOLLER, F., PAHR, A. (1980): The Penninic ophiolites of the Eastern end of the Alps. Ofioliti. **5,** 65—72.

KOTSIS, T. (1965): Mineralogical and petrological investigations of talcum in Felsőcsatár (Western Hungary). M. Sc. Diss. Univ. of Szeged. (In Hungarian)

KUBOVICS, I. (1983): Petrological characteristics and genetic features of crossitite from Western Hungary Földtani Közlöny. **113,** 207—224. (In Hungarian wiht English abstract.)

NAGY, E. (1972): Investigations in Kőszeg Hills. Annual report Hung. Geol. Inst. for 1970, 197—205. (In Hungarian with German abstract.)

POLINO, R., LEMOINE, M. (1984): Detritisme mixte d'origine continentale et oceanique dans les se-

diments jurassico-cretaces supra-ophiolitiques de la Tethys ligure: la serie du Lago Nero (Alpes occidentales franco-italiennes). C. R. Acad. Sci. Paris. Ser. 2. **298**, 359—364.

PUPIN, J. P. (1980): Zircon and granite petrology. Contrib. Mineral. Petrol. **73**, 207—220.

PUPIN, J. P. (1985): Magmatic zoning of Hercynian granitoids in France based on zircon typology. Schweiz. Min. Petr. Mitt. **65**, 29—56.

SCHMIDT, W. (1956): Die Schieferinseln am Ostrand der Zentralalpen von Rechnitz, Bernstein und Möltern. Mitt. Geol. Gesselschaft in Wien. **47**, 360—365.

SCHÖNLAUB, H. (1973): Schwamm-Spiculae aus dem Rechnitzer Schiefergebirge und ihr stratigraphiser Wert. Jb. Geol. Bundesanst. **116**, 35—48.

SZEBÉNYI, L., FÖLDVÁRY, A., NOSZKY, J., SZENTES, F. (1948): Geological notes from the Kőszeg Hills. Jel. Jöv. Mélykut. 1947/48 évi Munk. 5—31. (In Hungarian)

VARRÓK, K. (1963): Geochemical survey of crystalline schists in Western Hungary. Annual Report Hung. Geol. Survey for 1963, 149—153. (In Hungarian with English abstract.)

VOGGENREITER, W. (1986): Vorlaufige Ergebnisse morphologische untersuchungen an Zirconen aus Quartziten und Quartzschiefern des Penninikums und Unterostalpins des Weisseneck-Schareck-Gebietes der südlichen Radsadter Tauern (Ostalpen, Österreich). Jb. Geol. Bundesanst. **129**, 149—159.

WEISSERT, H., BERNOULLI, D. (1985): A transform margin in the Mesozoic Tethys: evidence from the Swiss Alps. Geologische Rundschau. **74**, 665—679.

Manuscript received, 21 December, 1987

Acta Mineralogica-Petrographica, Szeged, XXIX, 27—33, 1987—1988

ELECTRON MICROPROBE ANALYSIS OF TOURMALINE GRAINS, MECSEK MOUNTAINS, HUNGARY

O. SZTANÓ—K. BODÓ—A. BARTHA—K. GÁL-SOLYMOS

Department of Petrology and Geochemistry,
Loránd Eötvös University

ABSTRACT

Some outcrops of Bakonya Member of Kővágószőlős Sandstone Formation (detrital complex of the Upper Permian of Mecsek) contains a considerable amount of tourmaline. Optically these grains can be divided into different groups. In addition to different genesis of grains some of them has syntaxial rim. It is well known that tourmaline is an excellent indicator of rock types. The result of microprobe investigations of tourmaline grains were plotted on the diagrams of HENRY and GUIDOTTI (1985). The differences in composition of cores correspond to different metamorphic rocks. The grains after getting into Permian sedimentary basin had overgrown diagenetically, due to the new geochemical conditions.

INTRODUCTION

The directions of transport of Permian sedimentary complex and the source areas as well as the mineralogy of sandstone were investigated by FAZEKAS (1987). She has an opinion that the Upper Permian sandstone of Mecsek Mts. is mainly composed of eroded Paleozoic metamorphics and migmatic-granite materials of Mórágy mass in its southern and south-eastern areas. Tourmaline grains derived from the same area and are characterized by various optical properties, and these may explain their distinct origins. Electron microprobe analyses of tourmaline grains were performed so that we could obtain more exact data on their genesis.

GEOLOGICAL STRUCTURE OF WESTERN MECSEK ACCORDING TO PREVIOUS AUTHORS

The first investigation of Western Mecsek Mountains was carried out by BÖCKH (1876). VADÁSZ (1935) in his monography also wrote about this region in detail. After discovery of uranium deposits the research of this region became more intensive. Nowadays the Permian and Lower Triassic sediments are well known by the results of investigations of Ore-Mining Company (MÉV).

BARABÁS (1979), BARABÁS-STUHL (1981) and FAZEKAS (1987) gave exact descriptions of these formations.

The older parent rocks may belong to crystalline basement and carboniferous molasse.

SZEDERKÉNYI (1977), JANTSKY (1979). LELKES—FELVÁRI (1981) and ÁRKAI (1984) delt with this topic and they arrived at different conclusions. The oldest

H—1088. Budapest, Múzeum krt. 4/A Hungary.

formation of the basement consists of Paleozoic crystalline rocks (mica-schist, gneiss, amphibolite). There are younger Silurian anchi-metamorphic schists also; which is proved by microfossils, and serpentinite subdivided into Devonian.

The origin and age of migmatic alkaline-rich granite are significant and very discussed questions.

The examined Kővágószőlős Sandstone Formation belongs to the third Permian sedimentary cycle. When the Bakonya Member was deposited, the direction of the sediment transport must have been from the west, south, south-east, so that we have to look for the source area towards these directions. The investigated area is illustrated by *Fig. 1.*

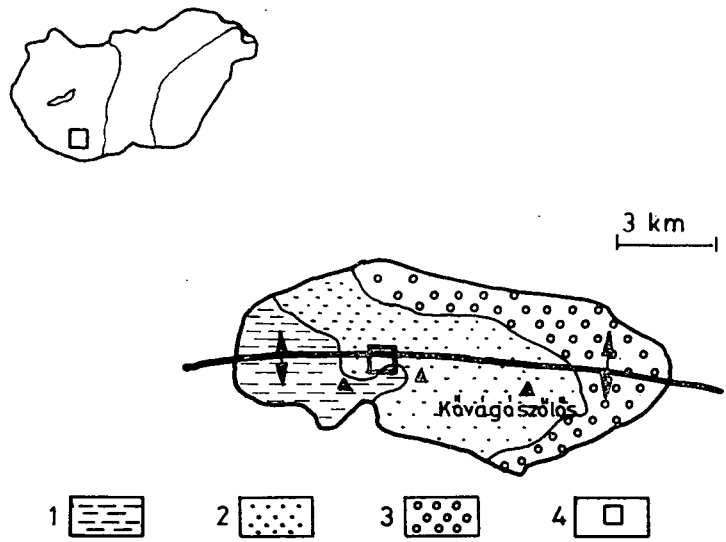

Fig. 1. Geological sketch about Kővágószőlős anticline (after BARABÁS, 1979). 1. Boda Aleurolite Formation. 2. Kővágószőlős Sandstone Formation. 3. Jakabhegy Sandstone and Conglomerate. 4. The investigated area.

OPTICAL PROPERTIES OF THE ANALYSED TOURMALINE GRAINS

The tourmaline grains examined in this work are mostly anhedral and sometimes subhedral. Their size are between 0.05 mm and 0.5 mm (see *Fig. 2* and *Fig. 3*). These tourmalines can be divided into two groups on the basis of their pleochroism. The first one is characterized by pink and black colours and the second has brown and greenish-brown tone.

The *pink tourmaline* is represented by a sole, 0.3 mm long grain, only. It shows a strong pleochroism. Passing towards the a-axis it is black and to the c-axis it is pink *(Fig. 4a, b)*.

The *greenish-brown tourmaline*'s pleochroism depends on the orientation of the segment. If the segments are paralell with the c-axis, they have a strong pleochroism; towards the c-axis it shows a pale yellow shade or it is colourless. The segments which are perpendicular to the c-axis, show usually a greenish-brown colour but they have no any visible pleochroism.

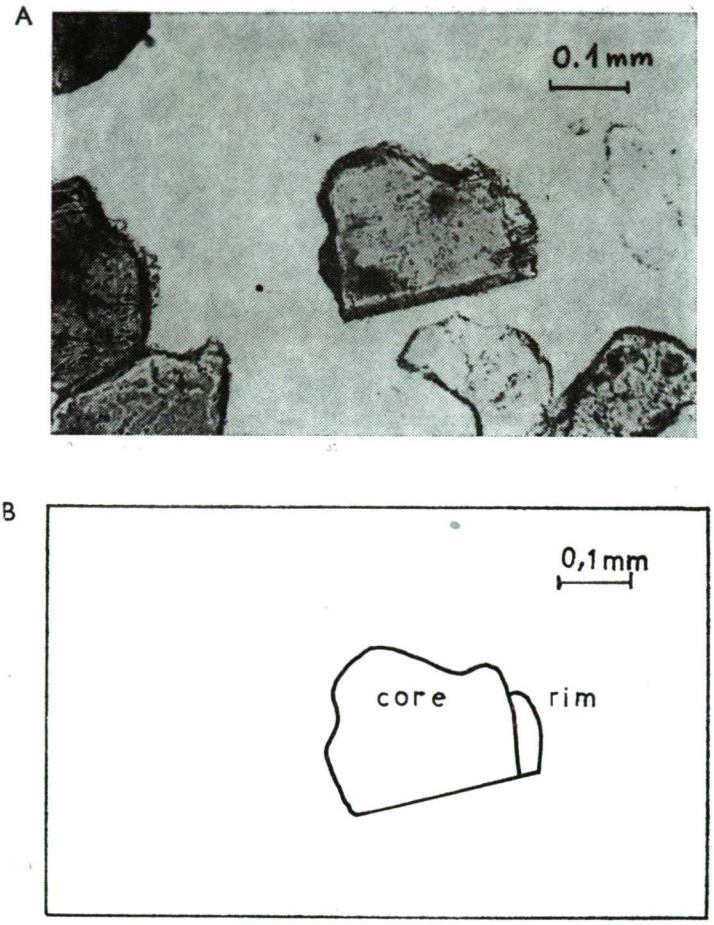

Fig. 2a, b. Pink—black coloured tourmaline grain with its blue rim.

In some grains several inclusions of garnet, rutile (?) and muscovite were recognized. In the others some zircons, ilmenites and apatites occur.

Some grains have greenish-blue syntaxial rim. The main features of these rims are the following:

— discontinous core-to-rim zoning,

— rich in inclusions, which are perpendicular to the c-axis.

— strong pleochroism: towards the a-axis the colour is greenish-blue, and towards the c-axis it is colourless.

There are some grains which have continous zoning from the core to the rim. The core is greenish-brown and the rim is greenish-blue. A small colour difference exists between the core and the rim, only.

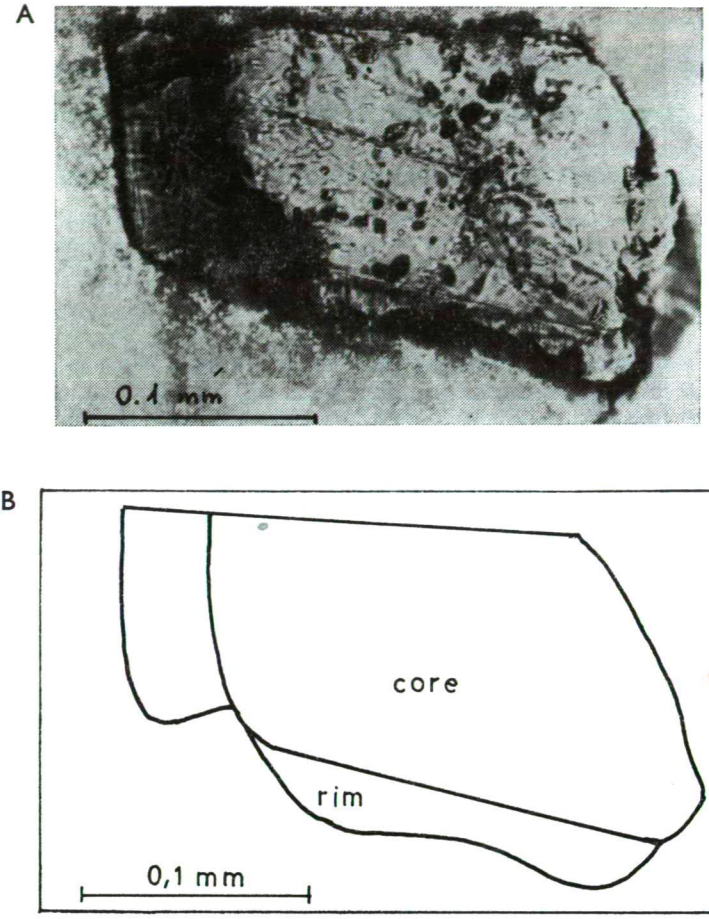

Fig. 3a, b. Greenish-brown tourmaline grain with its blue rim.

ELECTRON MICROPROBE ANALYSES OF TOURMALINE GRAINS

The tourmaline grains for the electron microprobe analyses were chosen by the favourable results of their optical examinations. Both the core as well as the rim of the grains were checked from each groups.

— It was unexpected that the composition of the other greenish-brown grain (B. in the Table 1) was similar to that of the epigenetic rims. According to its end-members it is an alkali-rich grain, which has different genesis from that of the previous ones.

In spite of our expectation we was not able to identify grains derived from the granite. Previously we supposed that the pink-black tourmaline grain may have this origin, but if it is true, its composition should have changed, during the diagenese or epigenese which caused an enrichment of the Mg, and a loss of the Fe.

These results show, that the sources of the Upper Permian detrital complex could have been various rock types exposed in the adjoining area.

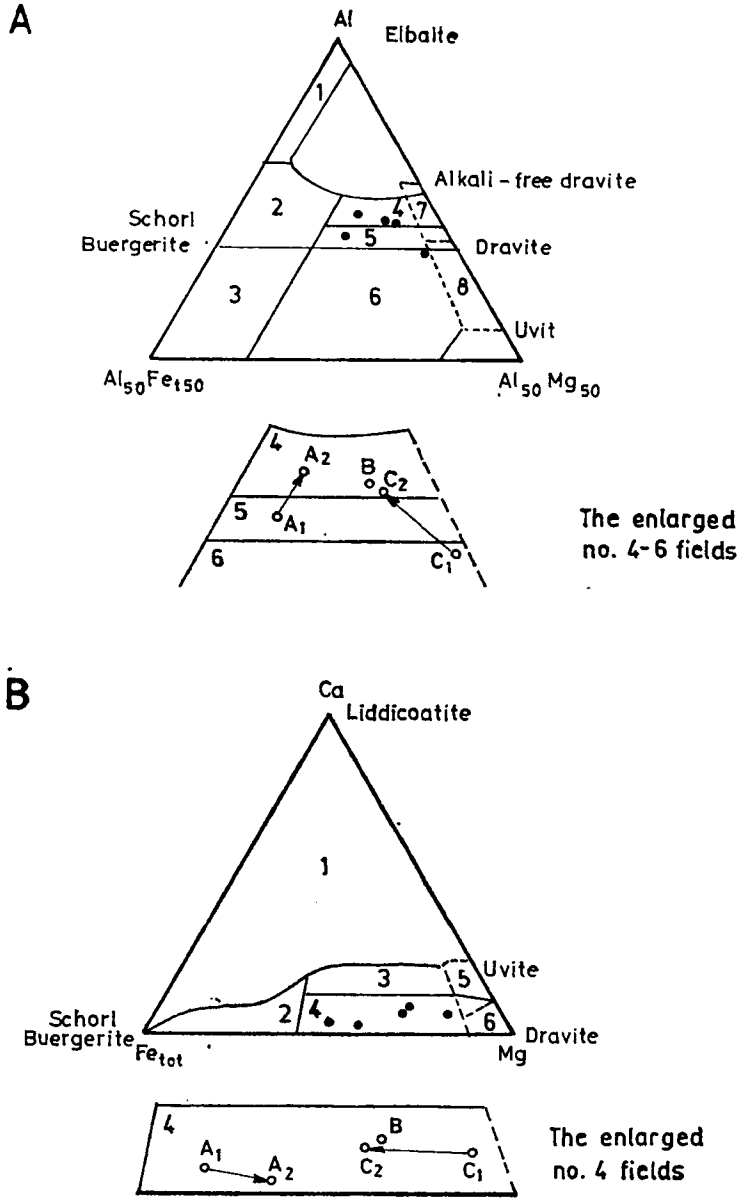

Fig. 4a. Al-Fe_{tot}-Mg diagram for tourmalines of various rocks (after HENRY and GUIDOTTI, 1985). Fields of the diagram represent the compositional ranges of tourmalines from different kind of rocks.) 1. Li-rich granitoid, pegmatite and aplite. 2. Li-poor granitoids and associated pegmatites and aplites. 3. Fe-rich quartz-tourmaline rocks (hydrotermally altered granites). 4. Metapelites and metapsammites coexisting with Al-saturating phase. 5. Metapelites and metapsammites not coexisting with Al-saturating phase. 6. Fe-rich quartz-tourmaline rocks, calcsilicate rocks and metapelites. 7. 7. Low-Ca metaultramafics, Cr-V-rich metasediments. 8. Metacarbonates and metapyroxenites. A.1 Core of the pink – black grain. A.2 Margin of the pink – black grain. B. Little greenish-brown grain (core). C.1 Core of the greenish-brown grain. C.2 Margin of the greenish-brown grain.

Fig. 4b. Ca-Fe_{tot}-Mg diagram for tourmalines of various rocks (after HENRY and GUIDOTTI, 1985). 1. Li-rich granitoid, pegmatite and aplite. 2. Li-poor granitoids and associated pegmatites and aplites. 3. Ca-rich metapelites, metapsammites and calcsilicate rocks. 4. Ca-poor metapelites, metapsammites and quartz-torumaline rocks. 5. Metacarbonates. 6. Metaultramafics. The A.1, A.2, B, C.1 and C.2 symbols are the same that of *Fig. 4a.*

TABLE 1

Electron microprobe analyses of tourmaline grains

	A.1	A.2	B	C.1	C.2
BO_3	10.0	10.0	10.0	10.0	10.0
SiO_2	37.0	38.0	37.6	36.7	37.3
TiO_2	0.31	0.04	0.82	0.65	0.77
Al_2O_3	30.5	32.8	31.4	31.2	33.3
FeO	9.8	7.8	5.1	3.5	5.6
MgO	5.7	6.0	7.7	10.5	8.0
CaO	0.32	0.14	0.86	0.82	0.87
Na_2O	2.19	1.79	2.17	2.69	2.10
total	95.82	96.57	95.65	96.06	97.94

Kation numbers

	1	2	3	4	5
B	3.000	3.000	3.000	3.000	3.000
Si	6.143	6.149	6.112	5.931	5.926
Al (T)	0.0	0.0	0.0	0.069	0.074
Al (Z)	5.970	6.000	6.000	5.875	6.000
Al (Y)	0.000	0.257	0.017	0.0	0.163
Fe	1.361	1.056	0.639	0.473	0.744
Mg	1.411	1.447	1.865	2.529	1.894
Ti	0.039	0.005	0.100	0.079	0.092
total	2.811	2.760	2.675	3.081	2.893
Ca	0.057	0.024	0.150	0.142	0.148
Na	0.705	0.562	0.684	0.843	0.467
total	0.762	0.586	0.834	0.985	0.615

Calculated on the basis of 24.5 oxigen

End-member proportions

	1	2	3	4	5
Schorl	50.8	42.0	26.0	17.0	28.3
Dravite	28.1	25.1	50.0	33.5	25.0
Uvite	6.4	2.9	16.5	16.0	16.8
Alkali-defected tourmaline	14.7	30.0	7.5	33.5	29.9

A.1, A.2, B, C.1 and C.2 symbols are the same that of Fig. 4a

The microprobe analyses were run on a JXA—50A type insrument. The accelerator voltage was 15 kV. The adsorbed electron current intensity was 30 nA and the diameter of the electronfile was 1 μm. Albite, olivine and sphene standards were used. The analyses were carried out by G.-SOLYMOS in the Department of Petrology and Geochemistry of the Loránd Eötvös University, Budapest.

Results of analyses are shown on a table and figures. The *Table 1.* represents concentrations expressed in weight perecentages and the calculated kation numbers as well as the percentages of the tourmaline end-members. The percentage of boron was calculated on the basis of structural formula. It is assumed that there are 3 boron atoms in the formula and the weight percent of B_2O_3 are as much as 10%.

The cation numbers were plotted on the Al-Fe_{tot}-Mg and Ca-Fe_{tot}-Mg triangle diagrams *(Fig. 4a, b)*. These diagrams show relationship between the various rocktypes and the composition of tourmaline grains derived from these rocks. We have to note that the fields of the diagrams may overlap each other.

CONCLUSIONS

The following conclusions can be reached from the results of the analyses:

— According to the triangle diagrams the tourmaline grains having a pink-black pleochroism (A.1 in the Table 1) may be derived from metapelites or metapsammites.

— The origin of the greenish-brown grain (C.1 in the Table 1) is difficult to explain, because the region no. 6 of the Al-Fe_{tot}-Mg diagram represents three different types of the rocks. In spite of this uncertainity, we can suppose that it comes from another type medium-grade metamorphic schist.

— These grains having different origin and arriving to the sedimentary basin after the burrying they had overgrown diagenetically and have produced a blue margin. Unfortunately there is no region for epigenetic tourmalines on HENRY and GUIDOTTI's (1985) diagram. Improvement of this method needs further investigations.

ACKNOWLEDGEMENTS

Our thanks are extended to S. JÓZSA, A. DEMÉNY, K. TÖRÖK and Cs. SZABÓ for their many helpful discussions. We are also grateful to Prof. I. KUBOVICS who made possible to do this work.

REFERENCES

ÁRKAI, P. (1984): Polymetamorphism of the crystalline basement of the Somogy—Dráva basin (South-Western Hungary). Acta Miner. Petr. Szeged. **XXVI/2,** 129—153.

BARABÁS, A. (1979): A perm időszak földtani viszonyai és a külszíni kutatás feladatai a mecseki ércelőhelyen. (Geological conditions of the Permian and tasks of surface geological investigations at the Mecsek ore deposits.) Földt. Közl. **109/3—4,** 357—365.

BARABÁS—STUHL, A. (1981): A Kővágószőlősi homokkő formációt alkotó kisciklusok földtani vizsgálata. (A geological study of the microcycles forming the Kővágószőlős Sandstone Formation.) Földt. Közl. **111/1,** 26—42.

BÖCKH, J. (1876): Pécs városa környékének földtani és vízi viszonyai. (Geological and hydrogeological relations of Pécs and its environs.) Földt. Int. Évk. **1876.**

DEMÉNY A. (1987): Turmalin szemcsék geokémiai vizsgálata (Kőszegi hegység). (Geochemical studies of tourmaline grains (Kőszeg Mts).) Földt. Közl. **117/2,** 131—140.

FAZEKAS, V. (1987): A mecseki perm és alsó triász korú törmelékes formációk ásványos összetétele. (Mineralogical composition of Permian and lower Triassic clastics from the Mecsek Mts.) Földt. Közl. **117/1,** 11—30.

HENRY, D. J.—GUIDOTTI, C. V. (1985): Tourmalines as petrogenetic indicator mineral: an example from the staurolite grade metapelites of NW-Maine. The Amer. Miner. **70/1—2,** 1—15.

JANTSKY, B. (1979): A mecseki kristályosodott alaphegység földtana. (Geology of crystalline basement of Mecsek Mts.) Földt. Int. Évk. **60,** 3—193.

LELKES-FELVÁRI, GY. (1981): Outlines of the pre-Alpine metamorphism in Hungary. In: Karmata, S.—Sassi, F. P. (eds.) IGCP. 5 Newsletter **3,** 89—99.

SZEDERKÉNYI, T. (1977): Geological evolution of South Transdanubia (Hungary) in Paleozoic time. Acta. Miner. Petr. Szeged. **XXIII/1,** 3—14.

VADÁSZ E. (1935): A Mecsek hegység — Magyar Tájak Földtani leírása (Das Mecsek Gebirge), Budapest.

Manuscript received, 5 April, 1988

Acta Mineralogica-Petrographica, Szeged, XXIX, 35—46, 1987—1988

GEOCHEMICAL INVESTIGATION OF OLIVINES FORM ALKALI BASALT AND THEIR XENOLITHES (NÓGRÁD-GÖMÖR REGION, HUNGARY)

I. KUBOVICS—G. B. ÁRGYELÁN—CS. SZABÓ—K. G. SOLYMOS

Department of Petrology and Geochemistry, Loránd Eötvös University

ABSTRACT

Neogene-Quaternary alkaline basalts in the Nógrád-Gömör region bear several kinds of inclusions and xenocrysts. Olivine appears in both the lherzolitic and wehrlitic series of the inclusions, is frequent among xenocrysts and appears in the host alkaline basalts as phenocrysts and in the groundmass. Deformation lamellae and subgrain boundaries in xenocrysts and in a wehrlite sample indicate a complex history of the inclusion before embedding in the host alkaline basalt. The REE-poor olivine with the highest mg-value is characteristic for lherzolite and dunite inclusions of the upper mantle origin. Main element composition of the xenocrysts is similar to that of the wehrlitic series (cumulate). Their mg-values indicate crystallization from a Fe-rich, tholeiitic magma; magma mixing (possibly assimilation) caused their embedding in the host alkaline basalt. REE spectra of individual grains suggest cognate phenocrysts and groundmass olivines from the alkaline basalts. High mg-values of phenocrysts indicate crystallization in the upper mantle, while groundmass olivines are products of near-surface process.

INTRODUCTION

Neogene- to Quaternary alkaline basalts and their pyroclastics are widely distributed within the Carpathian-Pannonian region (BALOGH *et al.*, 1981, 1982, 1986). in Steiermark and Burgenland (Austria), in the Little Plain and Balaton Highlands (Hungary) and in the Nógrád-Gömör region (Hungary and Czechoslovakia). These rocks contain mafic and ultramafic xenoliths and megacrysts (DIENES, 1968; KURAT, 1971; RICHTER, 1971; EMBEY-ISZTIN, 1976, 1977, 1984; HOVORKA, 1978; HOVORKA and FEJDI, 1980; KURAT *et al.*, 1980; SCHARBERT *et al.*, 1981; JÁNOSI, 1984; DIETRICH and POULTIDIS, 1985; KUBOVICS *et al.*, 1985; BÉRCZI and BÉRCZI, 1986; FORGÁČ *et al.*, 1987).

Olivine appears in the so-called lherzolitic and wehrlitic series, and as xenocrysts, phenocrysts and in the groundmass of the alkaline basalts in the Nógrád-Gömör region.

Localities are shown in *Fig. 1;* the samples are listed in Table 1, together with the samples of HOVORKA and FEJDI (1980), JÁNOSI (1984) and FORGÁČ *et al.*, (1986).

TEXTURE ANALYSIS

The lherzolite and dunite xenoliths (Fig. 2) belong to the porphyroclastic, mosaic-porphyroclastic and equigranular texture types of MERCIER and NICOLAS (1975), MERCIER and CARTER (1975), PIKE and SCHWARZMAN (1977), HARTE (1977). The

H—1088 Budapest, Múzeum krt. 4/A Hungary.

wehrlite and olivine-clinopyroxenite are considered as hypidiomorphic cumulates (Fig. 2).

The ultramafic xenoliths and olivine xenocrysts display conspicuous traces of deformation in the microscope. We have observed deformation lamellae, subgrain boundaries as well as triple junctions after BOLAND *et al.* (1971), BOLAND and BUISKOOL—TOXOPEUS (1977), BUISKOOL—TOXOPEUS (1977), DEER *et al.*, (1982), MERCIER (1983), NICOLAS (1984).

TABLE 1

Number of investigated olivines from the Nógrád-Gömör region

Locality	Lherzolite dunite	Wehrlite olcpxite	Xeno-cryst	Pheno-cryst	Ground-mass
THIS PAPER:					
Eresztvény-Nagybánya	1,7		21		
Eresztvény-Középbánya	12,13		18		
Bárna-Nagykő	3,4		17	30	33
Strázsahegy	6		22		
Fülek	9,10		16		
Magyarbánya	11	35,37	19		
Terbeléd (Trebeľ ovce	5,8				
Kercsiktető (Kerčik)	2		20		
Nagy-Salgó		36			
Medves	34				
Ajnácskő (Hajnačka)			24	28,29	
Pécskő			14		
Pogányvár (Pohansky)			23	27	
Tilic (Tilic)			15		32
Zabodakő (Zabda Skala)				25,26	
Fányakő				31	
JÁNOSI (1984):					
Maskófalva (Maškova)	+				
Nagy-Salgó			+		
HOVORKA and FEJDI (1980):					
Maskófalva (Maškova)			+		
Patakalja (Podrečany)			+		
Fülek (Fiľakovo)			+		
Sátoros (Šiatoros)			+		
FORGÁČ et al. (1986):					
Ajnácskő			+	+	
Bolgárom (Bulhary)			+	+	
Korláti (Konrádovce)			+	+	

Deformation lamellae form a set of long, parallel platelets of different extinction, made by cross-sliding *(Fig. 3)*. The most favoured sliding surface is a function of temperature and stress. Below 1000 °C the deformed olivines are characterized by translation lamellae, while these lamellae above 1000 °C easily move in the sliding plane, forming twinning seen in ultramafic xenoliths (CARTER and AVE LALLEMANT, 1970).

There are a lot of small, polygonal olivine grains around the large, porphyroclastic olivines and some xenocrysts of the porphyroclastic and mosaic-porphyroclastic ultramafic xenoliths *(Fig. 4)*; these are called subgrains. The above mentioned authors consider that subgrains are formed when P—T conditions change around crystals, when magma mixing or incorporation in magma occurs and P—T changes produce

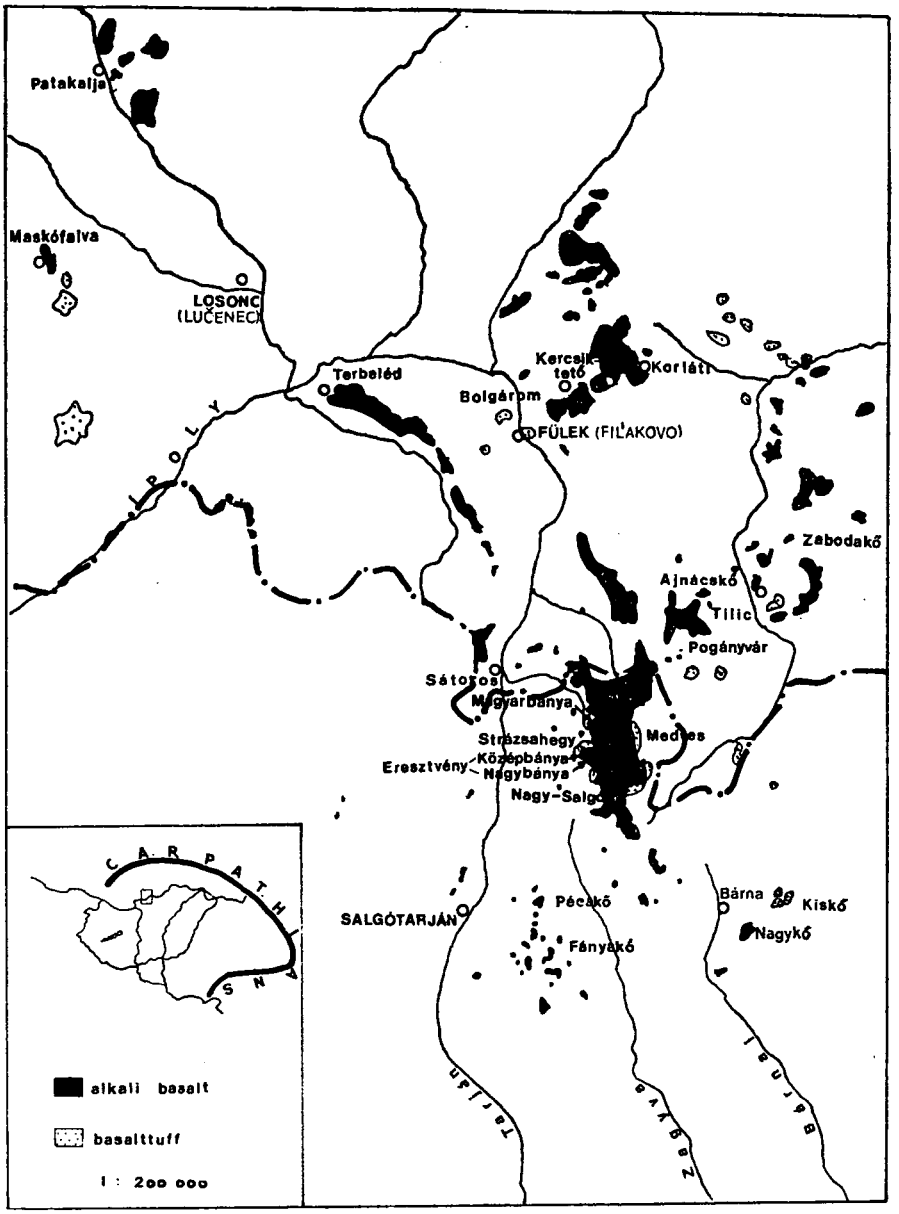

Fig. 1. Distribution of alkali basalt and basalt tuff in the Nógrád-Gömör region (after JÁNOSI, 1984).

multi-directed strain. The dislocations are expelled from the crystals or arranged in a plane. The dislocations can not move under low temperatures due to low diffusion, but these can be arranged in planes under high temperatures *(Fig. 5)* (GREEN and RADCLIFFE, 1972). These planes are the boundaries of subgrains where crystals are fractured and new grains are formed *(Fig. 4)*. The formation of substructures is due to complex deformation, which could be caused by flowing-mixing magma.

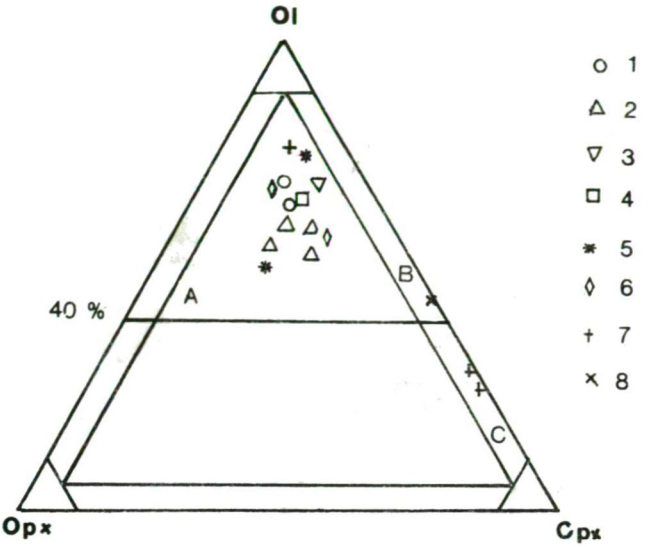

Fig. 2. Ol-Opx-Cpx plot of ultramafic xenoliths from the Nógrád-Gömör region; fields after STRECKEISEN's (1974) classification of plutonic rocks.

Localities:
1 — Terbeléd
2 — Eresztvény-Nagybánya
Eresztvény-Középbánya
3 — Strázsahegy
4 — Kercsiktető
5 — Bárna-Nagykő
6 — Fülek
7 — Magyarbánya
8 — Nagy-Salgó
A — Lherzolite
B — Wehrlite
C — Olivine-clinopyroxenite

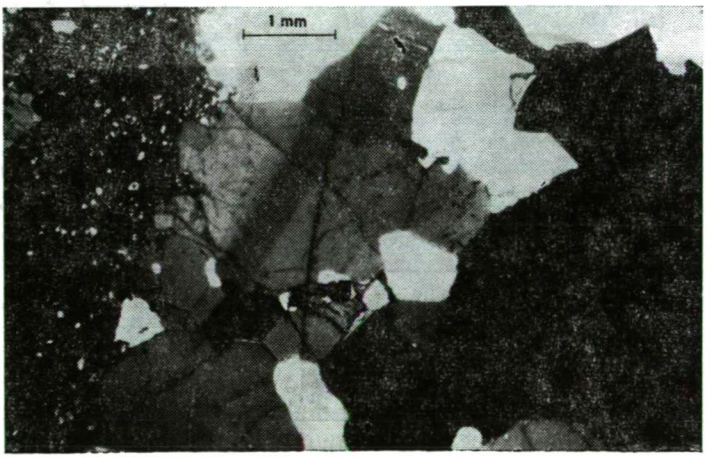

Fig. 3. Photomicrograph of twinning olivine in a lherzolite xenolith from the Nógrád-Gömör region. Crossed nicols.

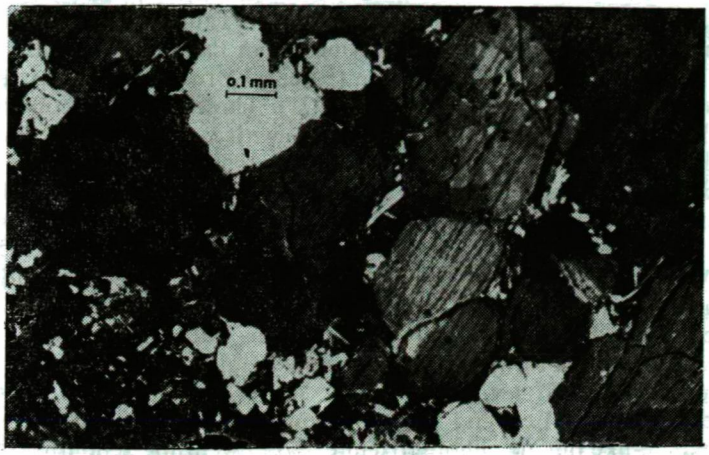

Fig. 4. Photomicrograph showing development of sugbrains in an olivine xenocryst from the Nógrád-Gömör region. Croossed nicols.

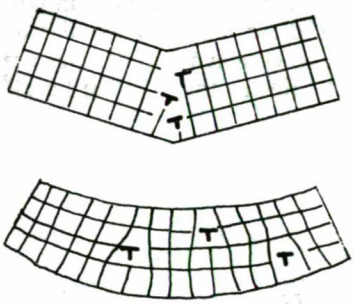

Fig. 5. Development of sugbrain in olivine.

The formation of triple junctions are made by recrystallization; these are more or less characteristic for the texture of the examined peridotite xenoliths.

Primary and secondary recrystallizations are known. In the former process energy is spent — within the crystals — to the elimination of dislocations, while during the latter one for decrease of surface energy. Secondary recrystallization in our ultramafic xenoliths is shown by mosaic texture, with slightly curved outline of grains and 120° triple junctions (NICOLAS, 1984). These deformations were found in the xenocrysts and olivines of some wehrlite samples, indicating a complex history of the xenocrysts and xenoliths before embedding in the host alkaline basalts.

GEOCHEMISTRY

Electron microprobe analyses were made by a JXA—50A microprobe (accelerating voltage 15 kV, 30 μA, electrobeam diameter: 1 μm). Olivine standard was applied. Minerals were checked for homogenity at five or more points. The representative data are presented in Table 1. Cation numbers were calculated on the basis of 4 oxygens.

Two groups of olivines were found in the ultramafic xenoliths. The lherzolite and dunite xenoliths with strongly deformed texture bear olivines with very low

FeO, MnO, low CaO contents and high mg-values (Table 2; *Fig. 6*). Data in Table 2 show fair correlation with those of olivines from lherzolite xenoliths in alkaline basalts in the Carpatho-Pannonian region (EMBEY-ISZTIN, 1976; KURAT *et al.*, 1980; DIETRICH and POULTIDIS, 1985; RICHTER, 1971). These olivines show no chemical inhomogenity or zonation and are in equilibrium with associated orthopyroxenes and clinopyroxenes. Data of DEER *et al.*, (1982) indicate that olivines in lherzolite xenoliths from the worldwide spread alkaline basalts show mg-values mostly between 89 and 92, like in our samples (Fig. 6).

KUBOVICS *et al.*, (1985) described olivines from ultramafic xenolithes from the Nógrád-Gömör region showing mg-values like above. These xenoliths were in equilibrium between 800—1000 °C under 1.0—1.5×10⁶ kPa pressure. The alkaline basaltic melt derived from 60—80 km depth. This value is in good correlation with the conditions of worldwide spread alkaline basalt source regions (e.g. WILKINSON, 1975; SKEWES and STERN, 1979; TAKAHASHI, 1980; PRESS *et al.*, 1986; etc.).

Olivines shows high FeO and MnO, but low CaO and very low MgO concentrations in cumulate-like olivine-clinopyroxenite and in wehrlitic xenoliths (see Table 2). The presented vol% data are similar to those of chrysolitic olivines of mafic plutonic rocks (DEER *et al.*, 1982). The two associated minerals in olivine-clinopyroxenite and wehrlite xenoliths (olivine and clinopyroxene) are in equilibrium with each other as seen in the microscope; but these are in disequilibrium with their environment, indicated by unclear grains, and concave outline. Despite displaying igneous texture, these xenoliths are foreign bodies in the alkaline basalts; the olivine compositions

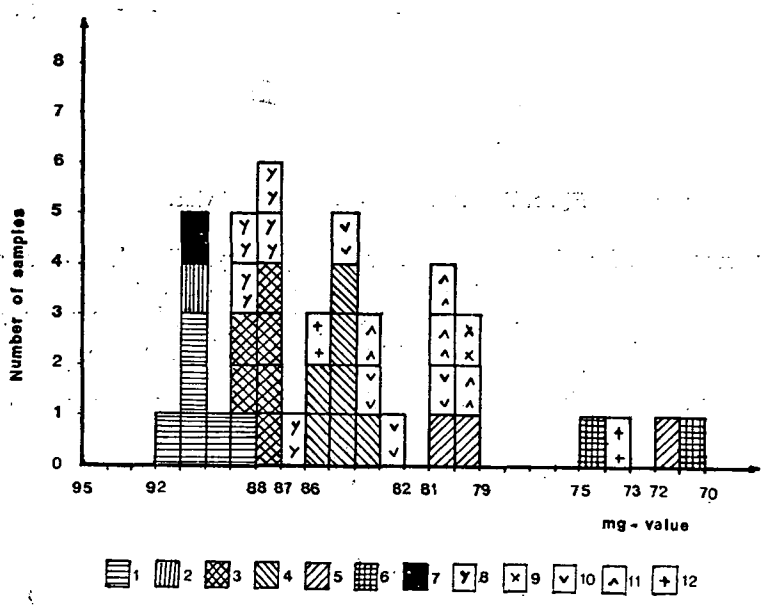

Fig. 6. Histograms of mg-values of olivines from the Nógrád-Gömör region

1 — lherzolite
2 — dunite
3 — phenocryst
4 — xenocryst
5 — wehrlite, olivine-clinopyroxenite
6 — groundmass
7 — dunite (JÁNOSI, 1984)
8 — phenocryst (FORGÁČ *et al.*, 1986)
9 — xenocryst (JÁNOSI, 1984)
10 — xenocryst (FORGÁČ *et al.*, 1986)
11 — xenocryst (HOVORKA and FEJDI, 1980)
12 — xenocryst (SZABÓ, 1984)

indicate crystallization from a Fe-rich, mafic melts in not too high temperature (low CaO-contents) (STORMER, 1973).

Composition of discrete olivine (resorbed outline, mostly deformed and larger than 2 mm grains, interpreted as xenocrysts after ÁRGYELÁN (1987), are well separeted in Table 2 and *Fig. 6* from the phenocrysts (euhedral, rarely skeletal, less than 2 mm grains). The xenocrysts contain more FeO and less MnO, but less MgO than the phenocrysts. Changes of mg-values in our samples display these characters very well *(Fig. 6)*. Considering the data of JÁNOSI (1984), HOVORKA and FEJDI (1980) and FORGÁČ *et al.*, (1986) some of the xenocrysts — described by us as megacrysts — shows strong chemical relationships with olivines of olivine-clinopyroxenite and wehrlite (Fig. 6). It means that part of the xenocrysts crystallized from the same Fe-rich melt, like the wehrlite and olivine-clinopyroxenite. This suggestion is supported by the CaO-FeO plot *(Fig. 7)*, where the points of xenocrysts (discrete inclusions called as megacrysts by HOVORKA and FEJDI, 1980; JÁNOSI, 1984; FORGÁČ *et al.*, 1986) are very near or within the field of tholeiites. Location of the field of mg-values of xenocrysts *(Fig. 6)* indicate that Fe/Mg ratio widely varied in the source melt. The phenocrysts are well separated from the xenocrysts (mg-values: 79—87) and from the mg-field of the olivine-clinopyroxenite and wehrlite, and display much less compositional variation *(Fig. 6)*.

This narrow mg-value field (87—88) indicates much more constrained crystallizations, than of the xenocrysts. We suggest 1200—1300 °C crystallization temperature (considering the low pressure experimental data of ROEDER and EMSLIE, 1970), which are similar to the alkaline lamprophyre data of KUBOVICS and SZABÓ (1987).

The olivine crystals of the groundmass from a well-separated group by their highest FeO, MnO and lowest MgO concentrations (Table 2, *Fig. 6*). These are located between the basanite and alkaline basalt fields of in the CaO-FeO plot *(Fig. 7)*. Their high CaO contents are characteristic for low-pressure olivines crystallized under near-surface conditions (SIMKIN and SMITH, 1970; STORMER, 1973).

Some xeno- and phenocrysts — of different size — bear barely perceptible zonation. Concentration changes of the most sensitive components: FeO, MgO, MnO and CaO were examined (Table 3), and two-way trends were shown *(Fig. 8)*.

Type I. (normal zonation) is represented by a xenocryst from Fülek and two phenocrysts — of different sizes — from Zabodakő. Composition of the rim zone of the xenocryst is located near the groundmass olivines, while phenocryst rims cross the field of xenocrysts and appear in the tholeiite field. The Fülek xenocryst shows steeply increasing CaO content, related to the fall of pressure. The unchanged CaO content of phenocrysts can be related to the decrease of crystallization temperature (STORMER, 1973).

The above characters unanimously prove that normal zonation can be formed by the change of different physical and/or chemical conditions, acting in different times. We noted that NAGY (1983) tried to determine the rate of cooling by the composition of the diffusion zone of phenocrysts, and to determine the equilibrium temperature by the olivine-spinel pair.

Type II. (reverse zonation) is represented by a xenocryst from Ajnácskő *(Fig. 8)*. A similar phenomenon was observed by NABELEK and LANGMUIR (1986) in a basalt sample from the Atlantic Ridge. *Fig. 7* shows that the zone of the xenocryst displays the same composition as the core of the phenocrysts. It clearly indicates that the zone was formed when the xenocryst was embedded in the melt of the host basalt. It means that xenocryst showing reverse zonation were crystallized from a Fe-rich tholeiitic melt, while the zones and the phenocrysts were formed due to the mixing of tholeiitic

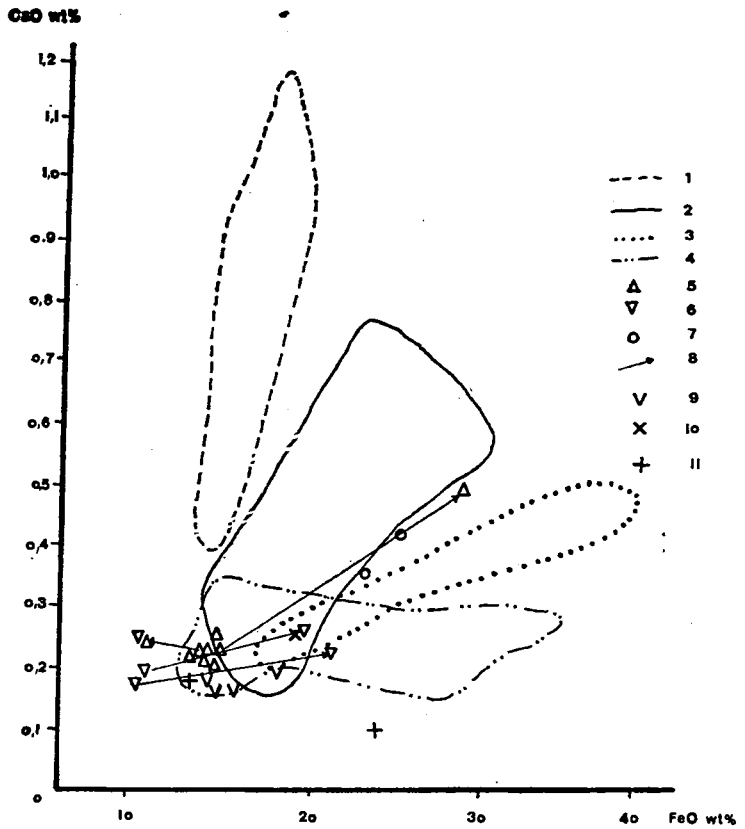

Fig. 7. CaO(wt%) versus FeO(wt%) in olivines from the Nógrád-Gömör region.

1 — nephelinite
2 — basanite
3 — alkali basalte
4 — tholeiite
5 — xenocryst
6 — phenocryst

} STORMER (1973)

7 — groundmass
8 — core — rim trend
9 — xenocryst (HOVORKA and FEJDI, 1980)
10 — xenocryst (JÁNOSI, 1984)
11 — xenocryst (SZABÓ, 1984)

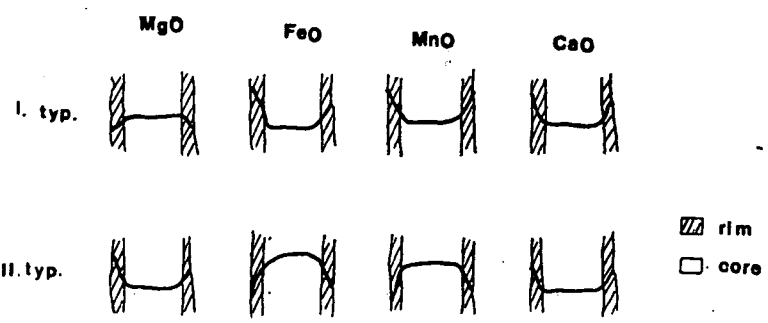

Fig. 8. Schematic profils across normally zoned olivines (type I) and reversely zoned olivines (type II) from the Nógrád-Gömör region.

and Mg-rich magmas. JÁNOSI (1984) noted a similar magma mixing by a preliminary examination of pyroxene nodules of alkaline basalts from the Nógrád—Gömör region, proved by DOBOSI (1987) later.

DUDA and SCHMINCKE (1985), WÖRNER and WRIGHT (1984) suggested magma mixing in the alkaline volcanic complex at Laacher See by the geochemistry of xeno- and phenocrysts of similar composition.

REE GEOCHEMISTRY

REE and other trace element contents of separates of different olivine types (determined by optical and microprobe analysis) were determined by neutron activation analysis (Table 4).

Olivines of ultramafic xenoliths were shown to contain only Sc, Sm, La, Yb and rarely Ce, Lu and U. Comparing the resultes with a small number of samples from Graz (KURAT *et al.*, 1980) and from the Balaton Highlands (BÉRCZI and BÉRCZI, 1986) we can say REE concentrations of these olivine types are extremly low and less differenciated only. Sc, Sm and rarely La were determined in xenocrysts in similar amounts as in olivines of ultramafic xenoliths. Phenocrysts and especially groundmass olivines are characterized by higher REE and trace element contents, except the two samples from Zabodakő (25, 26). The latter two ones are considered as phenocrysts (Table 1) or xenocrysts (Table 4). This contradiction shall be resolved by further investigations.

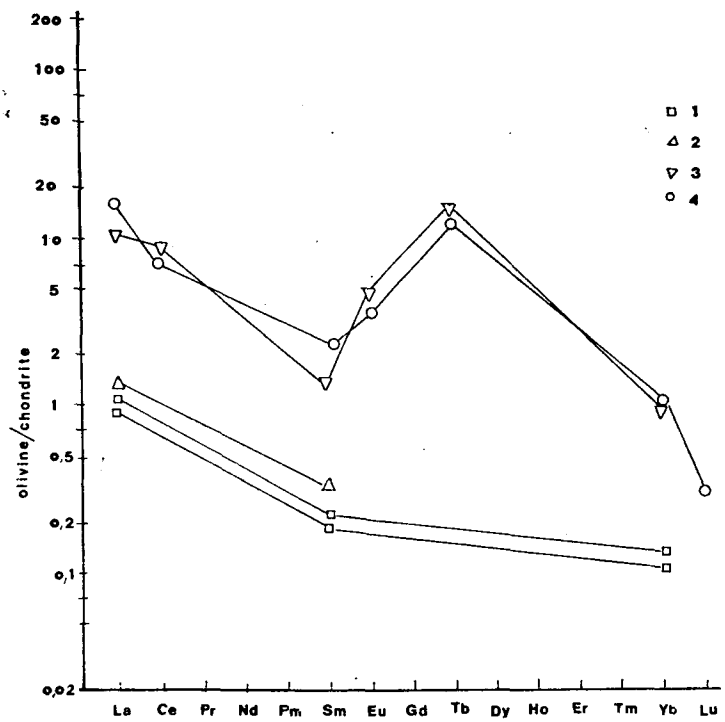

Fig. 9. REE pattern (normalised to chondrite, NAKAMURA, 1974) of olivines from the Nógrád-Gömör region. 1 — lherzolite; 2 — xenocryst; 3 — phenocryst ; 4 — groundmass

All olivine types were recognized at Nagykő near Bárna *(Fig. 1)*. The results clealy show the REE spectra of olivine crystals of different origin in the alkaline basalts of the Nógrád-Gömör region *(Fig. 9)*.

TABLE 3

Compositions of zoned olivines

	Xenocrysts				Phenocrysts			
	16		24		25		26	
	core	rim	core	rim	core	rim	core	rim
FeO_t	15.2	26.9—30.5	14.7	11.3	11.6	17.7—19.7	11.8	18.3—22.1
MnO	0.22	0.97	0.20	0.18	0.17	0.42	0.17	0.22
MgO	45.0	35.0	45.2	48.0	47.4	42.0	47.5	40.5
CaO	0.23	0.48	0.21	0.26	0.17	0.23	0.20	0.23

The numbers of samples are listed in Table 1.

Ratios of some lantanides show parallel changes in the xenocrysts, lherzolites, phenocrysts and groundmass olivines despite their different concentrations. In the latter group the Eu shows a minor enrichment. The enrichment of Tb is unclear to us in absence of reference materials. Relationships of phenocrysts and groundmass olivines are clear, but similarities among xenocrysts and lherzolite olivines are considered to be random, due to dissimilarities in texture an chemical composition.

CONCLUSIONS

Three genetic groups were recognized among the olivine phases of the Nógrád-Gömör Neogene-Quaternary alkaline basalts:

1. REE-poor olivines of lherzolitic, dunitic inclusions displaying deformed texture are considered upper mantle components, well known from alkaline basalt xenoliths all over the Earth.

2. Genetic relationships among olivines of olivine-clinopyroxenite and wehrlite nodules on the one side and xenocrysts on the other are suggested by similarities in main element composition. We think that xenoliths and xenocrysts have been crystallized in a Fe-rich, differenciated tholeiitic melt under lower crust — upper mantle condition, and got to the host alkaline basalt by magma mixing (possibly assimilation). This event was recorded by the large amount of texture deformation, anhedral resorbed outline, revers zonation yielded by incorporation by a huge mass of high temperature more mafic melt.

3. The phenocrysts — together with groundmass olivine — are in relationship with the host alkaline basalt, supported by main element composition, REE distribution and absence of deformed texture. This host magma, being a mixed melt, was less differenciated that the system producing the xenocrysts, clinopyroxenite and wehrlite inclusions. After mixing — with upper mantle mg-values — the phenocrysts, and after ascending near the surface the groundmass olivines were crystallized.

ACKNOWLEDGEMENT

We should like to thank M. BALLA (Training Reaktor of Budapest Technical University) for the INAA measurements.

Main element contents of olivines from the Nógrád-Gömör region, in wt %

TABLE 2

	1	2	3	4	5	6	34	35	36	37	23	14	24	16	16	17	18	26	25	30	28	29	28	32	33
SiO_2	40.4	40.3	40.4	40.5	40.2	40.4	40.3	38.0	38.6	38.8	39.7	39.5	39.7	39.6	39.6	39.5	39.7	40.2	40.0	40.2	40.4	40.2	40.3	37.4	37.5
Al_2O_3	nd	nd	nd	nd	nd	nd	nd	nd	nd	nd	0.04	0.04	0.03	0.04	0.03	0.03	0.03	0.03	0.05	na	na	na	na	0.03	0.03
FeO_t	10.8	10.5	9.30	8.90	9.50	8.90	9.16	25.6	15,4	18.4	14.0	13.6	14.7	15.2	15.2	15.0	15.0	11.8	11.6	11.7	11.8	11.3	11.3	23.1	25.9
MnO	0.16	0.16	0.12	na	0.13	0.12	0.12	0.30	0.29	0.29	0.19	0.18	0.20	0.22	0.22	0.21	0.20	0.20	0.17	na	0.18	0.18	0.18	0.61	0.70
MgO	48,6	48,9	50.7	50.1	49.6	50.0	49.1	35.7	41.6	42.3	45.8	46.0	45.2	44.6	45.0	45.4	45.2	47.5	47.4	47.7	47.5	48.0	48.1	37.9	35.5
CaO	0.10	0.16	0.07	0.20	0.06	0.06	0.12	0.04	0.06	0.04	0.23	0.21	0.21	0.21	0.23	0.22	0.20	0.20	0.19	na	0.25	0.26	0.26	0.33	0.41
Σ	100.06	100.02	99.79	99.50	99.49	99.48	98,80	99.64	95,95	99.83	99.94	99.53	100.04	99.97	100.28	100.36	100.33	99.90	99.39	99.60	99.43	99.94	100.14	99.37	100.04
Si	0.994	0.992	0.991	0.993	0.990	0.992	0.996	1.007	0.991	0.993	0.994	0.991	0.996	0.997	0.993	0.989	0.994	0.996	0.995	0.997	0.998	0.994	0.994	0.987	0.996
Al	—	—	—	—	—	—	—	—	—	—	0.001	0.001	0.001	0.001	0.001	0.001	0.001	0.001	0.002	—	—	—	—	0.001	0.001
Fe	0.223	0.216	0.191	0.178	0.196	0.183	0.189	0.568	0.417	0.394	0.293	0.285	0.308	0.332	0.319	0.314	0.316	0.245	0.241	0.243	0.244	0.234	0.233	0.510	0.575
Mn	0.003	0.003	0.003	—	0.003	0.003	0.003	0.007	0.006	0.006	0.004	0.004	0.004	0.005	0.005	0.004	0.004	0.004	0.004	—	0.004	0.004	0.004	0.014	0.016
Mg	1,783	1,793	1,824	1,831	1,820	1.830	1.808	1.410	1.592	1.613	1.708	1.721	1.689	1.673	1.682	1.695	1.687	1.754	1.758	1.763	1.749	1.768	1.768	1.491	1.405
Ca	0,003	0.004	0.002	0.005	0.002	0.002	0.003	0.001	0.002	0.001	0.006	0.006	0.006	0.006	0.006	0.006	0.005	0.005	0.005	—	0.007	0.007	0.007	0.009	0.012
Fo%	89.0	89.2	90.7	91.1	90.3	91.0	90.3	71.0	79.0	80.1	84.9	85.4	84.2	83.0	83.6	84.0	83.9	87.4	87.5	87.9	87.3	87.8	87.9	73.7	70.0
mg-value	88.9	89.2	90.5	91.1	90.3	90.9	90.5	71.3	79.2	80.4	80.5	85.8	84.6	83.9	84.1	84.4	84.2	87.7	87.9	87.9	87.8	88.3	88.4	74.5	71.0

nd = not detected; na = not analysed; FeO_t = total iron as FeO

No. 1—6, 34 from lherzolite and dunite xenoliths; No. 35—37 from wehrlite, olivine-clinopyroxenite xenoliths
No. 14—23 xenocrysts; 25—30 phenocrysts; 32—33 groundmass
The numbers of the samples are listed in Table 1

Trace element contents of olivines from the Nógrád-Gömör region, in ppm

TABLE 4

	1	2	3	4	5	6	7	8	9	10	11	12	13	14	15	16	17	18	19	20	21	22	26	25	27	28	30	31	32	33
Sc	2.55	3.73	3.35	5.93	4.80	4.94	2.06	1.94	4.08	1.92	4.58	3.61	1.77	3.83	3.72	3.37	3.71	3.37	3.43	2.65	2.40	3.49	3.74	3.66	3.80	4.64	4.39	4.57	5.18	4.95
Ta	—	—	—	—	—	—	—	—	—	—	—	—	—	—	—	—	—	—	—	—	—	—	—	—	0.49	2.44	0.89	0.73	0.98	0.79
Hf	—	—	—	—	—	—	—	—	—	—	—	—	—	—	—	—	—	—	—	—	—	—	—	—	0.75	3.52	1.38	1.22	4.29	1.32
Th	—	—	—	—	—	—	—	—	—	—	—	—	—	—	—	—	—	—	—	—	—	—	—	—	—	—	—	—	—	—
U			0.04	—	—	—	—	—	—	—	—	—	—	—	—	—	—	—	—	—	—	—	—	—	—	0.31	0.53	0.19	0.73	—
La	0.84	—	0.38	0.24	0.77	0.48	0.55	—	0.44	0.32	0.78	0.11	0.62	1.16	—	—	0.39	—	0.76	—	0.48	—	0.99	1.60	2.205	2.600	3.22	1.88	4.34	4.90
Ce	—	—	—	—	—	—	0.08	—	—	—	—	—	—	—	—	—	—	—	—	—	—	—	—	—	4.14	19.70	7.80	6.70	8.60	6.40
Nd	—	—	—	—	—	—	—	—	—	—	—	—	—	—	—	—	—	—	—	—	—	—	—	—	4.26	3.82	—	8.78	9.53	—
Sm	0.065	0.030	0.035	0.035	0.060	0.063	—	0.020	0.020	0.025	0.180	0.20	0.09	—	0.024	0.030	0.060	0.040	0.050	0.020	0.030	0.020	0.067	0.110	0.190	0.180	0.245	0.205	0.240	0.420
Eu	—	—	—	—	—	—	—	—	—	—	—	—	—	—	—	—	—	—	—	—	—	—	—	—	0.13	1.05	0.31	0.22	0.18	0.24
Tb	—	—	—	—	—	—	—	—	—	—	—	—	—	—	—	—	—	—	—	—	—	—	—	—	0.40	1.59	0.68	0.63	0.79	0.59
Yb	0.21	—	0.02	0.02	0.05	0.23	—	—	0.42	0.09	0.13	—	—	—	—	—	—	—	—	—	—	—	—	—	0.25	0.51	0.15	0.09	1.40	0.48
Lu	—	—	—	—	—	—	—	—	—	—	0.07	—	—	—	—	—	—	—	—	—	—	—	—	—	0.03	—	—	0.01	0.006	0.008

No. 1—13 from lherzolite xenoliths; No. 14—26 xenocryst; No. 27—31 phenocryst; No. 32—33 groundmass.
The numbers of samples are listed in Table 1.

REFERENCES

ÁRGYELÁN, G. (1987): A Nógrád-Gömöri bazaltok bázisos és ultrabázisos zárványainak kőzettani-geokémiai vizsgálata (Petrological and geochemical investigations of mafic and ultramafic xenoliths from basalts of Nógrád-Gömör, Hungary). M. Sc. thesis. Library of Dept. Petrol. Geochem. of Univ. Loránd Eötvös, Budapest. Manuscript (in Hungarian).

BALOGH, K., MICHALIKOVÁ, Á., VASS, D. (1981): Radiometric dating of basalts in Southern and Central Slovakia. Zap. Karp. Ser. Geol. **7**, 113—126.

BALOGH, K., JÁMBOR, Á., PARTÉNYI, Zs., RAVASZ-BARANYAI, L., SOLTI, G., NUSSZER, A. (1983): Petrography and K/Ar dating of tertiary and quarternary basaltic rocks in Hungary. Ann. Inst. Geol. Geof. **LXI**, 365—373.

BALOGH, K., ÁRVA-SÓS, E., PÉCSKAY, Z., RAVASZ-BARANYAI, L. (1986): K/Ar dating of Post-Sarmatian alkali basaltic rocks in Hungary. Acta Min. Petr. Szeged. **XXVIII**, 75—93.

BÉRCZI, Sz., BÉRCZI, J. (1986): Rare earth element content in the Szentbékkála series of peridotite inclusions. Acta Min. Petr. Szeged. **XXVIII**, 61—74.

BOLAND, J. N., BUISKOOL-TOXOPEUS, J. M. A. (1977): Dislocation deformation mechanism in peridotite xenoliths in kimberlites. Contrib. Miner. Petrol. **60**, 17—30.

BOLAND, J. N., MCLAREN, A. C., HOBB, B. E. (1971): Dislocation associated with optical features in naturally deformed olivine. Contrib. Miner. Petrol. **30**, 53—63.

BUISKOOL-TOXOPEUS, J. M. A. (1977): Deformation and recrystallization of olivine during mono- and poliphase deformation. N. Jb. Miner. Abh. **129**, 233—268.

CARTER, N. L., AVÉ LALLEMANT, H. G. (1970): High temperature flow of dunite and peridotite. Bull. Geol. Soc. Am. **81**, 2181—2202.

DEER, W. A., HOWIE, R. A., ZUSSMANN, J. (1982): Rockforming minerals, orthosilicates, Longmans, London.

DIENES, I. (1968): Klinopiroxén megakristályok a medvesi bazaltból (Clinopyroxene megacrystals from the basalt of Medves Hill) Ann. Rep. of. Hung. Geol. Survey from **1968**, 125—130. (in Hungarian with German abstract.)

DIETRICH, H., POULTIDIS, H. (1985): Petrology of ultramafic xenolith in alkali basalts from Klöch and Stadner Kogel (Styria, Austria) N. Jahr. Miner. Abh. **151**, 131—140.

DOBOSI, G. (1987): The zoned clinopyroxenes of the post orogen young alkali basalts of Hungary, and their petrogenetic implication. 5th MEGS-Abstracts, **27**. ("Orogeny, magmatism and metallogeny in Europe", Dubrovnik).

DUDA, A. H., SCHMINCKE, U. (1985): Polybaric differentiation of alkali basaltic magmas evidence from green core clinopyroxenes (Eifel, FRG). Contrib. Miner. Petrol. **91**, 340—353.

EMBEY-ISZTIN, A. (1976): Felsőköpeny eredetű lherzolitzárványok a magyarországi alkáli olivinbazaltos, bazanitos vulkanizmus kőzeteiben (Lherzolite modules of upper mantle origin in the olivines basaltic, basanitic rocks of Hungary) Földt. Közl. **106**, 42—51. (in Hungarian with English abstract).

EMBEY-ISZTIN, A. (1977): Az alkáli bazaltok peridotitzárványainak ásvány-kőzettana, eredete és összefüggése hazánk és a Massif Central nagyszerkezetével. (Mineralogy, petrology and origin of the peridotite xenoliths from alkali basalt, and the structures of Massif Central and Hungary). Ph. D. thesis. Library of Hung. Ac. Sci. Budapest. Manuscript (in Hungarian).

EMBEY-ISZTIN, A. (1984): Texture types and their relative frequencies in ultramafic and mafic xenoliths from Hungarian alkali basaltic rocks. Ann. Hist. Nat. Mus. Natn. Hung. **76**, 27—42.

FORGÁČ, J., HATÁR, J., KRIŠTIN ,J., MEDVEĎ, J. (1986): Olivines Western Carpathians basalts. Geol. Carp. **37**, 145—165.

GREEN, H. W., RADCLIFFE, S. W. (1972): Dislocation mechanisms in olivine and flow in upper mantle. Earth Planet. Sci. Lett. **15**, 239—247.

HARTE, B. (1977): Rock nomenclature with particular relation to deformation and recrystallization textures in olivine-bearing xenoliths. J. Geol. **85**, 279—288.

HOVORKA, D. (1978): Uzavrevy spinellovych peridotitov v basanite pri Maskovej-rezidium vrchneho plasta (Upper mantle rezidium). Min. Slov. **10**, 97—112. (in Slovak with English abstract).

HOVORKA, D., FEJDI, P. (1980): Spinel peridotite xenoliths in West Carpathian late tectonic alkali basalts and their tectonic significance. Bull. Volc. **43**, 95—105.

JÁNOSI, M. (1984): A Nógrád-Gömöri bázisos vulkanitok kőzet- és megakristály-zárványainak kőzettani-geokémiai vizsgálata (Petrological and geochemical investigations of megacrysts and xenoliths from mafic volcanic rocks of Nógrád-Gömör, Hungary). M. Sc. thesis. Library of Univ. Loránd Eötvös, Budapest. Manuscript (in Hungarian).

KUBOVICS, I., G. SÓLYMOS, K., SZABÓ, Cs. (1985): Petrology and geochemistry of ultramafic xenoliths in mafic rock of Hungary and Burgenland (Austria). Geol. Carp. **36**, 433—450.

KUBOVICS, I., SZABÓ, Cs. (1987): Az AD-2 fúrással harántolt alkáli bázisos, ultrabázisos telérkőzetek ásvány-kőzettani és geokémiai vizsgálata (Mineralogical, petrological and geochemical investigation on alkali mafic and ultramafic dikes from AD-2 borehole). Annales of Hung. Geol. Survey (in press)

KURAT, G. (1971): Granat-Spinell-Websterit und Lhersolit aus dem Basalttuff von Kapfenstein, Steiermark. Tscherm. Miner. Petrol. Mitt. **16**, 192—214.

KURAT, G., PALME, H., SPETTEL, B., BADDENHAUSEN, H., HOFMEISTER, PALME, CH., WÄNKE, H. (1980): Geochemistry of xenoliths from Kapfenstein, Austria: evidence for a variety of upper mantle processes. Geochim. Cosmochim. Acta. **44**, 45—60.

MERCIER, J. C. C. (1985): Olivine and pyroxenes (in Wenk, H. A. (ed): Preferred orientation in deformed metals and rocks an introduction to modern texture analysis). Academic Press. Inc. Orlando, San Diego, New York, London, Toronto, Montreal, Sydney, Tokyo.

MERCIER, J. C. C., CARTER, N. L. (1975): Pyroxene geotherms. J. Geophys. Res. **80**, 3349—3362.

MERCIER, J. C. C., NICOLAS, A. (1975): Textures and fabries of upper mantle peridotites as illustrated by basalt xenoliths. J. Petrol. **15**, 454—487.

NABELEK, P. I., LANGMUIR, C. H. (1986): The significance of unusual zoning in olivines from FAMOUS area basalt 527-1-1. Contrib. Miner. Petrol. **93**, 1—8.

NAGY, G. (1983): Cooling history of young Hungarian basalts based on zoning of olivine phenocrysts. Acta Geol. Hung. **26**, 321—339.

NAKAMURA, N. (1974): Determination of REE, Ba, Fe, Mg, Na and K in carbonaceous and ordinary chondrites. Geochim. Cosmochim. Acta. **38**, 757—775.

NICOLAS, A. (1984): Principes de Tectonique, Masson Paris, New York, Barcelona, Milan, Mexico. Sao Paulo.

PIKE, J. E. N., SCHWARZMAN, E. C. (1977): Classification of textures in ultramafic xenoliths. J. Geol. **85**, 9—61.

PRESS, G., WITT, G., SECK, H. A., EONOV, D., KOVALENKO, V. I. (1986): Spinel peridotite xenoliths from the Tariat Depression Mongolia; I. Major element chemistry and mineralogy of a primitive mantle peridotite suite. Geochim. Cosmochim. Acta. **50**, 2587—2599.

RICHTER, W. (1971): Ariegite, Spinell-Peridotite und Phlogopit-Klinopyroxenite aus dem Tuff von Tobaj im Südlichen Burgenland. Tscherm. Miner. Petrol. Mitt. **16**, 227—251.

ROEDER, D. L., EMSLIE, R. J. (1970): Olivine-liquid equilibrium. Contrib. Miner. Petrol. **29**, 275—289.

SCHARBERT, H. G., PAULTIONS, CH., HÖLLER, H., KOLMER, H., WIRSCHING, U. (1981): Vulkanite im Raume Burgenland-Oststeiermark. Forschr. Miner. **59**, 69—88.

SIMKIN, T., SMITH, J. V. (1979): Minor element distribution in olivine. J. Geol. **78**, 304—325.

SKEWES, M. A., STERN, C. (1979): Petrology and geochemistry of alkalibasalts and ultramafic inclusions from the Palei-Aike volcanic field in Southern Chile and the origin of the Patagonian plateau lavas. J. Volc. Geoth. Res. **6**, 3—25.

STORMER, J. C. (1973): Calcium zoning in olivine and its relationships to silica activity and pressure. Geochim. Cosmochim, Acta. **37**, 1815—1821.

STRECKEISEN, A. (1974): Classification and nomenclature of plutonic rocks. Geol. Rundschau. **63**, 773—786.

SZABÓ, Cs. (1984): Az Alcsutdoboz-2 (AD-2) fúrással harántolt alkáli bázit zárványainak ásvány-kőzettani és geokémiai vizsgálata, eredete, genetikai jelentősége. (Mineralogy, petrology and geochemistry of ultramafic modules in lamprophyre dikes of Alcsutdoboz-2 borehole [Bakonyicum, Hungary]: their origin and genetic implication). M. Sc. thesis. Library of Dept. Petrol. Geochem. of Univ. Loránd Eötvös, Budapest. Maniscript (in Hungarian).

TAKAHASHI, F. (1980): Thermal history of lherzolite xenoliths I. Petrology of lherzolite xenoliths from Ichinomegata crater, Oga peninsula, Northeast Japan. Geochim. Cosmochim. Acta. **44**. 1643—1658.

WILKINSON, J. F. G. (1975): Ultramafic inclusions and high pressure megacrysts from a nephelinite sill, Nanderwasr Mountains, North-Eastern New South Wales, and their bearing on the origin of certain inclusions in alkaline volcanic rocks. Contrib. Miner. Petrol. **51**. 235—262.

WÖRNER, G., WRIGHT, T. L. (1984): Evidence for magma mixing within the Laacher See magma chamber. (East Eifel, Germany). J. Volc. Geoth. Res. **22**, 301—327.

Manuscript received 24 July, 1988.

Acta Mineralogica-Petrographica, Szeged, XXIX, 47—56, 1987—1988

GEOCHEMISTRY OF BIOTITE AND ITS SIGNIFICANCE AS A GUIDE TO THE ORIGIN OF THE GRANITOID ROCKS OF EL-IMRA AREA, EASTERN DESERT, EGYPT

By

A. K. A. SALEM, M. A. HEIKAL, M. L. KABESH, M. A. SALEM

Earth Sciences Laboratory, National Research Centre

ABSTRACT

Biotites from the granitoid rocks of El-Imra, Eastern Desert, Egypt have been examined. The chemical data of 8 new analyzed biotites are presented. The behaviour of major and trace elements in the examined biotites are discussed according to different variation diagrams. The chemical composition of biotites has proved a reasonable guide to the magmatic origin of the host granitic rocks.

INTRODUCTION

The present study deals with the geochemistry of biotites separated from some granitoid rocks of El-Imra area, Eastern Desert, Egypt *(Fig. 1)*. The granitic stock of El-Imra consists mainly of pink, pinkish — white and grey granites. They comprise porphyritic and equigranular, non-porphyritic types. Biotite is generally the sole mafic mineral in these granites. The biotite is mostly pleochroic from straw – yellow to chestnut brown. It occurs largely as irregularly – sphaped flakes reaching 0.18 mm in length. In some varieties, biotite show subparallelism and is associated with clusters of minute epidote granules. Occasionaly it froms stout flakes with torn ends. Rarely muscovite also is present in the groundmass as marginal gradation around bioitite. The main inclusions present in biotite are zircon, apatite and iron ores.

The work reported in this paper forms part of a continuing research program carried out in the Earth Sciences Laboratory National Research Centre, by Kabesh and co- workers (KABESH and SALEM, 1981, KABESH *et al.*, 1982).

ANALITICAL METHODS

The samples of the host granitic rocks were crushed to pass through a 100-mesh and 120 mesh sieve (U. S.). The crushed fraction was individually separated with bromoform, followed by removal of magnetite by hand magnet. Biotite separated from heavy fraction was purified by using the FRANTZ isodynamic separator. Finally, the pure sample of biotite was pulverized in agte mortar under acetone untill all pass through 200-mesh sieve (U. S.). The chemical analysis was carried out by using volumetric, gravimetric and colourimetric methods of silicate analysis according to BENNETT and READ (1971) and VOGEL (1968). Trace elements were determined by inductively coupled plasma emission spectrometry at the Nuclear Materials Corporation, Cairo using the technique described by WALSH (1980) and McLaren *et al.*, (1981).

Dokki-Cairo, Egypt.

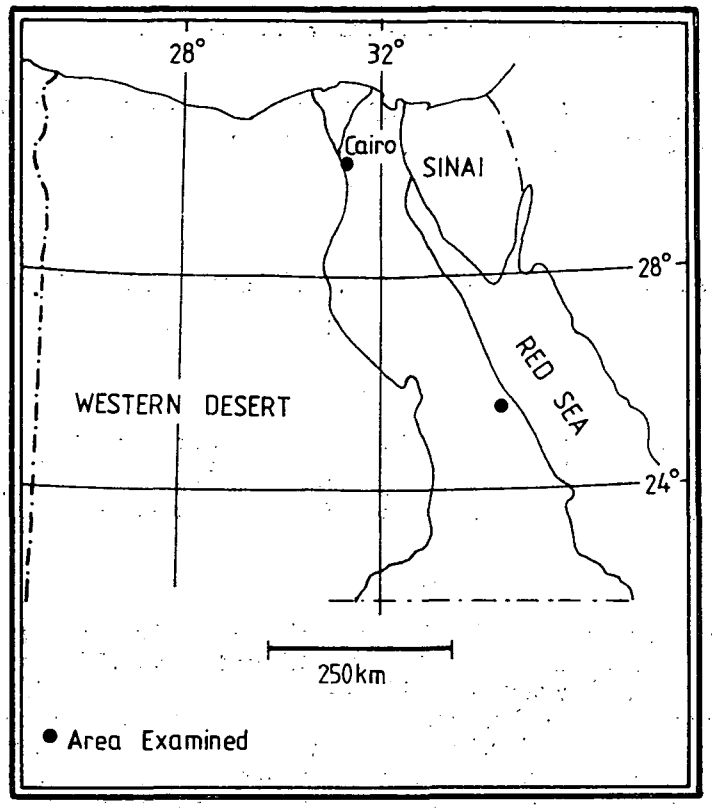

Fig. 1. Location map of the investigated area.

CHEMISTRY OS BIOTITES

Eight new chemical analyses of biotites from El-Imra granitoid rocks are used to elucidate the petrogenesis of these rocks. The major element compositions of the examined biotites are given in Table 1, in addition, one analysis of biotite from Kadabora granitic mass (KABESH *et al.*, 1977) and one analysis from the granodiorite of Sierra Nevada Batholith (DODGE *et. al.*, 1969) are given for comparison.

The chemical data are plotted on GOKHALE variation diagram *Fig. 2,* showing the ternary diagram MgO, FeO and Al_2O_3. It is observed that all the examined biotites fall wihin the zone drown by GOKHALE (1968) for biotites of magmatic nature.

Structural formulae of biotite

The structural formulae of the examined biotites are given in Table 2. The calculation is based on 24 (O, OH) to the general mica formulae $X_2 M_6 Z_8 O_{20}$ (OH, F, Cl) and the results are listed in the same table.

Fig. 3 shows the ternary diagram Mg ($Fe^{3+} + Ti/ + Al^{VI}$) and Fe^{2+} (FÖSTER, 1960). It is clear from the diagram that all the analysed biotites fall within the field Mg-iron rich varieties.

TABLE 1

Chemical analyses of biotices from granitoid rocks of El Imra

Oxide	1	2	3	4	5	6	7	8	average	A	B	C
SiO_2	35.15	35.67	35.53	30.06	35.53	35.00	35.64	36.11	35.59	35.40	35.99	36.90
Al_2O_3	4.27	14.54	15.15	15.20	15.30	15.98	15.30	14.45	14.95	16.66	14.94	15.40
Fe_2O_3	36.36	6.43	6.47	5.06	7.01	5.78	7.23	5.56	6.24	5.17	6.11	3.90
Fe O	19.47	21.66	18.57	19.29	17.67	18.48	19.23	19.23	19.20	21.61	16.91	16.60
MnO	0.25	0.12	0.21	0.18	0.18	0.19	0.29	0.25	0.21	0.45	0.14	0.52
MgO	9.73	8.04	8.58	9.89	7.81	9.36	7.13	9.01	8.69	6.23	12.90	10.90
CaO	1.42	2.03	2.23	1.52	2.77	2.00	1.52	1.77	1.91	1.40	0.14	0.22
Na_2O	1.53	1.09	1.66	1.52	1.71	1.19	1.09	1.71	1.44	0.34	0.12	0.04
K_2O	7.30	6.22	7.38	7.60	7.08	6.94	7.20	6.60	7.04	6.34	7.81	9.10
Ti O_2	1.89	1.24	1.01	1.05	1.83	2.10	1.68	2.09	1.61	2.18	2.73	2.90
H_2O^-	0.15	0.20	0.30	0.21	0.16	0.46	0.35	0.26	0.26	0.32	—	0.20
H_2O^+	2.52	2.59	2.91	2.42	2.42	2.95	3.11	3.30	2.83	3.10	2.50	31.0
total	99.83	100	100	100	100	99.99	99.96	99.87	99.97	99.29	99.43	99.18

A — Biotite from Kadabora (KABESH and SALEM, 1981)
B — Biotite from Ras Barud, Eastern Desert Egypt (KABESH *et al.*, 1977)
C — Biotite from granodiorite from Sierra Nevada Batholith, California (DODGE *et al.*, 1969).

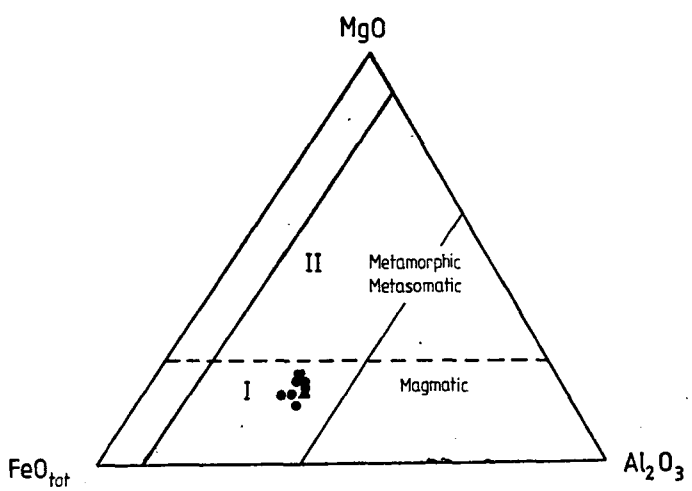

Fig. 2. Plot of Al_2O_3-MgO-FeO_{tot} in the investigated biotites. ● Analised samples, ▲ The average of biotites (after GOKHALE, 1968).

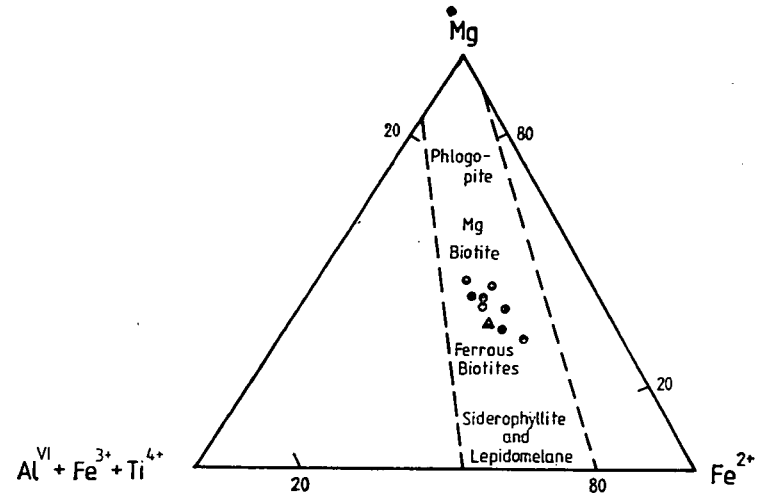

Fig. 3. Relation between octahedral cations of the studied biotite (after FOSTER, 1960). Symbols are same as *Fig. 2.*

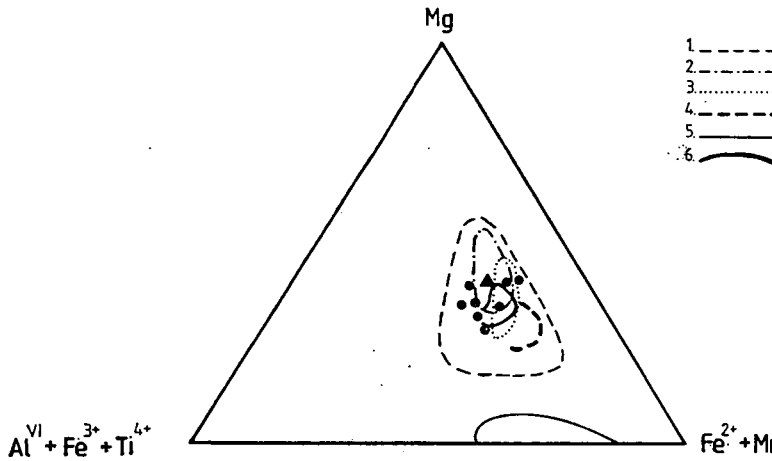

Fig. 4. Comparison of the composition of biotites in the granites of the studied masses with composition of biotites from igneous and metamorphic rocks. (1) granite, (2) monzonite, quartz-monzonite and granodiorite, (3) quartz-diorite, (4) nepheline syenite, (5) gneiss and schist, (6) pegmatite. Symbols are same as *Fig. 2.*

The value of the Y– group cations; Mg, $(Al^{IV} + Fe^{3+} + Ti^{4+})$ and $(Fe^{2+} + Mn^{2+})$ are plotted on FOSTER's diagram *Fig. 4.* It is evident from the figure that the analyzed samples of biotite fall within the fields granite and granodiorite.

Fig. 5 shows the relation between $(Fe^{2+}/Mg) \times 100$ and $Al^{IV} \times 100$ of the examined biotites. It is evident from the diagram that all the analyzed biotites fall in the field of the magmatic differentiation (SHIBATA *et al.*, 1966).

Fig. 6 shows that the division between phlogopite and biotite compositional field is arbitarily chosen to be where Mg: Fe=2:1 (DEER *et al.*, 1966). The examined biotites are plotted on this figure which shows that all the analyzed samples fall within.

TABLE 2

Structural Formulate of biotites

		1		2		3		4		5		6		7		8		average	
Si	Z	5.52	8	5.63	8	5.56	8	5.57	8	5.53	8	5.56	8	5.55	8	5.63	8	5.57	8.00
AI^{IV}	Z	2.48		2.37		2.44		2.43		2.47		2.44		2.45		2.37		2.43	
Al^{VI}	Y	0.16	6.02	0.33	6.08	0.35	5.66	0.33	6.34	0.33	5.49	0.43	5.94	0.35	5.59	0.28	5.81	0.32	6.00
Fe^{3+}	Y	0.75		0.76		0.76		0.59		0.82		0.59		0.84		0.65		0.73	
Ti	Y	0.22		0.07		0.12		0.60		0.21		0.21		0.20		0.24		0.38	
Mg	Y	2.30		1.90		1.99		2.29		1.82		2.23		1.67		2.11		2.04	
Fe^{2+}	Y	2.55		3.00		2.42		2.48		2.29		2.45		2.49		2.50		2.50	
Mn	Y	0.03		0.02		0.02		0.05		0.02		0.03		0.04		0.03		0.03	
Ca	X	0.24	2.16	0.34	1.92	0.37	1.90	0.25	2.21	0.46	2.39	0.36	2.10	0.25	1.95	0.29	2.11	0.32	1.95
Na	X	0.46		0.33		0.05		0.46		0.52		0.34		0.27		0.51		0.22	
K	X	1.46		1.25		1.48		1.50		1.41		1.40		1.43		1.31		1.41	
OH		2.72		2.72		3.04		3.06		3.06		2.22		3.42		2.34		2.86	
		58.92		66.43		61.51		57.28		63.08		57.69		66.60		59.99		61.29	

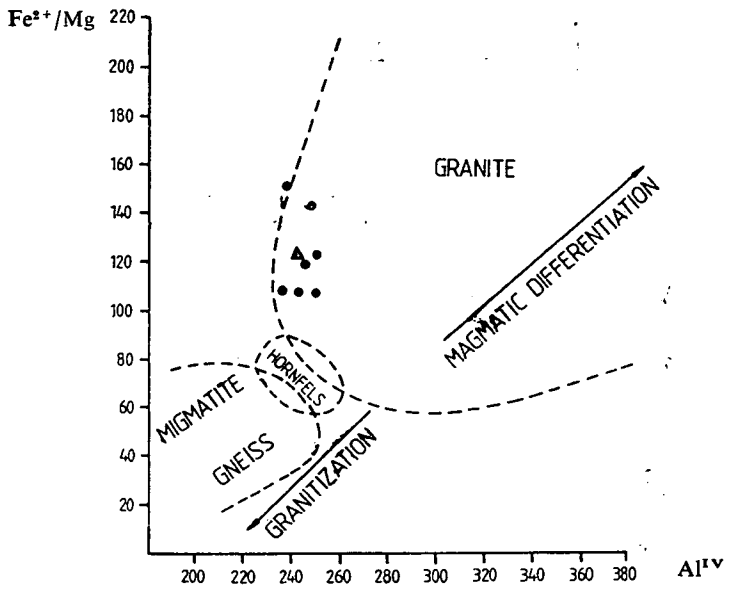

Fig. 5. The Fe^{2+}/Mg-Al^{IV} relations in biotite-formulas of granitic rocks of magmatic origin and metamorphic origin (after SHIBATA *et al.*, 1966). Symbols are same as *Fig. 2.*

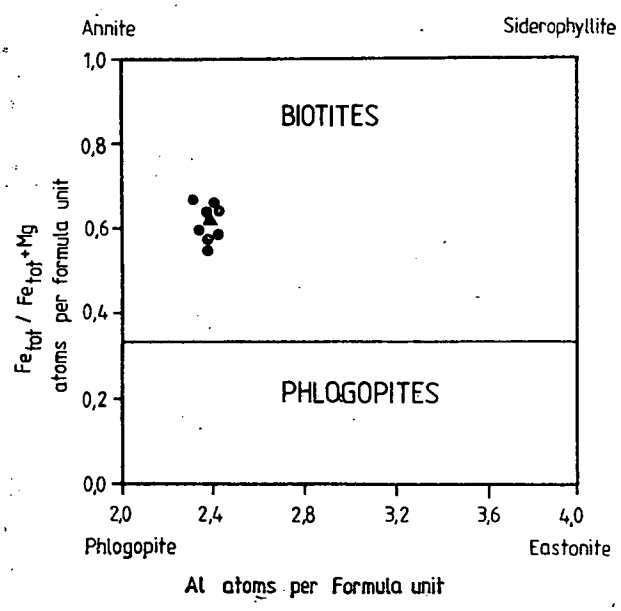

Fig. 6. Composition of biotite in terms of $Fe_{tot}/(Fe_{tot}+Mg)$-Al. The division between phlogopite and biotite fields is arbitarily chosen to be where $Mg:Fe_{tot}=2:1$ (DEER et al., 1966). Symbols are same as *Fig. 2.*

TABLE 3

Minor elements in biotites from granitoid rocks of El Imra with some other localities for comparison

	1	2	3	4	5	6	7	8	A	B	C
Ga	20	27	31	19	33	133	29	121	95	90	44
V	211	253	227	220	333	103	212	109	90	100	180
Cr	44	53	72	47	55	127	60	133	130	80	10
Nb	27	33	37	44	28	19	30	17	—	—	20
Co	18	17	18	22	19	33	27	40	60	40	34
Cu	11	8	13	7	6	30	8	28	*	25	50
Zn	0.2	0.3	0.2	0.2	0.5	1.5	0.5	1.5	*	*	—
Sc	7	5.5	3.5	5.5	4.5	33	4.5	4.1	*	*	44
Sr	3	7	5	7	8	17	4	22	6	6	20
Ba	2440	2360	2010	2518	2500	1122	2019	1215	450	340	*
Zr	62	57	70	50	73	40	60	33	*	57	60
Ni	13	22	19	30	25	62	30	72	95	25	10
Rb	930	1003	988	818	1111	630	1117	701	240	*	*
Li	150	165	140	111	159	277	172	301	310	*	*
Y	2	3	2	3	2	7	2	8	*	*	*

* not detected

A — Biotite from Kadabora (KABESH and SALEM, 1981)
B — Biotite from Ras Barud, Eastern Desert Egypt (KABESH *et al.*, 1977)
C — Biotite from granodiorite from Sierra Nevada Batholith, California (DODGE *et al.*, 1969).

TABLE 4

Elemental ratios of the examined of biotites

	1	2	3	4	5	6	7	8
$Cox10^3/Fe^2$	0.12	0.10	0.12	0.14	0.14	0.23	0.18	0.27
$Nix10^3/Fe^2$	0.09	0.13	0.13	0.20	0.18	0.43	0.20	0.47
$Nix10^3/Mg$	0.22	0.46	0.37	0.51	0.53	1.10	0.70	1.39
$Crx10^2/Fe$	0.10	0.12	0.16	0.13	0.11	0.31	0.34	0.34
$Vx10^2/Fe$	0.47	0.56	0.50	0.62	0.68	0.25	0.42	0.28
K/Rb%	51.5	65.2	62.0	77.0	53.0	91.4	53.5	68.2
Ni/Co	0.72	1.24	1.01	1.36	1.32	1.88	1.11	1.75

TRACE ELEMENTS

Trace elements data of the analyzed biotites are listed in Table 3. Elemental ratios recalculated from the trace elements of the examined biotites are given in the same table.

It is clear from Table 3 that the elements; Sc, Zn, Cu, Cr, Nb, Co, Cu, Sc, Sr, Zr, Ni, Rb, Li, and Y are concentrated in the biotites of the examined area. It is believed that the trace elements: Sc, Zn, Cu, Co, Ni, Nb, Cr, V. and Ga substitute major elements in octahedral sites, although some Ga may substitute for Al in tetrahedral coordination. Li is strongly concentrated in biotites. Li and Sc follow Mg according to various authors (DE ALBUQUERQUE, 1973). From the geochemical point of view barium and rubidium dan be expected from their affinity to potassium to occur in high amount in the biotites.

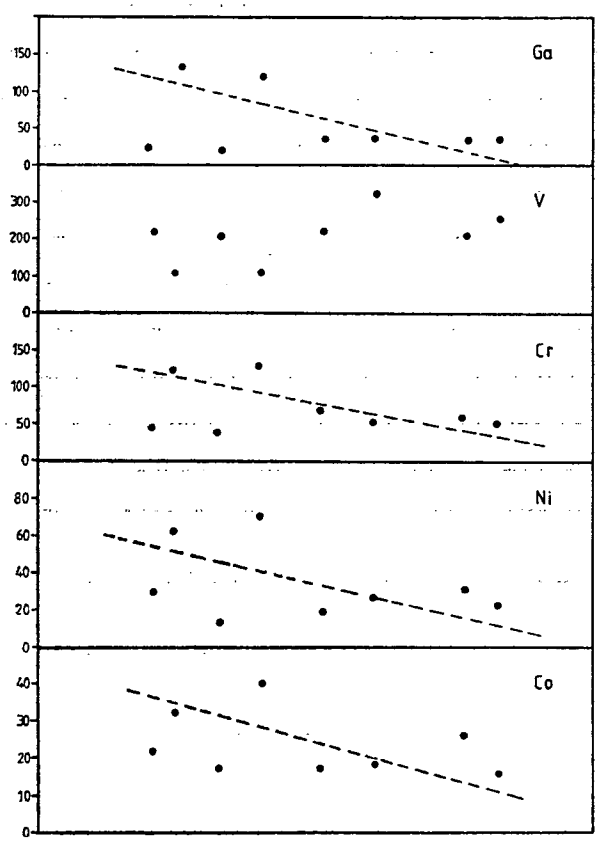

Fig. 7. Variation diagram of trace elements of the biotites.

Trace elements and elemental ratios are plotted on the following graphical representation:

The values of the function $Fe_{tot}/(Fe_{tot}+Mg)$ (Table 3) are plotted against V. Co, Ni, Ca *(Fig. 7)* and Cr. Ni, Co and Ga decrease with the increase of the value $Fe_{tot}/(Fe_{tot}+Mg)$. Vanadium shows no definite trend.

The values of $Fe_{tot}/(Fe_{tot}+Mg)$ are also plotted versus some elemental ratios Fig. 8. It is clear from the figure that $Ni\times10^3/Fe^{2+}$, $Ni\times10^3/Mg$, Co/Ni, $Cr\times10^2/Fe^{3+}$ and $V\times10^2/Fe^{3+}$ decrease with the increase of the value of the function, $Fe_{tot}/(Fe_{tot}+Mg)$.

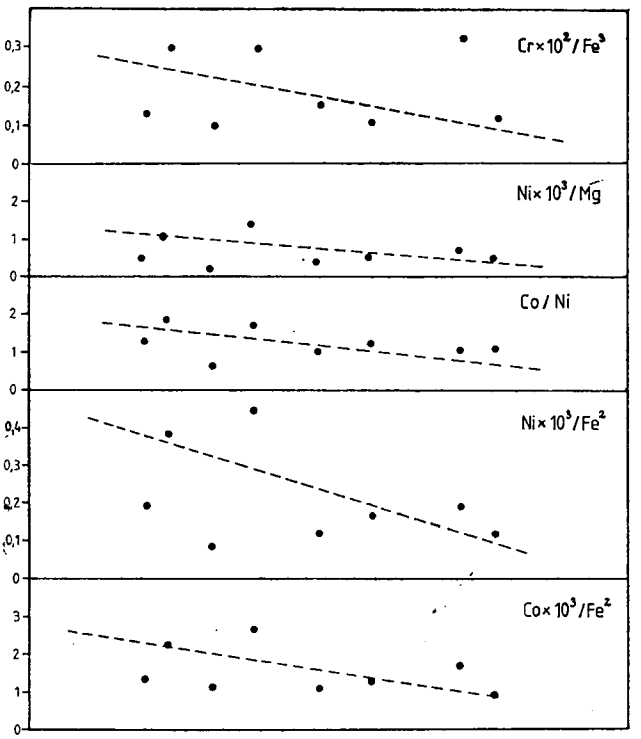

Fig. 8. Variation diagram of some trace elemental ratios.

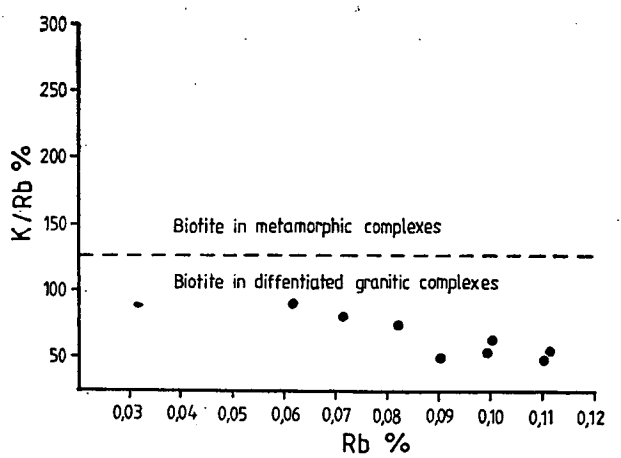

Fig. 9. Plot of K/Rb versus Rb% for the studied biotites (after STAVROV, 1971).

It is clear that the behaviour of the trace elements of the investigated biotites agrees fairly well with the expected behaviour of trace elements of biotites from the granitic rocks, North Portugal (DE ALBUQUERQUE, 1973).

Fig. 9 shows the relation between Rb% against the value of K/Rb of biotite according to STAVROV (1971). It is observed from the figure that all the biotites fall in the field of magmatic differentiation.

SUMMARY

Biotites from the granitic rocks of El-Imra mass have been investigated by geochemical methods. The behaviour of both major and trace elements are discussed according to several variation diagrams, in which the values of the function $Fe_{tot}/(Fe_{tot}+Mg)$ increases with the decrease of the values of the elements; Co, Ni, Cr, Ga as well as with elemental ratios.

It is concluded that the biotites of El-Imra confirm the magmatic origin of the host granitic rocks.

REFERENCES

BENNET, H. and REED, R. A. (1971): A Handbook, Chemical Methods of Silicate Analysis. Academic Press, London and New York.

DE ALBUQUERQUE, C. A. R. (1973): Geochemistry of biotites from granitic rocks, Northern Portugal. Geochemica et Cosmochimica Acta. **37**, 1779—1802.

DEER, W. A., HOWIE, R. A. and ZUSSAMANN, J. (1966): An Introduction to the Rock-forming Minerals. Longmans, London.

DODGE, F. C. W., SMITH, V. C. and MAYS, R. E. (1969): Biotites from granitic rocks of the Central Sierra Nevada Batholith, California. Journal of Petrology. **10**, Part 2, 250—71.

FOSTER, M. D. (1960): Interpretation of the composition of trioctahedral micas, U. S. Geol. Surv. Prof. Paper Washington. **354—B**, S., 11—49.

GOKHALE, N. W. (1968): Chemical composition of bioties as a guide to ascertain the origin of granites. Bull. Comm. Geol. Finlande. **40**, 107—111.

KABESH, M. L., HILMY, M. E., REFAAT, A. M., ABDALLAH, Z. M. (1977): Geochemistry of biotite from Ras Barud granitic rocks Eastern Desert N. Jb. Miner. Abh. **12**, №. 3, 201—210.

KABESH, M. L., SALEM, A. K. A. (1981): Geochemistry of biotite from Kadabora granitic batholith, Eastern Desert, Egypt. Egypt-J. Geol. **25**, №. 1—2, 37—47.

KABESH, M. L., SALEM, A. K. A. and EL-NASHAR, E. R. (1982): Remarks on the petrogenesis of Samadai granitic complex, Eastern Desert, Egypt. Z., Geol. Wiss. Berlin. **10 H. 11**, S. 1439—1447.

MCLAREN, J. W., BERMAN, S. S., BOYKO, V. J. and RUSSEL, D. S. (1981): Simultaneous determination of major, minor and trace elements in marine sediments by inductively coupled plasma atomic emission spectrometry, Anal. Chem. **53**, 1802—1806.

STAVROV, O. D. (1971): Ore content in granite and geochemistry of rubidium — Geochemistry International. **8**, 5, 739—754.

SHIBATA, H. OBA, N. and SHIMODA, N. (1966): Bearing of aluminium in mafic minerals in plutonic and metamorphic rocks. Sc. Rep. Tokyo Univ. Education Sec. **9**, №. **86**, 89—123.

VOGEL, A. I. (1968): A Text-book of Quantitative Inorganic Analysis 3rd ed. Longmans London.

WALSH, J. N. (1980): The simultaneous determination of the major, minor and trace constituents of silicate rocks using inductively coupled plasma spectrometry. Spectrochimica Acta **358**, 107—111.

Maniscript received, 25 February, 1988

Acta Mineralogica-Petrographica, Szeged, XXIX, 57—68, 1987—1988

GENETICAL PECULIARITIES OF THE MERCURY INDICATIONS NEAR SÁROSPATAK (TOKAJ MTS., NE-HUNGARY) ON THE BASIS OF FLUID INCLUSION STUDIES

F. MOLNÁR

Department of Mineralogy, Loránd Eötvös University

ABSTRACT

The mercury indications are NNW from Sárospatak, in area bounded by Királyhegy, Cinegés and Botkő. The cinnabar occurrences are situated in the metasomatically altered Badenian rhyolite tuff. The primary and pseudosecondary fluid inclusions of barites from Királyhegy and secondary gas-liquid inclusions of magmatic quartz grains from Botkő are studied. On the basis of fluid inclusion studies the barite crystals grew in a boiled paleohydrothermal system on temperatures 187 ± 13.1 °C and on pressures 6—20 bar. The solution composition was NaCl-$CaCl_2$-H_2O (-CO_2)-type with 2.31 ± 0.55 NaCl equiv. wt % concentration values. The secondary gas-liquid inclusions of the magmatic quartz grains preserved the boiled hydrothermal fluids also and the diluted, post-boiling fluids, which had lower temperatures and concentration values. The crystallisation of cinnabar probably was in connection with the boiling and the temperature depression produced by mixing of the subsurface cold waters and the hot hydrothermal fluids. On the basis of the geological and the fluid inclusion data the mercury indications as a shallow zone of a polymetallic (±Au, Ag) ore deposit are explained.

INTRODUCTION

Along the SE margin of Tokaj Mountains near Sárospatak and Sátoraljaújhely the traces of paleohydrothermal activity are well known. The cinnabar bearing mercury ore occurences are situated NNW of Sárospatak in the area of Királyhegy, and Cinegés as well as Botkő.

Geological investigations were carried out at the end of the 1960's regarding the lithology and geochemistry of the ore indication (KULCSÁR and BARTA, 1969; MÁTYÁS, *et al.*, 1971).

The present work' s aim to accurate our knowledge about the genetical relations of the mercury-bearing zone on the basis of the results of the fluid inclusion studies.

GEOLOGICAL SETTING

The Badenian—Sarmatian (Middle—Upper Miocene) products of the andesitic-rhyolitic volcanic activity are underlain by Middle Triassic carbonate rocks. The cinnabar occurences are situated in the Badenian rhyolite tuff. Products of the Sarmatian igneous activity are less acidic (mixed tuff, amphibole-andesite, pyroxene-andesite), but rhyolite tuff also occurs among them (see *Fig. 1.* JASKÓ and MÉHES, 1946; KULCSÁR and BARTA, 1969; MÁTYÁS *et al.*, 1971). The Királyhegy, Cinegés and Botkő are made of rhyolite tuff altered by silicification.

H—1088. Budapest, Múzeum krt. 4/A

On Királyhegy the double, intensively silicified alteration zones also display baritic alteration and they are aligned in S-N direction. The silicification was developed by crystallisation of the following minerals: tridymite, quartz, chalcedony I, opal I, chalcedony II, quartzin, opal II (TOKODY, 1965). The siliceous alteration is characterized by NW—SE strike on Botkő.

KULCSÁR and BARTA, (1969) described the following alteration processes: (1) siliceous metasomatism, (2) potassic metasomatism below the silicified zones, (3) baritic alteration in two phases (the younger one is developed mainly on Királyhegy), (4) alunitisation.

MÁTYÁS, *et al.* (1971) distinguished seven hydrothermal alteration facies: (1) siliceous; (2) siliceous-kaolinitic; (3) siliceous with kaoline knots; (4) hydrohematitic; (5) montmorillonitic; (6) illitic; (7) devitrificeous, respectively. The cinnabar occurs in the siliceous and hydrohematitic facies, singenetically with siliceous alteration, as well as in the cavities and brecciated zones of the silicified rocks.

The characteristic feature of the mercury indications is the existence of the cinnabar and the lack of other sulphides. The anomalous abundance of Sb, As, Tl, Ag, Ba and Sr indicates an epithermal environments and it would refer to a deeper polymetallic ore deposit. However, the drillings did not cut significant vein systems; the borehole No. Sp-14 cut some baritic-pyritic veinlets, only. The mercury-impregnated bodies on the surface are limited in the silizified zones.

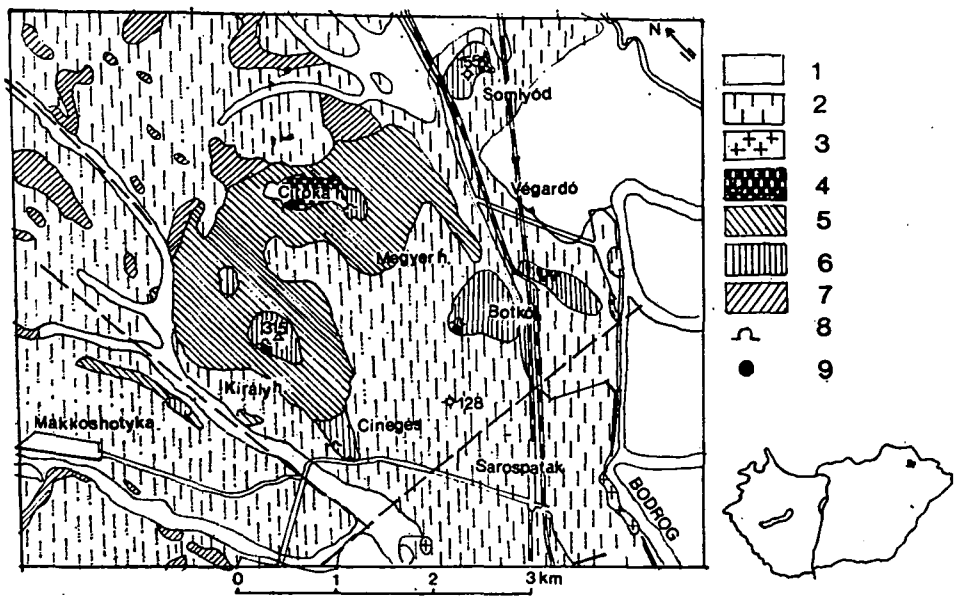

Fig. 1. Geological map of the cinnabar occurences (JASKÓ and MÉHES, 1946).
1 — Holocene, 2 — Pleistocene, 3 — Sarmatian andesite, 4 — rhyolite, 5 — limonitic rhyolite tuff, 6 — Badenian silicified rhyolite tuff, 7 — pumiceous rhyolite tuff, 8 — quarry, 9 — samples

FLUID INCLUSION STUDIES

On the basis of fluid inclusion studies it is possible to determine the temperature, pressure, solution composition and concentration of the mineralizing fluids (ROEDDER, 1984). Therefore some double polished, 0.5—1 mm thin sections from barites (Ki-

rályhegy) and hydrothermal and magmatic quartz grains (Botkő) were prepared for the fluid inclusion studies. Several phase-transition phenomena were observed during the change of the temperature with application a Chaixmeca-type microthermochamber and Amplival Pol microscope. The measurement reproductibility was ± 0.1 °C in negative and ± 0.2 °C in positive temperature interval.

1. Inclusion types. The 1—2 mm thick irregular, tabular barite crystals grew in the cavity of the baritised-silicified rhyolite tuff. They contain large amounts of fluid inclusions. Their diameters are max. 100—120 microns. The majority of the inclusions are pseudosecondary type and they are ordered along the crystal cleavage *(Fig. 2.)*. The two-phase inclusions contain liquids and 10—15 volume % gas. The large two-phase microobjects are primary type ones beside the inclusion rows *(Fig. 3.)*. The secondary inclusions have irregular, planar of flag-like shape, and they usually contain only liquid *(Fig. 4.)*. In certain growth zones of barite crystals the population of the large, liquid+gas and gas inclusions refer to the boiling of the mineralizing fluids (ROEDDER, 1984; *Fig. 5.*).

The short and long prismatic quartz crystals occur in the cavity of the silicified rhyolite tuff on Botkő. They often contain magmatic quartz grains in theirs cores.

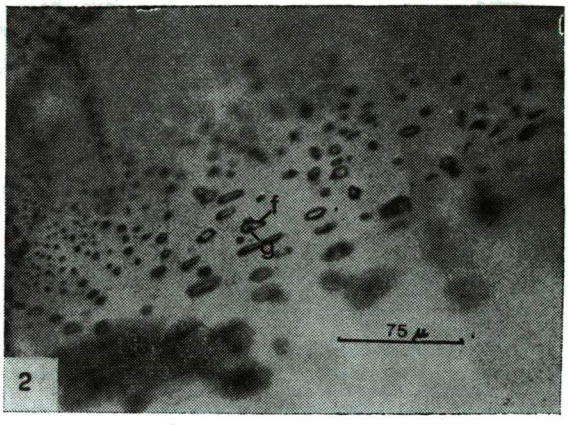

Fig. 2. Ps-S-type fluid inclusions along the cleavage of barite (Királyhegy)

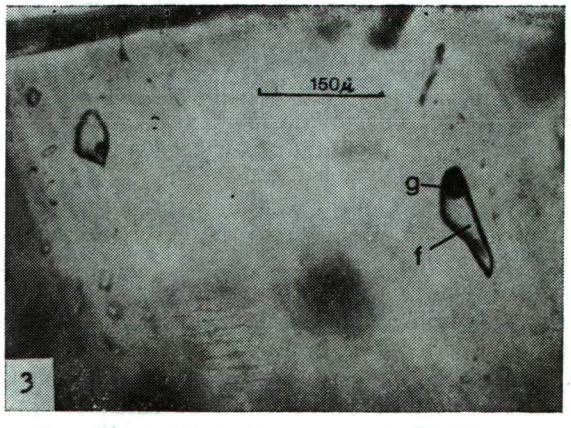

Fig. 3. P-type fluid inclusions in barite (Királyhegy)

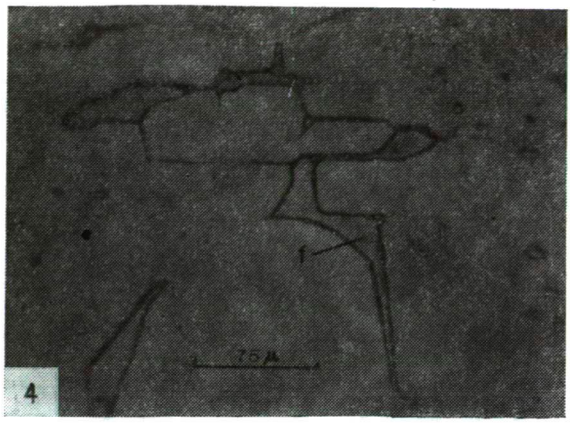

Fig. 4. S-type fluid inclusion in barite (Királyhegy)

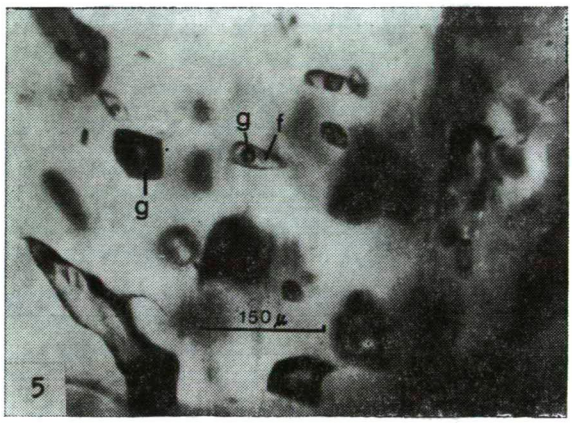

Fig. 5. Gas and gas-liquid inclusions in barite, referring to the boiling (Királyhegy)

The hydrothermal (α-) quartz crystals are unsuitable for phase-transition studies because they contain only secondary type, one-phase inclusions with small diameter.

The hexagonal-dipiramidal magmatic quartz grains occur mainly in the hollow-fractured zones of the silicified rhyolite tuff. The magmatic quartz crystals contain large amounts of volcanic glass inclusions *(Fig. 6.)*. The magmatic quartz grains became fractured in consequence of the tectonical forces, which affected the silicified brittle rock. The paleofluids penetrated into the microfractures and they dissolved the glass inclusions along the fractures and finally the fluids were captured in the cavity of the dissolved glass *(Fig. 7.)*. KOZLOWSKI, (1981) and KOZLOWSKI and METZ, (1985) described similar dissolution events in magmatic quartz grains.

The walls of the microcavity have often uneven, etched surfaces because of the dissolution *(Fig. 8.)*.

The glass inclusions reacted with the hydrothermal fluids, probably until the healing of the microfractures, so their dissolution would have been complete. The

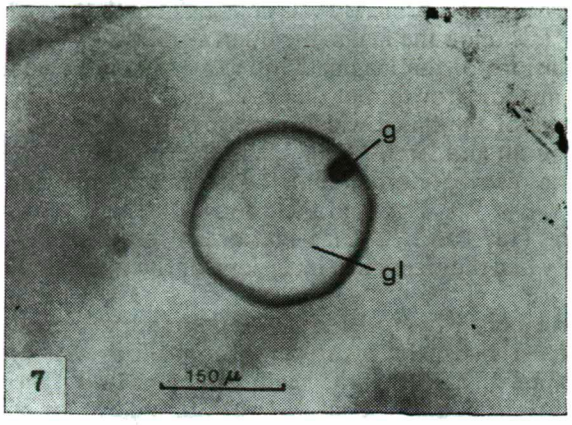

Fig. 6. Glass inclusion with gas bubble in magmatic quartz grain (Botkő)

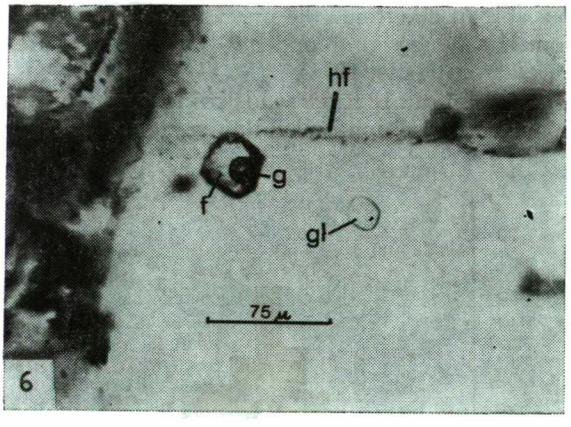

Fig. 7.: Fluid inclusion filling the place of the dissolved glass inclusion along a healed microfracture (Botkő)

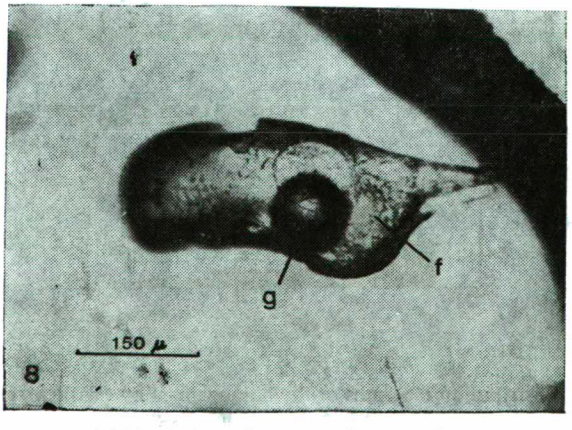

Fig. 8. Fluid inclusion with etched inner surface (Botkő)

healing of the microchannels probably was connected with the growth of the hydrothermal quartz crystals upon the magmatic quartz grains.

The fluid inclusions of the magmatic quartz grains are secondary type relating to the time of the mineral growth, but they are applicable to reconstruct the physicochemical parameters of the fluids which were present during the hydrothermal activity (e.g. TAKENOUCHI and IMAI, 1975).

2. Results. The distribution diagrams of the homogenization temperatures are showed on *Fig. 9.a and 9.b.* The fluid inclusions of the barites are homogenized at higher temperatures (187±13.1 °C) than that of had been prevailed in the paleohydrothermal system when the secondary inclusions of the magmatic quartz grains have been formed.

In the case of a boiled hydrothermal system the vapour pressure of the solution equal with (or higher than) the hydrostatic (in shallow system) or the lithostatic (in deeper system) pressure. During the heating of an inclusion the bubble dissappear when the pressure of the liquid is equal with its saturated vapor pressure. The results of this meditation are that in the case of a boiled hydrothermal system the homogenization temperatures of the inclusions approach the real temperature of a mineral growth and it is possible to determine the pressure of the hydrothermal system. The barites derived from Királyhegy grew under 6—20 bars pressure (with the application of data borrowed from HAAS, 1971).

It is important to point out that the values of the homogenization temperatures reflect the true temperature of a non-boiled fluid system, if they are corrected by the

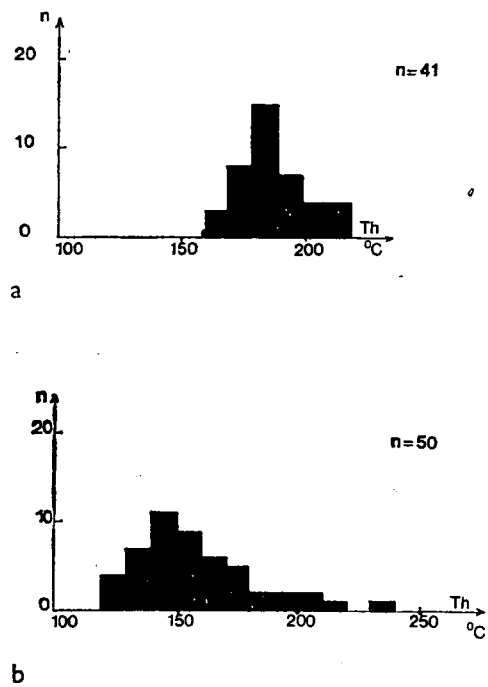

Fig. 9. Distribution diagrams of the homogenization (Th) temperatures
a — barites from Királyhegy
b — magmatic quartz from Botkő

so called „pressure correction". We think that the pressure values were not significantly different in time of the origin of the secondary fluid inclusions of the magmatic quartz, than the pressure values of the barite growth. On the basis of POTTER's (1977) pressure correction data this very low pressure values do not affect significantly the homogenization temperatures, so the mentioned homogenization data reflect the true temperature of the paleofluids for the Botkő samples, too.

The fluids froze below −40 °C during the cryoscopic studies. In all case we observed knot- or brush-like NaCl-hydrate. The melting temperature of the hydrate during the slow heating of the samples by the room air was also measured. The detected cotectic temperatures refer to a NaCl-$CaCl_2$-H_2O solution composition (HAYNES, 1985). The solution composition did not differ on the Királyhegy and Botkő (Table 1.). CO_2-hydrate was also observed in some inclusions which disappeared before the melting of the ice. The presence of the CO_2-hydrate refer to the low density CO_2-content of the gas phase of the inclusions.

The concentration data which were calculated from the melting point depression of the ice (POTTER *et al.*, 1978) are significantly different. The barites derived from Királyhegy grew from such solutions which had higher concentration values than the fluids on Botkő had *(Fig. 10.a* and *Fig. 10.b.)*. On the basis of the temperature and concentration data the density of the fluids were different from each other. The lower mean density values of the barites reflect the influence of a higher temperature (Table 1).

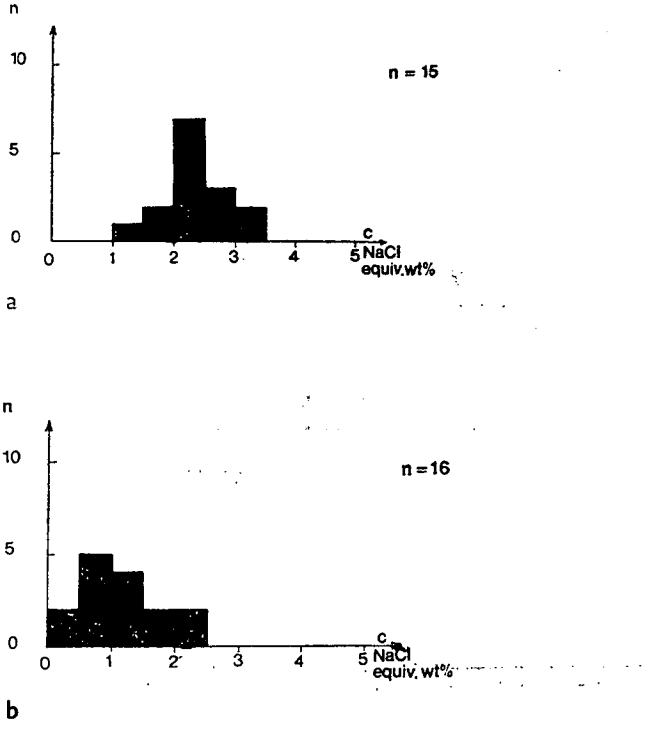

Fig. 10. Distribution diagrams of the concentration (c) values
a — barites from Királyhegy
b — magmatic quartz from Botkő

TABLE 1

Fluid inclusion data from Királyhegy (barite) and Botkő (magmatogenic quartz)

	Barite		Magmatogenic quartz	
	m	s. d.	m	s. d.
Th	187.9	13.1	158.1	23.7
T1	−26.7	5.5	−27.4	3.1
T2	−1.4	0.3	−0.9	0.8
c	2.31	0.55	1.45	1.35
d	0.895	0.016	0.911	0.024

Th — homogenization temperature
T1 — first melting point of ice (cotectic temperature)
T2 — melting temperature of ice
c — concentration (NaCl equiv. wt. %);
d — density (g/cm³)
m — mean value
s.d. — standard deviation

DISCUSSION

The boiling of the hydrothermal system was not obvious in the samples from Botkő by the fluid inclusion petrography. Comparing the *Figures 11.a and 11.b* it is clear that the fluid inclusion data of the magmatic quartz crystals reflect on the double evolution trends of the hydrothermal solution. The Th and T2 data of the magmatic quartz from Botkő have positive correlation in the high temperature interval, which is similar to the inclusion data of the barites. This correlation is characteristic to the boiled systems (HEDENQUIST and HENLEY, 1985b).

The melting temperatures of ice become higher in the inclusions which have lower homogenization temperatures in the samples from Botkő *(Fig. 11.b)*. This fact would refer to the mixing of the hydrothermal fluids and the subsurface ground water. So the secondary inclusions of the magmatic quartz grains also demonstrated the evolution of the paleofluids after the boiling. The decrease of the boiling probably was in connection with the cooling caused by influx of the cold ground water.

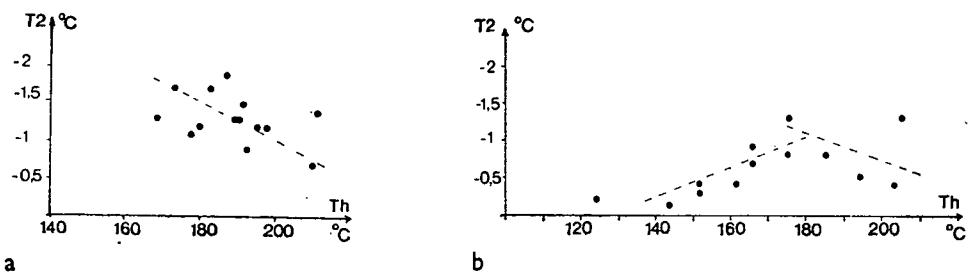

Fig. 11. Relations between the homogenization (Th) and melting temperatures (T2)
a — barites from Királyhegy
b — magmatic quartz from Botkő

The following factors are favourable for the deposition of cinnabar (SMIRNOV *et al.* 1983): (1) chemical changes during the reactions between the fluids and rocks, (2) rising of the oxygen fugacity in the shallow zone of the hydrothermal system, (3) The dilution of the fluid by influx of the vadose water.

About 150 °C temperature the low (< 9) pH values are favourable for the deposition of cinnabar (KOLONIN and PTITSIY, 1972). The low pH values are characteristics in the condensation zone of a boiled volcanic-subvolcanic hydrothermal system (DRUMMOND and OHMOTO 1985). The boiling is favourable for the separation of mercury from other elements (WHITE *et al.*, 1971).

At Sárospatak the cinnabar crystallised during two periods: syngenetically with the silification and another in the brecciated zones. We demonstrated the boiling of the hydrothermal system by fluid inclusion studies. The kaolinitic and alunitic alteration of the rocks refer to an acidic system, also. On the basis of the geological data (KULCSÁR and BARTA, 1969) the cinnabar in some case occur as a sublimated product on the walls of the cavities and fractures. The fluid inclusion data and the geological observations suggest that the cinnabar would crystallised at 170—200 °C during the boiling of the hydrothermal system.

The fluid inclusion studies also provided some proofs for the mixing phenomena between the hydrothermal (hot) fluids and the subsurface (cold) water. So the crystallisation of the cinnabar would be connected to the mixing events also because of the cooling and the (possible) increasing oxygen fugacity. The final conclusion is: the mercury indication have been formed in the near surface or marginal zone of a boiled system, where the condensation of the vapour and acidic gas and the mixing of the fluids are the characteristic phenomena. This result is in harmony with the anomalous Hg, As, Sb, Tl, Pb, Ba and Sr element population, which is very similar to the near surface element association of the recent ore deposition in the geothermal fields (Waiotapu, New Zealand; HEDENQUIST and HENLEY, 1985b).

The investigated mercury occurence is in the temperature interval of the mercury deposits characterized by the data of the Table 2. However, the ore indication displays transitional features to the volcanic-subvolcanic, epi-mesothermal polymetallic ore deposits by the connection between the temperature and concentration data *(Fig. 12)*.

Around Sárospatak and Sátoraljaújhely the silicified rhyolite tuff occurs on the Bányi-hegy, also. This volcanic rock was altered by potassium metasomatism, and it contains a sulphidic-gold type ore occurence which have been exploited in the MiddleAges on Bányi-hegy (GŐBEL, 1954; VARGA, 1961).

The potassium metasomatism had also passed off in the district of the mercury occurences (KULCSÁR and BARTA, 1969). The rock alteration zonality (siliceous, kaolinitic, illitic, montmorillonitic) is well known in the mercury-bearing „siliceous caps" of the precious metal deposits (Buckskin Mountains, Nevada; VIKRE, 1985), and similar hydrothermal alteration zones were described by MÁTYÁS, *et al.* (1971) near Sárospatak. On the basis of the possible analogy, the presumed genetical connection would accurate by further fluid inclusion studies between the mercury indication and the gold ore indication near Rudabányácska.

AKNOWLEDGEMENTS

The author acknowledges his thanks to J. KISS, I. GATTER and M. KÁZMÉR for the review of the manuscript and their valuable suggestions; to E. RÁBL and E. SCHÁD for the drawings and photographs.

TABLE 2

Fluid inclusion data from various Hg-deposits

Deposit	Mineral	Th	C	References
Djilkidal (I)	quartz	110—150	30.4 (3)	
Kurumdu-Ayri (I)	quartz	120—170	27.5	
	ankerite	130—160	12—15	
Kuvay (I)	quartz	145—170	10 (3)	
Cagan-Uzun (I)	quartz	150—190	8.2 (3)	
	ankerite	140—200	8.2 (3)	
Aktash (I)	quartz	120—190	10	
	calcite	130—215	0.5—2 c	
Ak-T ul (I)	quartz	130—150	3.5—6 c	BORISENKO *et al.* (1974)
	calcite	125—135	4—9	
Cheremshanka (I)	quartz	135—165	6—7 c	
Suhoskoe (I)	quartz	115—180	0.5—2.5 c	
Gorhon (II)	quartz	155—185	17.8 (4) c	
Gal-Haya (III)	fluorite	160—190	4.5—6 c	
	quartz	190—240	1.5—3 c	
	calcite	110—130	0.5—1.5	
Karasu (IV)	quartz	180—225	3.5 (5)	
Palianskoe (V)	quartz	130—220	1.5—4	
	quartz	75—140	0.5—1	
Terlinghay (VI)	quartz	100—165	17 (6)	
	quartz	120—145	25 (6)	
	barite	90—110	22 (6)	
	quartz	90—95	20—25	
	barite	70—80	20—25	BORISENKO *et al.* (1979)
	carbonates	70—80	12—15	
	fluorite	60	12—20	
Chazadir (VI)	quartz	120—180	40.9 (1)	
	barite	130—140	7—9 c	
	cinnabar	100—155	39.7 (3)	
	cinnabar	90—110	20	
Slaviansk	fluorite	225—240		ZATSIKHA (1973)
	siderite	220—280		
	quartz	200—220		
Rovni (VII)	quartz	230—210	2—11	ZATSIKHA and GALABURDA (1985)
Szilhegy (VII)	quartz	248—255	3	
Soymi (VII)	quartz	140	5 (2)	
Csontos (VII)	quartz	230	1.5	

Th — homogenization temperature (°C)
C — concentration: NaCl wt % (without symbols) Symbols: solution composition
(1) — NaCl+CaCl+KCl
(2) — NaCl+KCl
(3) — NaCl+Na_2CO_3
(4) — NaCl+$MgCl_2$
(5) — Na_2CO_3
(6) — NaCl+$CaCl_2$

c — CO_2 in the solution
I — High-Altai
II — East-Sayan
III — Yakutia
IV — Middle-Asia
V — Chukotka
VI — Tuva
VII — Transcarpathia

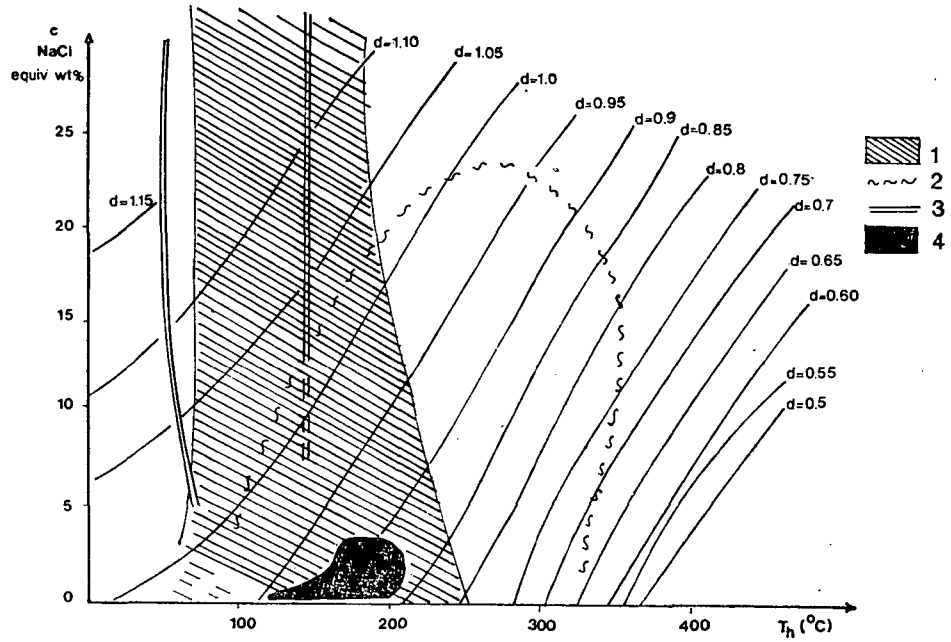

Fig. 12. Distribution of the fluid inclusion homogenization temperatures (Th) and concentration (c) values from various mercury deposits.

1 — mercury deposits (references are on the table 2.)
2 — volcanic-subvolcanic polimetallic deposits (GATTER, 1985)
3 — Mississipy-Valley type deposits (GATTER, 1985)
4 — data from Sárospatak
d — density of fluids

Symbols on the photomicrographs: f=liquid, g=gas, gl=volcanic glass, hf=healed microfracture

REFERENCES

BORISENKO, A. S., LEBEDEV, V. I., OBOLENSKI, A. A., ZAYKOV, V. V., TULKIN, V. G. (1979): Physico chemical pecularities of the hydrothermal ore deposition in Western-Tuva — In: Parameters of the natural processes of the endogene ore deposition, T.2. "Nauka", Novosibirsk, p. 226—235. (in Russian).

BORISENKO, A. S., VASILYEV, V. I., OBOLENSKIY, A. A., SHUGOROVA, N. A. (1974): Composition of gasliquid inclusion in minerals of mercury deposits and the chemistry of ore-bearing solutions. Akad. Nauk. SSSR Doklady **214. № 3.** 673—676. (in Russian).

DRUMMOND, S. E., OHMOTO, H. (1975): Chemical evolution and mineral deposition in boiling hydrothermal systems. Econ. Geol. **80.,** 126—147.

GATTER I. (1985): Fluid inclusion discrimination diagram for various genetical types of polimetallic deposits — Poster. ECRFI Symp., Göttingen, 1985.

GŐBEL, E. (1954): Mining-geological description of the surroundings of Nagybányi Hill near Rudabányácska. Ann. Rep. of Hung. Geol. Survey for 1954 year, 45—55. (in Hungarian).

HAAS, J. L. (1971): The effect of salinity on the maximum thermal gradient of a hydrothermal system at hydrostatic pressure. Econ. Geol. **66.,** 940—946.

HAYNES, F. M. (1985): Determination of fluid inclusion composition by sequential freezing. Econ. Geol. **80.,** 1436—1439.

HEDENQUIST, J. L., HENLEY, R. W. (1985a): Hydrothermal eruption in the Waiotapu geothermal system, New Zealand; their origin, associated breccias and relation to precious metal mineralization. Econ. Geol. **80.,** 1640—1668.

HEDENQUIST, J. L., HENLEY, R. W. (1985b): The importance of CO_2 on freezing point measurements of fluid inclusions: evidence from active geothermal systems and implications for epithermal ore deposition. Econ. Geol. **80.**, 1379—1408.

JASKÓ S., MÉHES K. (1946): Geological description of the surroundings of Sátoraljaújhely and Sárospatak. Ann. Rep. of. Hung. Geol. Survey for 1945—47 years II, 67—75. (in Hungarian).

KOLONIN, G. R., PITTSIY, A. B. (1972): Physico-chemical conditions of the mercury-sulphide deposition from hydrothermal solutions. Akad. Nauk. SSSR. Doklady **T. 206. №. 2.**, 459—462. (in Russian).

KOZLOWSKI, A. (1981): Melt inclusions in pyroclastic quartz from the Carboniferous deposits of the Holy-Cross Mountains, and the problem of magmatic corrosion. Acta. Geol. Polon. **31.** No. **3—4.**, 273—284.

KOZLOWSKI, A., METZ, P. (1985): Origin of quartz-filled inclusions in pyrogenic quartz. N. Jb. Miner. Mh. **H. 6.**, 277—288.

KULCSÁR L., BARTA I. (1969): Petrological-geochemical investigations concerning a mercury-ore prospecting carried out near Sárospatak. T. 2266, p. 96. Doc. Dept. of Hung. Geol. Survey, Budapest. Manuscript. (in Hungarian).

MÁTYÁS E., MRS. KOPP, K., SÁNTA, P., MRS. SZÉP, É. (1971): Preliminary report about results of the mercury-ore prospecting carried out near Sárospatak. T. 3137, p. 106. Doc. Dept. of Hung. Geol. Survey, Budapest. Manuscript. (in Hungarian).

POTTER, R. W. (1977): Pressure corrections for fluid inclusion homogenization temperatures based on the volumetric properties of the system $NaCl-H_2O$. U. S. Geol. Surv. J. Res. **5**, 603—607.

POTTER, R. W., CLYNNE, M. A., BROWN, D. L. (1978): Freezing point depression of aqueous sodium chloride solutions Econ. Geol. **73**, 284—285.

ROEDDER, E. (1984): Fluid incusions — Reviews in Mineralogy **12**, Min. Soc. of America, p. 644.

SMIRNOV, V. I., GINZBURG, A. I., GRIGORIEV, V. K., YAKOVLEV, V. M. (1983): Studies of mineral deposits. Eng. Trans. "Mir" Publ. House, Moscow, p. 288.

TAKENOUCHI, S., HIDEKI, I. (1975): Glass and fluid inclusions in acidic igneous rocks from some mining areas in Japan. Econ. Geol. **70**, 750—769.

TOKODY, L. (1965): The minerals of Király Hill near Sárospatak. Földt. Közl. **95**, 95—98. (in Hungarian).

VARGA—MÁTHÉ, K. (1961): Potassium metasomatism and enrichment on the area located between Sátoraljaújhely and Vágáshuta. Földt. Közl. **91.** 391—396. (in Hungarian).

VIKRE, P. G. (1985): Precious metal vein systems in the National District, Humbold County, Nevada. Econ. Geol. **80**, 360—393.

WHITE, D. E., MUEFLER, L. J. P., TRUESDELL, A. H. (1971): Vapor dominated hydrothermal systems compared with hot-water systems. Econ. Geol. **66**, 75—97.

ZATSIKHA, B. V., PETRICHENKO, O. I., DOLYSHNY, B. V., LASKOV, V. A. (1973): Genetic pecularities of mineral formation in the Slaviansk mercury deposit. L'vov. Min. Sb. **27**, No. **4.** 326—332. (in Russian).

ZATSIKHA, B. V., GALABURDA, YU. A. (1985): Physico-chemical conditions of formation of the mercury and arsenicmercury deposits of the Transcarpathia. Geokhimiya **5**, 657—666. (in Russian).

Manuscript received, 21 July, 1988

Acta Mineralogica-Petrographica, Szeged, XXIX, 69—79, 1987—1988

CHROMITE OCCURRENCES IN IRAQI ZAGROS

G. BUDA

Department of Mineralogy, Eötvös Loránd University

ABSTRACT

Ultrabasic rocks (harzburgite, wherlite and dunite) occurring in the northeastern Iraqi Zagros thrust zone, contain massive podiform, schliern and accessory type chromites.

Aluminium and chromium-rich chromites have been distinguished in the ophiolitic complexes of Mawat and Penjwin Mountains. The first variety was probably originated as cumulite whereas the second one was residuum after partial melting of rising mantle. Fe-rich accessory-type chromite have been found in Bulfat formed as a differentiated product of a large gabbro intrusion.

Alteration of chromite is widespread and probably was formed simultaneously with the serpentinization. Reaction between chromite and host rock, initiated by water, resulted the formation of iron-rich rim around chromite grains and chlorite or serpentine, depending on the chromite composition.

INTRODUCTION

Chromite-bearing ultramafic rocks located at Penjwin, Mawat and Bulfat areas in northeast Iraqi Zagros thrust zone *(Fig. 1.)*. The former two localities belong to the ophiolitic complexes and have very similar petrological characters whereas the latter one may be a differentiated product of a large gabbroic intrusion.

Fig. 1. Location map.

H—1088 Budapest, Múzeum krt. 4/A Hungary.

Complete ophiolitic rock sequences occur in Mawat. The ultramafic rocks are mostly serpentinized harzburgite, wherlite and dunite (olivine Fo_{93-97}) with chromite (BUDA *et. al.*, 1977). The upper part of the ultrabasic body contains olivine websterite (*Fig. 2.*, Table 1.) which forms dikes in the peridotite, too. Above the ultrabasic rock there is an about 1000 metre thick gabbroic body emplaced tectonically. Two types of gabbro can be distinguished: a strongly sheared, banded, and foliated amphibole- and a coarse-grained pyroxene gabbro. Small plagiogranite and diorite intrusions occur along the main tectonic zones probably as leucocratic differentiates of the gabbroic body. The upper part of gabbro grades into diabase which was metamorphosed under the conditions of the greenschist facies together with the basalt which occurs above the diabase. The chemical composition of basalt is oceanic tholeiite or sometimes spilitic. Pillow structure can be observed. The Penjwin ophiolitic complex has same suite but the volcanic sequences are completely missing. The ultrabasic rocks are mostly harzburgite (olivine Fo_{95-97}), dunite and wherlite (*Fig. 2.* Table 1.). The two ophiolitic complexes are emplaced tectonically without any contact metamorphism. The only thermal contact which occurs at Penjwin (Asnawa) is due to a later dioritic intrusion after the emplacement of the ophiolitic complex.

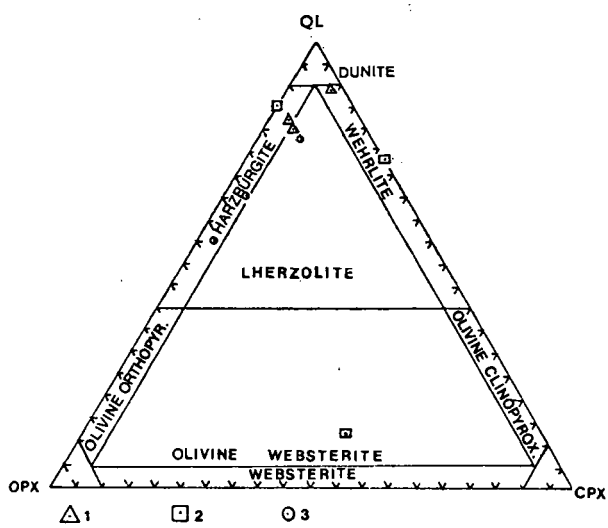

Fig. 2. Cassification of ultrabasic rocks from Mawat, (1) Penjwin (2) and Bulfat (3)

The Bulfat ultrabasic and gabbroic complex differs from the others. It is an intrusion with high temperature contact aureole (cordierite+K-feldspar+sillimanite hornfels, predazzite, ophicalcite). The ultrabasic rocks are rich in pyroxene (*Fig. 2.* Table 1.) and contain iron-rich chromite in small amount.

METHOD OF STUDY

About 40 polished ore and thin sections of chromite and chromite bearing rocks were studied in reflected and transmitted light and by microprobe. Universal stage was used for determining optical properties of silicate minerals (olivine, pyroxene,

TABLE 1

Chemical analyses of ultrabasis rocks from Northeast Iraq

	Penjwin			Mawat			Bulfat		
	1.	2.	3.	1.	2.	3.	1.	2.	3.
SiO_2	35.64	40.00	39.82	40.99	42.93	49.50	40.14	38,71	38.51
TiO_2	0.00	0.00	0.00	0.03	0.06	0.13	0.06	0.14	0.09
Al_2O_3	0.85	0.85	0.32	2.13	2.63	2.75	0.60	0.90	1.27
Cr_2O_3	0.21	0.17	0.13	0.86	0.88	0.00	0.08	0.14	0.33
Fe_2O_3	4.31	3.23	3.64	2.02	1.11	3.30	3.60	6.78	7.10
FeO	3.35	4.14	3.85	5.06	7.27	3.72	4.03	1.84	2.00
MnO	0.10	0.10	0.10	0.08	0.13	0.03	0.10	0.09	0.13
MgO	40.70	43.00	42.96	44.01	37.36	24.86	42.86	38.20	35.56
CaO	2.03	1.40	1.61	1.17	7.43	11.83	1.75	1.40	1.32
Na_2O	0.10	0.15	0.10	0.09	0.15	0.24	0.10	0.15	0.10
K_2O	0.04	0.04	0.05	0.02	0.03	0.03	0.04	0.04	0.03
P_2O_5	0.10	0.07	0.10	0.00	0.00	0.00	0.07	0.10	0.09
CO_2	0.00	0.00	0.00	0.00	0.00	0.00	0.00	0.00	0.00
H_2O^+	9.86	5.10	6.00	4.03	0.30	3.51	5.00	10.69	11.93
H_2O^-	0.60	0.16	0.12	0.25	0.22	0.26	0.21	0.43	0.88
Total	97.89	98.41	98.80	100.74	100.55	100.2	98.64	99.61	99.34
CIPW NORMS									
Or	0.27	0.25	0.32	0.12	0.16	0.18	0.25	0.27	0.20
Ab	0.97	1.36	0.91	0.79	1.28	2.12	0.91	1.43	0.98
An	2.00	1.64	0.30	5.55	6.53	6.61	1.15	1.88	3.38
Di	6.84	4.16	5.95	0.37	24.39	42.77	5.99	4.07	2.73
Hy	3.00	12.90	13.47	13.02	—	32.57	13.30	26.41	34.99
Ol	79.04	74.12	72.83	75.32	64.32	10.50	72.36	55.51	46.32
Mt	7.15	4.03	5.69	3.04	1.65	4.39	5.59	6.09	6.48
He	—	—	—	—	—	—	—	3.46	3.74
Ap	0.27	0.18	0.25	—	—	—	0.17	0.26	0.24
Il	—	—	—	0.06	0.12	0.25	0.12	0.30	0.20
Cr	0.49	0.37	0.29	1.83	1,33	—	0.18	0.32	0.78

Penjwin: 1. Dunite-wehrlite (37A)*; 2. Harzburgite (107); 3. Harzburgite (111)
Mawat: 1. Harzburgite (average 4 analyses); 2. Wehrlite (1 analysis); 3. Olivine websterite (average 5 analyses)
Bulfat: 1. Harzburgite (213); 2. Harzburgite (166); 3. Harzburgite (212)
* Sample number

stc.) and Leitz MPV2 microscope photometer was applied for measuring the reflectivity of chromite using different wave lengths (542 nm, 584 nm, 640 nm). The chromite and olivine were separated by heavy liquide and were investigated by X-ray powder methods. The chromite cell sizes were measured following STRAUMANIS method and the forsterite content of olivine was determined by using the (130) reflection (YODER *et. al.*, 1957) and by 2V determination. Cameca microprobe was used for quantitative chemical analysis of chromite applying the MBXCOR computer software introduced at the 3th International Conference of X-ray Optics and Microanalisis held at Boston in 1977. FeO was re-expressed as FeO and Fe_2O_3 on the assumption that $RO = R_2O_3$ in spinel structure (Ti and Si were assumed to occupy trivalent sites). Some altered grains were selected and Fe, Cr, Al and Mg distribution were determined across these grains.

MINERALOGY AND PETROGRAPHY OF THE CHROMITE OCCURRENCES

At Penjwin and Mawat three types of chromite occurrences have been distinguished (1) accessory-type chromite (chromite content 2—5 V%). (2) schlieren-type chromitite (chromite content 20—25 V%). (3) massive chromite ore (chromite content is more than 80 V%).

In Bulfat only euhedral or subhedral accessory-type chromite have been found.

1. *Accessory-type chromite*

The ultrabasic rocks usually contain about 2—5 V% chromite which is mostly euhedral or subhedral, corroded and it normally has an altered iron-rich rim. The host rocks are strongly sheared, foliated and serpentinized. Besides serpentine, talc, Mg-chlorite, brucite and magnetite are also present. Magnetite is mostly secondary, originated by serpentinization of olivine. Talc and Mg-chlorite formed from Al-bearing pyroxene and from chromite altered during the serpentinization.

Before the complete or partial serpentinization the ultrabasic rocks were harzburgite, dunite in Penjwin, wherlite, harzburgite, dunite in Mawat and pyroxene-rich harzburgite in Bulfat (original compositions were estimated from chemical analyses).

1.1. Penjwin. The chromite is subhedral transected by cracks and altered along the rims and cracks into iron-rich chromite. The chromites in dunite are somewhat richer in Cr which contain a lower amount of Al (Table 2.). The reflectance is low ($R_{542\ nm}\% = 12.5\%$) which indicates a lower iron content, too. The grains are surrounded by serpentine. Increasing pyroxene content of the rocks resulted in a relative enrichment of aluminium.

1.2. Mawat. The same alteration phenomenon can be recognized in Mawat but differences between chromite compositions occurring in different rock types are more obvious. The chromite in dunite has high chromium content and in pyroxene—bearing rocks the chromite is aluminium-rich and the grains are surrounded by Mg-chlorite (Table 3.).

1.3. Bulfat. The chromite grains are always euhedral without any alteration rim and are surrounded by chromium-bearing Mg-chlorite and by magnetite. The chromite is rich in iron. (Table 2.). Under reflected light, it shows high reflectance ($R\%_{542nm} = 16,9$) due to the high iron content.

2. *Schlieren-type chromite*

This type occurs around the massive chromite lenses or scattered irregularly in peridotite. The grains are mostly rounded subhedral, corroded and reddish brown in transmitted light. The host rock is always dunite which is frequently altered to serpentine. The forsterite content of olivine is high (Penjwin $= Fo_{96}$, Mawat $= o_{93}$). The chemical composition of chromites are very similar in both occurrences, so called subferrichromite with high Cr_2O_3 content. (Table 2, 3).

3. *Massive chromite*

The shape of chromite bodies are variable occurring mostly as lens-like or podiform surrounded by dunite halos. The sizes of these bodies are larger in Mawat (thickness 0,5 m up to 2,7 m) than in Penjwin (0,1 m up to 0,5 m). In Mawat two types of ore can be distinguished: in the first one the main gangue mineral is tremolite ($\gamma/C = 19°$, $2V = -83°$) and the ore is slightly crushed and the grains are mostly sub-

TABLE 2

Chromite analyses

wt %	Penjwin								Bulfat	
	Accessory-type chromites				Schlieren-type chromite		Massive chromite		Accessory-type chromite	
	1.	2.	3.	4.	5.	6.	7.	8.	9.	10.
Cr_2O_3	46.43	48.10	42.40	41.87	59.26	54.59	58.10	54.06	46.92	48.39
Al_2O_3	19.23	16.67	19.91	23.62	10.35	10.77	9.59	9.22	6.58	10.61
Fe_2O_3	2.92	4.39	6.69	3.22	4,11	7.43	3.86	8.18	14.66	9.70
TiO_2	0.04	0.23	0.26	0.03	0.15	0.15	0.15	0.09	0.18	0.12
SiO_2	0.13	0.01	0.01	0.47	0.08	0.60	0.00	0.35	0.08	0.32
FeO	19.44	20.75	22.14	19.77	10.23	11.70	17.18	18.79	23.06	21.54
MgO	9.26	8.65	7.75	9.81	15.14	14.07	10.42	9.30	5.60	7.37
MnO	0.30	0.26	0.63	1.21	0.11	0.80	0.32	0.84	0.35	0.26
ZnO	0.87	0.28	0.84	—	0.06	—	0.03	—	0.31	0.30
Total	98.62	99.34	100.62	100.00	99.49	100.11	99.65	100.83	97.74	98.61
	Numbers of ions on the basis of 4 (O)									
Cr	1.187	1.241	1.075	1.033	1,501	1.381	1.523	1.416	1.320	1.299
Al	0.733	0.642	0.753	0.869	0.391	0.406	0.375	0.360	0.276	0.425
Fe^{3+}	0.071	0.108	0.162	0.076	0.099	0.179	0.096	0.204	0.393	0.248
Ti	0.001	0.006	0.006	0.001	0.004	0.004	0.004	0.002	0.005	0.005
Si	0.004	0.000	0.000	0.015	0.003	0.019	0.000	0.012	0.003	0.017
Fe^{2+}	0.526	0.567	0.594	0.516	0.274	0.313	0.476	0.521	0.686	0.612
Mg	0.446	0.421	0.371	0.456	0.723	0.671	0.515	0.459	0.297	0.373
Mn	0.008	0.007	0.017	0.032	0.003	0.022	0.009	0.024	0.011	0.008
Zn	0.020	0.007	0.020	—	0.001	—	0.001	—	0.008	0.008
$Cr/Cr+Al+Fe^{3+}$	0.59	0.62	0.54	0.52	0.75	0.69	0.76	0.71	0.66	0.65
$Al/Cr+Al+Fe^{3+}$	0.37	0.32	0.38	0.44	0.20	0.20	0.19	0.18	0.14	0.21
$Fe^{3+}/Cr+Al+$ $+Fe^{3+}$	0.04	0.05	0.08	0.04	0.05	0.09	0.05	0.10	0.20	0.12
$Mg/Mg+Fe^{2+}$	0.45	0.42	0.37	0.45	0.72	0.67	0.51	0.46	0.30	0.37

1. Chromite core (with altered rim) from serpentinized dunite (No. 37B); 2. Chromite core (with altered rim) from serpentinized dunit (No.82); 3. Chromite core (with altered rim) from serpentinized dunite (No.28A); 4. Chromite core (with altered rim) from peridotite (No. 82); 5. Chromite from olivine chromitite (No. 77); 6. Chromite from olivine chromitite (No. 78); 7. Chromite from olivine chromitite (No. 79); 8. Massive chromite with pyroxene gangue (No. 80); 9. Chromite from peridotite (No. 166B); 10. Chromite from peridotite (No. 131).

hedral with corroded rims. The colour is yellowish brown with reddish brown rim under transmitted light. These grains are slightly altered to Fe-rich chromite along their cracks and margins and are coated by thin layer of Mg-chlorite. According to the chemical composition, this type of ore is a slightly oxidized aluminochromite ($RO/R_2O_3=0,96$). The second ore type is a very strongly crushed and oxidized ($RO/R_2O_3=0.79$) reddish brown (under transmitted light) aluminochromite (Table 3). The only gangue mineral is Mg-chlorite.

In Penjwin the gangue mineral of massive chromite is clinopyroxene and small amount of amphibole together with Mg-chlorite. The chromite is frequently euhedral, corroded and slightly crushed with dark reddish brown colour under transmitted light. Iron content is high ($FeO=18.79$ wt% $Fe_2O_3=8.18$ wt%) and the aluminium

TABLE 3

Chromite analyses

	Mawat				
	Accessory-type chromite		Schlieren chr.		Massive chromite
	1.*	2.*	3.*	4.	5.
Cr_2O_3	46.50	65.50	56.50	48.43	49.06
Al_2O_3	20.75	—	10.00	18.80	18.76
Fe_2O_3	4.94	6.66	5.83	2.96	8.70
TiO_2	—	—	—	0.21	0.06
SiO_2	—	—	—	0.71	0.90
FeO	11.21	15.85	13.91	14.23	8.80
MgO	15.50	10.20	12.60	12.60	13.60
MnO	—	—	—	0.15	0.16
ZnO	—	—	—	0.48	—
Total	98.90	98.17	98.84	98.57	100.04
	Numbers of ions on the basis of 4 (0)				
Cr	1.132	1.824	1.468	1.195	1.186
Al	0.754	—	0.388	0.692	0.676
Fe^{3+}	0.115	0.176	0.144	0.069	0.200
Ti	—	—	—	0.005	0.001
Si	—	—	—	0.020	0.020
Fe^{2+}	0.289	0.465	0.382	0.372	0.225
Mg	0.712	0.535	0.618	0.586	0.620
Mn	—	—	—	0.040	0.005
Zn	—	—	—	0.011	—
				Ni 0.004	
$Cr/(Cr+Al+Fe^{3+})$	0.67	0.91	0.73	0.60	0.60
$Al/(Cr+Al+Fe^{3+})$	0.38	—	0.20	0.19	0.32
$Fe^{3+}/(Cr+Al+Fe^{3+})$	0.05	0.35	0.07	0.06	0.10
$Mg/(Mg+Fe^{2+})$	0.71	0.54	0.62	0.59	0.73
a_0	8.267 ± 0.007	8.336 ± 0.007	8.301 ± 0.004	8.268 ± 0.004	8.272 ± 0.003
R % 542 µm	11.9 ± 0.15	core rim 14.9 17.0	13.3 ± 0.16	12.2 ± 0.10	12.3 ± 0.1
Fo content of olivine	93	92	90	—	—

1. Chromite from peridotite (No. 161, 201); 2. Chromite from dunite (No. 160); 3. Chromite from olivine chromitite (No. 211); 4. Massive chromite with tremolite gangue (No. 64); 5. Massive chromite with pyroxens gangue (No. 272)
* Determined by physical properties

content is low ($Al_2O_3 = 9.22$ wt%) (Table 2). The ore is subferrichromite according to PAVLOV (1949) nomenclature.

The matrix of the first chromite ore type of Mawat was also clinopyroxene but altered to tremolite. Local reactions between tremolite and chromite resulted, through diffusion of Al, the formation of Mg-chlorite. The matrix of the second ore type was originally olivine which was altered to serpentine and then to Mg-chlorite.

On the basis of the chemical composition of chromites, four groups *(Fig. 3)* can be distinguished:

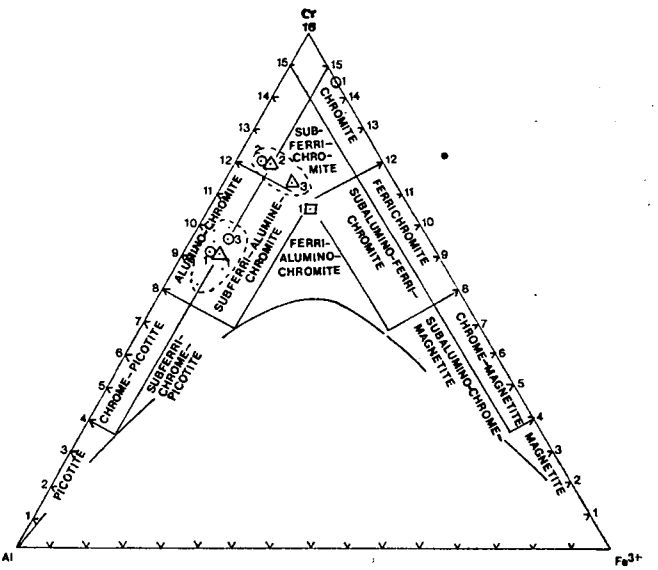

Fig. 3. Atomic proportions of Cr, Al and Fe^{3+} of chromites from Mawat, Penjwin and Bulfat

⊙1 Mawat △1 Penjwin □1 Bulfat	Average composition of accessory chromite
⊙2 Mawat △2 Penjwin	Average composition of schlieren chromite
⊙3 Mawat △3 Penjwin	Average composition of massive chromite

1. *Aluminochromite.* This group is rich in aluminium (average $Al_2O_3 = 19.01$ wt%) and in ferrous iron (average FeO = 15.99 wt%). In Mawat, it forms both the accessory and massive-type of chromites ($a_0 = 8.267 - 8.272$ Å, $R\%_{542nm} = 11.9 - 12.3$), whereas in Penjwin it constitutes accessory-type chromite only. The host rock usually contains orthopyroxene in addition to olivine.

2. *Subferrichromite.* Chromites of this group contain a rather high amount of chromium (average $Cr_2O_3 = 56{,}6$ wt%) and magnesium (average MgO = 12,35 wt%). They form the so-called schlieren-type chromitite in Penjwin, Mawat and the massive ore-type of Penjwin. The unit cell parameter of subferric chromite is larger than that of aluminochromite ($a_0 = 8.296$—8.306 Å).

3. *Chromium-rich chromite.* These chromites ($Cr_2O_3 = 65.5$ wt%) occur in small amount in dunitic rocks of Mawat ($a_0 = 8.336$ Å, $R\%_{542\,nm} = 14.9$).

4. *Ferrichromite.* This chromite contains high amount of ferric and ferrous iron ($Fe_2O_3 = 12.10$ wt%, FeO = 22.3 wt%,); and is found only in the pyroxene-rich (harzburgite) rocks of Bulfat. The reflectance is strong ($R\%_{542\,nm} = 17$) due to the high iron content.

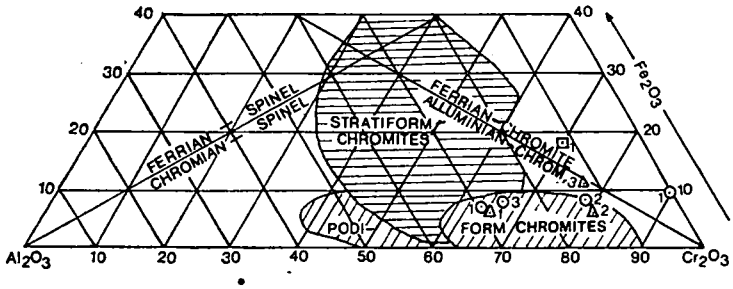

Fig. 4. Cr_2O_3, Al_2O_3 and Fe_2O_3 variation in chromites from Mawat, Penjwin and Bulfat (after THAYER, 1964).

⊙1 Mawat, △1 Penjwin, □1 Bulfat — Average composition of accessory chromite
⊙2 Mawat, △2 Penjwin — Average composition of schlieren chromite
⊙3 Mawat, △3 Penjwin — Average composition of massive chromite

The Al_2O_3, Fe_2O_3 and Cr_2O_3 contents of chromites were plotted in THAYER's (1964) triangular diagram *(Fig. 4)* which show that the composition of Mawat and Penjwin chromites are similar to the composition of Alpine-type podiform chromites. The aluminium-rich chromites are very near or in the field of stratiform chromites where two compositional fields overlap. The subferrichromites are little far but also in or near to the field of podiform chromite. Dunitic accessory chromite of Mawat is on the Fe_2O_3-Cr_2O_3 line. The accessory ferrichromite of Bulfat is far from the fields of stratiform and podiform chromites indicating a different origin.

The low TiO_2 content of Mawat and Penjwin chromites (0,03—0,26 wt%) is also characteristic of the podiform chromites (in stratiform chromite TiO_2 content is higher than 0,3 wt%, according to DICKEY, 1975).

In Mawat and Penjwin average of the $Cr/(Cr+Al+Fe^{3+})$ cation ratio of chromite in pyroxene-bearing rocks is 0.61 and in dunitic chromite 0.72 which indicates an aluminium enrichment in chromites occurring with pyroxenes. In Bulfat the lower Al and higher Fe content of chromite indicates a lower crystallization temperature in harzburgite with closed genetic connection of overlying gabbro.

TEMPERATURES OF FORMATION

Temperatures of formation of chromites can be calculated from cation distribution between coexisting olivine and chromian spinel, if equilibrium and ideal solid solution exist in the system, following the equations introduced by *IRVINE,* (1963) and *JACKSON,* (1969). The temperature of formation obtained from this equation was about 1350 °C in harzburgite and dunite in Mawat and Penjwin and 1150 °C in Bulfat. Unfortunately the host rock of massive chromite of Mawat is altered and was not possible to measure the cation distribution directly, therefore it was estimated. The range of estimated temperatures was around 1200—1250 °C. These values correspond to the temperature of formation of the Alpine-type peridotite, for example Burro Mountain (LONEY *et. al.,* 1971) and Massif due Sud, New Caledonia (RODGERS, 1973).

ALTERATION

Alteration of ultrabasic rocks is a widespread phenomenon in all occurrences. Along the main tectonic zones the rocks are completely altered and behaved as a lubricant for advancing tectonic movement. The olivine altered to serpentine and pyroxene altered to talc, tremolite and chlorite depending on Al and Ca content of the different types of pyroxenes. The nearly equal MgO/SiO_2 ratios in peridotite (1.03) and in serpentinite (1.02) require larger amount of brucite formation (COLEMAN, 1971). However, only small amount of this mineral was detected due to the leaching caused by latter processes. The kink-bands and serpentinization along the cracks of deformed olivine, and alteration of the chromite along fractures suggest a deformation before and during serpentinization. The presence of other fractures in chromite without alteration indicate a further deformation after serpentinization.

A special attention was given to the alteration processes which affected chromites. Detailed microprobe traverses were carried out across different types of chromites to investigate the main element distribution in the altered rims and in the core of the crystals. One traverse was carried out across the accessory chromite of serpentinized pyroxene-poor olivine-rich harzburgite of Penjwin area and another across the accessory chromite of harzburgite from Mawat. According to these investigations the altered, strongly reflecting chromite rim is very rich in iron and poor in chromium, magnesium and aluminium in both cases. The iron content is gradually decreasing towards the core and chromium content increasing. Magnesium and aluminium contents are very low in the rim which suddenly increase at the very border of the altered and unaltered parts.

The chromite from Mawat is richer in Al *(Fig. 5)* and coated by Mg-chlorite. It is supposed that during the alteration, Al-rich chromite released aluminium by diffusion to form Mg-chlorite from the surrounding Mg-silicates. Accordingly, relative enrichment of iron took place in the rim, indicated by its strong reflectance. The relatively aluminium poor chromite from Penjwin *(Fig. 6)* had not released enough aluminium to form chlorite, therefore the altered chromite grains surrounded by serpentine, only. Along the cracks, inside the crystals iron enrichment also occurs. This phenomenon supports the theory of the simple alteration. According to this theory the volatiles caused the alteration of chromite and the silicates, too. However, the possibility of secondary chromite overgrowth as suggested by ULMER, (1974) could not be excluded.

Well developed alteration rim did not formed around the euhedral iron-rich Al-poor chromite in Bulfat. However, in few cases a very narrow magnetite rim occurs. The grains are surrounded by sometimes Mg-chlorite which can be found in other parts of the rock, too, without any connection with the chromite but attached to the altered parts of pyroxenes. Therefore chlorite most probably formed from Al-containing orthopyroxene. The sources of water which was needed for the alteration are obscure because ultramafic melts do not contain enough water for extensive serpentinization (BOWEN *et al.*, 1949). Therefore, excess water could have been derived either from the mantle (HESS, 1962) or from the wet sediments.

CONCLUSIONS

The ultrabasic rocks of the ophiolitic complexes of northeast Iraqi Zagros thrust zone contain two main types of chromite: an Al-rich one ($Cr/Al=1.6$) occurs in pyroxene-bearing ultramafite (harzburgite) which can be a cumulite; and Cr-rich

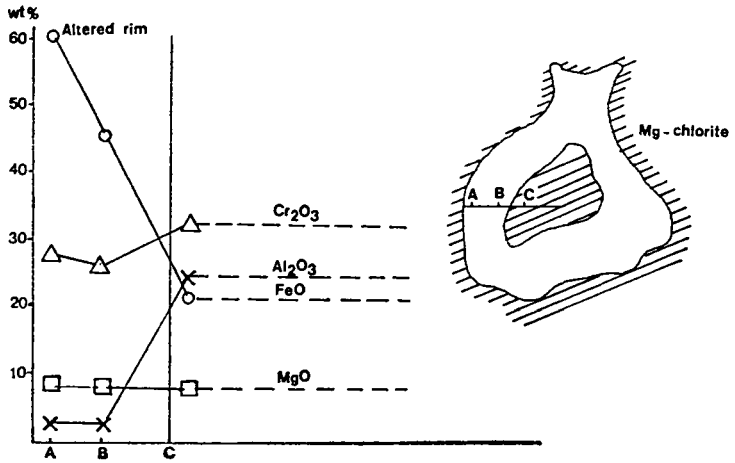

Fig. 5. Microprobe traverse across an altered accessory chromite from Mawat (surrounded by Mg-chlorite)

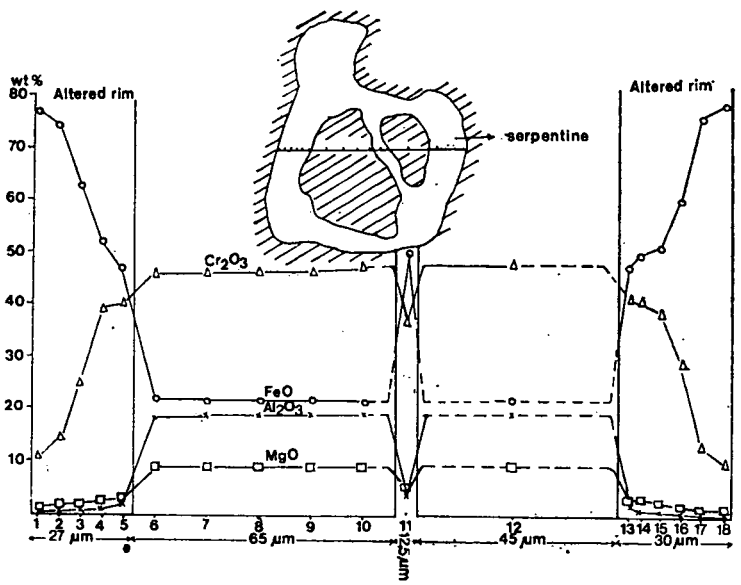

Fig. 6. Microprobe traverse across an altered accessory chromite from Penjwin (surrounded by serpentine).

one (Cr/Al=3.8) mostly in olivine-rich rock formed as a residuum after partial melting of rising mantle material. Fe-rich chromite of the pyroxene-bearing rock of Bulfat Mountain most probably formed as a differentiated product of a large gabbroic intrusion.

The Mg-content of chromite ($Fe^{2+}/Mg=0.8$) of Mawat and Penjwin is higher than of Bulfat ($Fe^{2+}/Mg=1.97$) which is further confirmation of podiform (Alpine-

type) origin of the previous one and formation by differentiation of the latter one. The ophiolitic peridotite belongs to the olivine-pyroxene-spinel facies which can form at high temperature (1350 °C) and at moderately high pressure. Such conditions exist only in the upper part of the mantle (*MACGREGOR*, 1967).

The lenticular occurrences of massive, strongly fractured schliern- and accessory-type chromites and kink-bands in olivine indicate a strong deformation which probably happend when the peridotite was carried up as a solid slab (no thermal contact). After the emplacement a serpentinization of the olivine and alteration of the pyroxene and chromite took place. The second phase of deformation crushed the chromite again when the igneous massif was overthrusted on the sediments. In Bulfat the extensive high temperature contact of gabbro suggests a postorogenic intrusion.

ACKNOWLEDGEMENTS

Thanks are due to J. ASTRUC for carry out the microprobe analyses and to DR. K. MALKE and to the staff of the X-ray department at the State Organization for Minerals for their help and cooperation.

REFERENCES

BOWEN, N. L., TUTTLE, O. F. (1949): The system MgO-SiO_2-H_2O. Geol. Soc. Amer. Bull. **60**, 439—460.

BUDA, G. and AL-HASHIMI WISSAM, S. (1977): Petrology of Mawat ophiolitic complex northeast Iraq. Jour. Geol. Soc. Iraq. X, 69—98.

COLEMAN, R. G. (1971): A hypothesis of origin for podiform chromite deposits. Geochim. Cosmochim. Acta. **39**, 1061—1074.

DICKEY, J. S. (1975): A hypothesis of origin for podiform chromite deposits. Geochim. Cosmochim. Acta. **39**, 1061—1074.

HESS, H. N. (1962): History of ocean basins. Geol. Soc. Amer. Petrology studies, a volume in honour of Buddington, A. F. Petrology studies, 599—620.

IRVINE, T. N. (1963): Chromian spinel as a petrogenetic indicator. Part I. theory. Can. J. Earth Sci. **2**, 648—672.

JACKSON, E. D. (1969): Chemical variation in coexisting chromite and olivine in chromitite zone of the Stillwater complex. Symposium on magmatic ore deposits. Econ. Geol. Monograph. **4**, 41—71.

LONEY, R. A., HIMMELBERG, G. R. COLEMAN, R. G. (1971): Structure and Petrology of the Alpine type peridotite at Burro Mountain, California, U. S. A. Jour. Petrology. **12**, part 2, 245—309.

MACGREGOR, I. D. (1967): Mineralogy of model mantle compositions. In Ultramafic and related rocks. pp. 382—393.

PAVLOV, N. V. (1949): Chemical composition of chromespinelids in relation to petrographic composition of ultrabasic intrusive rocks. Tr. Jn. Geol. Nauk. An. U. S. S. R. no. **103**,

RODGERS, K. A. (1973): Chrome-spinels from the Massif du Sud, southern New Caledonia. Min. Mag. **39**, 326—339.

THAYER, T. P. (1964): Principal features and origin of podiform chromite deposits and some observations on the Guleman Soridag District. Turkey. Econ. Geol. **59**, 1497—1524.

ULMER, G. C. (1974): Alteration of chromite during serpentinization in the Pennsylvania Maryland District. Am. Min. **59**, 1236—2342.

YODER, H. S., SAHAMA, Th. G. (1957): Olivine X-ray determinative curve. Am. Min. **42**, 475—491.

Manuscript received, 23 April, 1987

Acta Mineralogica-Petrographica, Szeged, XXIX, 81—93, 1987—1988

REDEPOSITED VOLCANOCLASTIC LIMESTONE IN THE EASTERN MECSEK MTS., SOUTHERN HUNGARY

SZ. HARANGI

Department of Petrology and Geochemistry, Eötvös University

ABSTRACT

In the eastern Mecsek Mts. of Southern Hungary, various volcano-sedimentary mixed rocks have been recognized: redeposited volcanoclastic limestone, intrusive breccia?, and local mixing at the contacts between limestone and magmatites. The redeposited volcanoclastic limestone described in detail in this paper, consists of volcanogenic and sedimentary clasts and limestone matrix. The rock is underlain by Oxfordian limestone and overlain by Lower Cretaceous basaltic lava breccia. The volcanic fragments exhibit different petrographic features (various texture, vesicularity, alteration and composition) indicating that they were derived from different lava flows. The rock formed by debris flow in a rough basin topography, associated with a continental rift-type basaltic volcanism.

INTRODUCTION

The Mesozoic sequence of the eastern Mecsek Mts., Southern Hungary is known from the Lower Triassic. During the Middle and Upper Jurassic pelagic sediments (limestone, calcareous marl) were deposited dominantly; the Oxfordian cherty limestone and radiolarite indicate the greatest depth of the sea. The paroxysm of the submarine basaltic volcanism was reached during Valanginian and Hauterivian time. Various mixed rocks composed of volcanogenic and sedimentary components formed due to the volcanic activity and the accompanying tectonic movements. Based on their origin 3 groups can be separated:

1. Upper Jurassic-Berriasian redeposited volcanoclastic limestone. It is composed of volcanogenic and sedimentary clasts and limestone matrix. This rock appears in the area of the Kisújbánya basin *(Fig. 1)*, in the middle of the Márévár valley, one of the left tributaries of Singödör valley and in the borehole Hosszúhetény XX.

2. Contact between sediments and volcanics, as local mixing occurs frequently. Calcareous sediments were penetrated by volcanic fragments, while lava flows incorporated limestone clasts. The original texture was preserved in some of these sedimentary fragments. At the Márévár valley small (2—3 mm) limestone amygdales can be found in the basalt. Such a local mixed rock appears especially in the vicinity of the Singödör valley, in the Hidas valley and Márévár valley.

3. Volcanoclastic mixed rock. It may be intrusive breccia in the area of Máza and Váralja-South (NE-Mecsek). Two boreholes (Váralja-11, BÓNA *et al.*, 1983; and Váralja-29) display this rock composed of volcanic and sedimentary (mainly siltstone and sandstone) clasts embedded in a fine grained matrix. The position in the sequence and its petrographical features indicate intrusive breccia origin. Investigation of this rock is in progress.

H—1088 Budapest, Múzeum krt. 4/A Hungary.

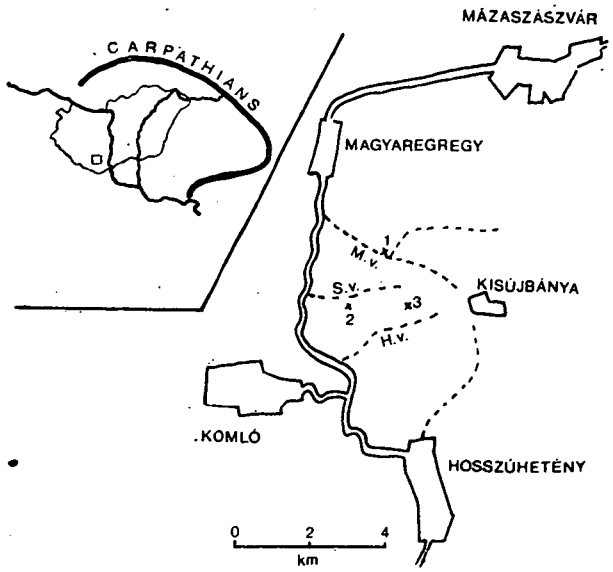

Fig. 1. Localities of redeposited volcanoclastic limestone: 1. Márévár valley, at the mouth of Somosi csörge 2. Left tributary of the Síngödör valley 3. Borehole Husszúhetény XX. (M. v.=Márévár valley, S. v.=Síngödör valley, H. v.=Hidas valley)

In this paper the redeposited volcanoclastic limestone is described only from the aspect of petrography and origin.

The first description of the Mecsek mixed rocks was made by NAGY, (1967), concentrating on the contact effects of the volcanic material in the limestone. He supposed that the volcanic clasts had got through joints into the limestone. Based on textural features BILIK, (1979) divided the volcanic clasts into three groups in the borehole Hosszúhetény XX. NAGY, (1986) investigated the mixed rocks in a new aspect. After describing the resedimentation features in thin sections he set up a model. He supposed a long time preserving of calcareous mud in unconsolidated state. Based on his micropaleontological and sedimentological investigations he explained the formation of mixed rocks with submarine resedimentation.

KOVÁCS, (1988) described olistostromes composed of volcanic and sedimentary components in the Uppony Mts., Northeastern Hungary, which may be similar genetically to the Mecsek redeposited mixed rock.

In the Lahn Dill area (FRG) and Eastern Thüringia (GDR) volcano-sedimentary mixed rocks have been reported under various name (Schalstein s. l., Dillenburger Schichten, Langenaubacher Breccia). Although they underwent low-grade metamorphism, on the basis of the microscopic features (LEHMANN, 1941) and petrographical descriptions (LIPPERT *et al.*, 1970; RÖSLER, 1960) the similarity to the Mecsek mixed rocks is conspicuous. In the Black Flysch and Rarau-Haghimas Syncline of the Eastern Carpathians similar rocks occur as well (SANDULESCU *et al.*, 1981; RUSSO—SANDULESCU *et al.*, 1979).

FIELD DESCRIPTION

The redeposited volcanoclastic mixed rock is underlain by Oxfordian siliceous limestone and overlain by Valanginian (?) lavabreccia and hyaloclastite.

At the Singödör locality a long sequence from the Bajocian marl to the Lower Cretaceous volcanics is exposed in a small tributary. The 4.5 m thick mixed volcanic-limestone unit is situated in the middle of the valley, underlain by vertical cherty limestone layers. Within this unit Upper Jurassic and Berriasian volcanic-free limestone boulders (up to 1.5 m in diameter) are embedded in a soft volcano-sedimentary material *(Fig. 2.A)*.

The Márévár valley locality exposes a ca. 20 m long green, greyish green and in some places brown, friable to hard mixed sequence. Its real thickness can be up to 5—6 m only — the rock dip to the SE *(Fig. 2.B)*. The varying hardness of the rock is due to its variable proportions of volcanic material content. Numerous rounded,

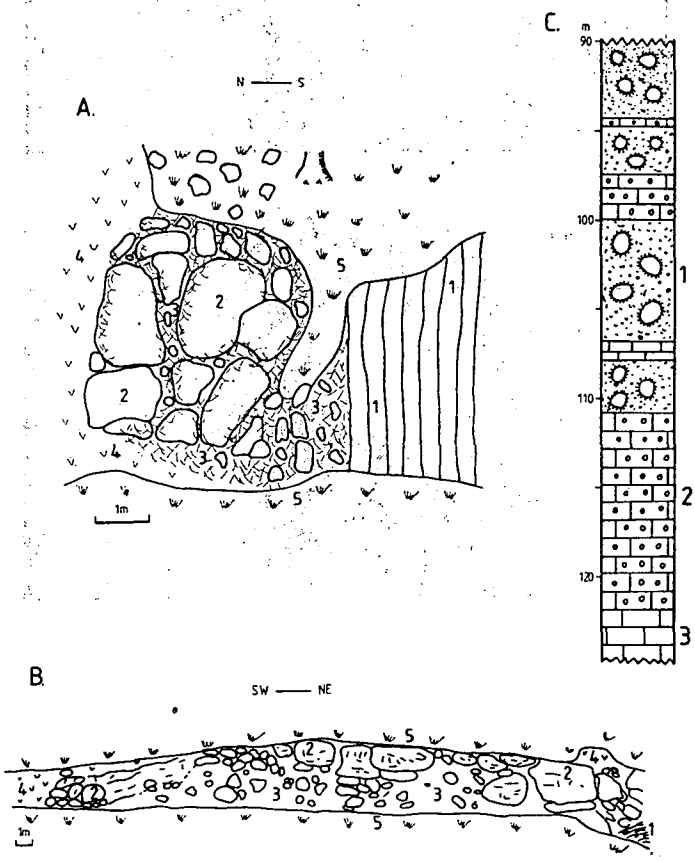

Fig. 2. Sketch of the outcrops of redeposited volcanoclastic limestone: A.) Síngödör tributary; B.) Márévár valley (1. Oxfordian siliceous limestone; 2. limestone boulders embedded in volcanoclastic mixed rock; 3. Volcanoclastic mixed rock with fine grained clasts; 4. Weathered lava breccia, hyaloclastite; 5. Soil and debris.) (after HARANGI, 1987, modified) C.) Borehole Hosszúhetény XX. between 90 m and 125 m. (1. lava breccia; 2. redeposited volcanoclastic limestone; 3. limestone) (after BILIK, 1979, modified).

hard fist-sized limestone blocks with low volcanogenic content are enclosed by a frequently exfoliated, friable — weathered — carbonate material with high volcanogenic content. In the inner part of the limestones no volcanic material can be observed, but in its marginal parts volcanic clasts appear. The contact between these two field is indistinct *(Figs. 3, 4, 5)*.

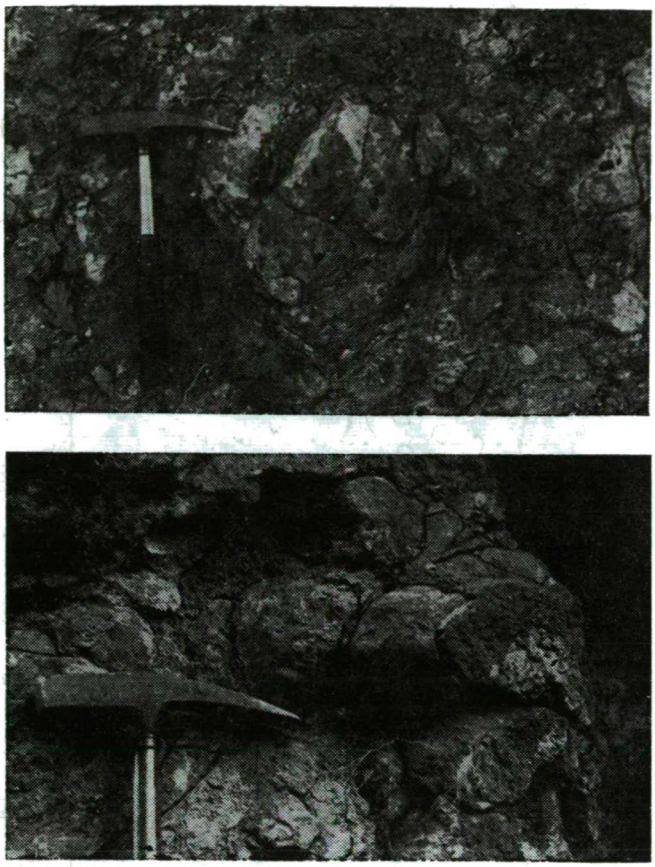

Fig. 3—4. Rounded hard siliceous limestone clasts are surrounded by soft vocanoclastic mixed material (Márévár valley).

The borehole Hosszúhetény XX. between 90 m and 125 m exposes alternating volcano-carbonate mixed rock and basaltic lavabreccia units *(Fig. 2.C)*. These are underlain by Upper Jurassic limestone (BILIK, 1979).

In this paper the first two localities are described in detail.

In both outcrops we can often find some slickensides and shear surfaces due to the post-consolidation movement of the rocks. The volcano-carbonate mixed rock can be crumbled in some places, where most of the volcanic clasts are weathered to clay-minerals and limonite, but generally it is medium hard. The harder limestone fragments have predominantly green-greenish blue colour. Especially in the Márévár valley the rock often diplays oriented texture with alternating bands of limestone

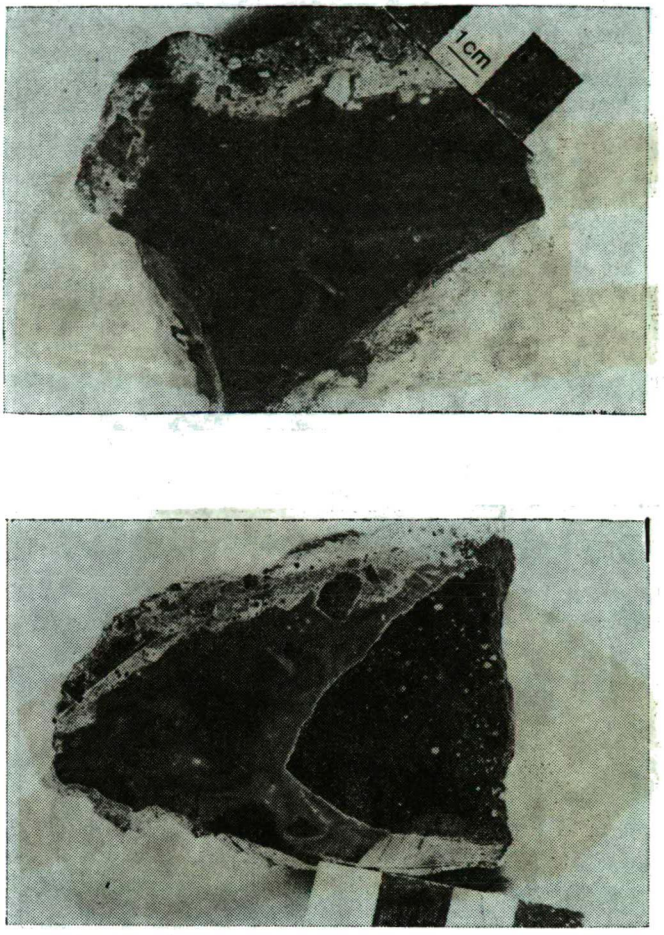

Fig. 5—6. Volcanoclastic mixed material appear in the marginal part of siliceous limestone core, which may contain larger (up to 8 cm diameter) volcanic clast.

matrix rich in volcanic clasts and dark green radiolarian limestone schliers and lenses poor in clasts *(Fig. 8)*.

The larger (5—15 cm) clasts are generally more or less rounded *(Fig. 7, 9, 10)*, but the cherts and radiolarites fragments are angular. The green clast-poor siliceous limestone frequently shows a banded, flow structure, which can be observed to the naked eye too, but in some parts the deep and light green bands blend chaotically.

The volcanic clasts are up to 15 cm, however, most of them are less than 1 cm in diameter. Most of the volcanic fragments are brown or grey, with carbonate and chlorite amygdales. The unweathered fragments are larger, they fall into the range of 5—15 cm in size, containing often fresh pyroxene phenocrysts. Numerous clasts are surrounded by a thin (up to 0.05 mm) light-coloured rim.

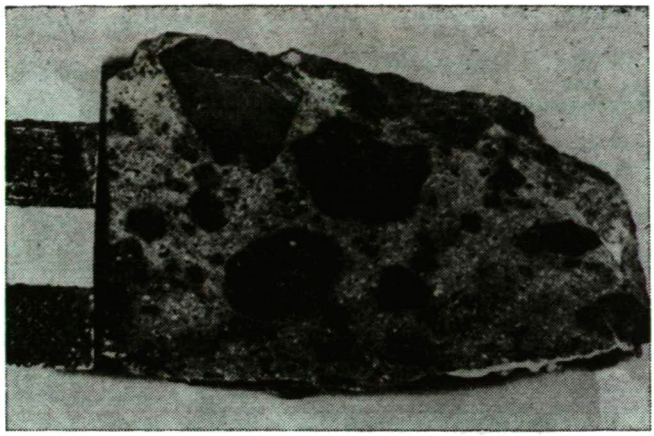

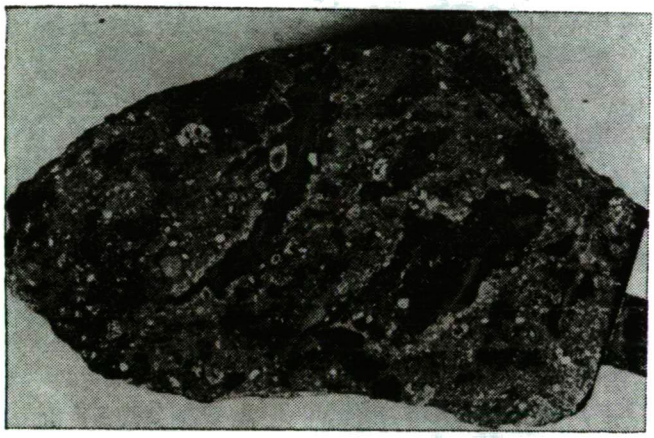

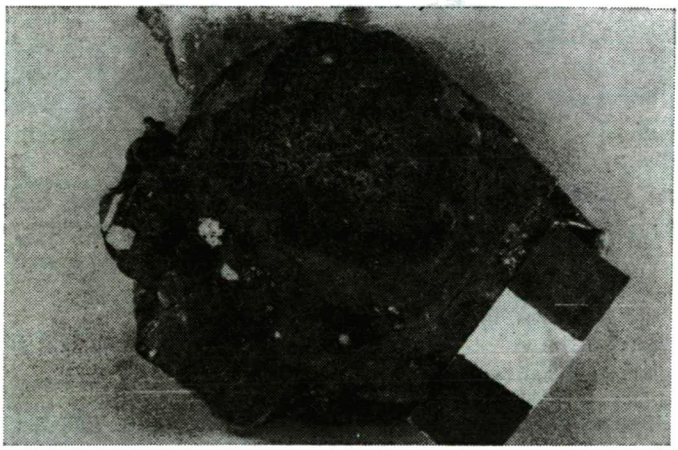

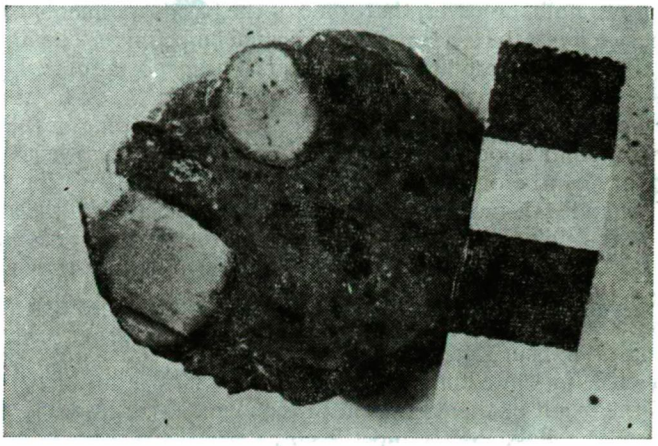

*Fig. 7—10.*Characteristic polished surfaces of the redeposited volcanoclastic limestone. There are more or less rounded clasts in the limestone matrix. Oriented radiolarian limestone lensens poor in clasts appear in the mixed rock frequently

PETROGRAPHY

The volcano-carbonate mixed rock consists of the matrix and the clasts:

Matrix: limestone, clayey limestone — the volcanoclastic parts are coloured by limonite.

Clasts: (1) Volcanic clasts: totally altered glass shards, amygdaloidal alkaline carbo-chloro basalt, alkaline chloro-nontro basalt, carbobasalt, basalt, trachytoid feldspar basalt, spilitic basalt. (2) Sedimentary clasts: calpionellid limestone, radiolarian siliceous limestone, radiolarite, chert. (3) Crystal clasts: plagioclase, pyroxene, pseudomorphs after mafic minerals, calcite, quartz.

The greatest part of the clasts are volcanogenic (ca. 75%), the sedimentary portion amounts to 20% (in vol% it is greater) and the crystal clasts are present in minor proportions (5%).

We could obtain information about the composition of the redeposited volcanoclastic limestone mainly on the basis of microscopic study considering the small sizes of the clasts.

The banded character of the rock can be recognized in thin section samples, too. Grey micritic-, brown clayey-limonitic-, radiolarian siliceous limestone bands and bands with coarse calcite crystal clasts alternate, interfinger with each other or chaotically blend one another in the volcanic clast-free limestone parts. The calcite crystals frequently appear oriented within the bands. The limestone parts with clasts coloured by limonite are not bordered sharply by the clast-free parts, there is a continuous transition between them. Compaction features occur and the calcite crystals are oriented around some clasts showing the direction of the embedding.

The shape of the clasts are variable, there are perfectly rounded, but amoeba-like irregular and angular forms, too. According to FLOYD, (1986) the degree of angularity attained by volcanic clasts is the function of both cooling fracture brecciation and submarine erosion. The highly vesicular glassy clasts are irregular shard-like fragments, the larger, glassy or holocrystalline basalt clasts have more rounded

margins. We have to note, however, that some of the basalt fragments have irregular, branching shape, wich may be explained by semisolid embedding. The limestone clasts are predominantly rounded produced by submarine transportation.

The contact between the carbonate matrix and the clasts can be „static" or „dynamic". In the first case the boundary is sharp, rectilinear, while in the other case a more complicated contact occurs, they interfinger with each other or sometimes indistinct boundary can be observed between them. NAGY. (1986) separated strong, distinct, indistinct and statistical boundary relating to the nature of the accumulation. Around most of the volcanic fragments a dark limonitic rim appear with various width (0.01—0.04 mm) *(Fig. 11, 12)*. LEHMANN, (1941) explained the dark rim at the contact between the „weilburgit" and the carbonate wall-rock in the Lahn-Dill area (FRG), with physical and chemical influences of the magma penetrating the sediments. BILIK, (1979) suggested that the limonitic rim-zones around the volcanic fragments prove the hot-state embedding of the volcanics. I am of the opinion that the dark rim is the result of the migration of the elements released by the alteration (devitrification) of the glass shards and the glassy groundmass of the volcanic clasts. The water diffusing to the volcanic glass can remove some cations — especially Fe, Mg, Ti and Ca (PESTY, 1985). The Fe and Ti as magnetite and ilmenite may have accumulated at the rim of the volcanic clasts and other boundary of inhomogeneous fields (eg. at the margin of the amygdales). Later these rims were oxidized to limonite. HENTSCHEL and THEWS (1979) stressed that the half-opaque rim appearing at the margin of the vesicles and fragments and composed of Ti-minerals is characteristic to palagonite tuffs.

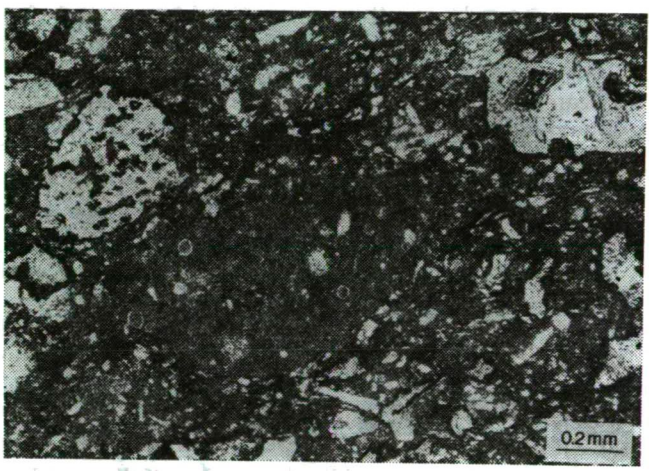

Fig. 11. Clast-free calpionellid limestone clast with indistinct boundary (in the middle of the picture.) The volcanoclastic limestone matrix encloses originally glass shards altered to carbonate minerals, with dark rim around them (Síngödör tributary).

(1) *Volcanic clasts*

According to the embedding state of the volcanics, two groups can be separated (I have to note that this embedding does not mean here only getting into the present matrix, but into a previous carbonate matrix as well.):

(1.1) Volcanic clasts embedded into the sediments in cold, solid-state: they can be characterized by predominantly rounded margin, compaction feature in the car-

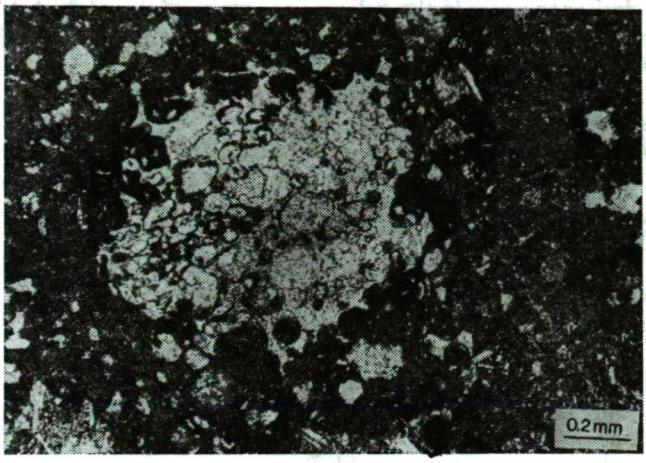

Fig. 12. Originally vesicular glass shard altered to calcite with dark rim around it embedded in limestone matrix (Márévár valley).

bonate matrix near their edges and the oriented calcite crystals around them. Dark rim zone appears rarely.

(1.2) Volcanic fragments embedded into the sediment in semisolid-state: amoeba-like, irregular shape and the „dynamic" contact are characteristic of this type of clasts. Incorporation of carbonate material by the volcanics is common. Dark rim-zone frequently occur (the chemical interaction may have been stronger in this case), but it can be absent, as well.

The volcanic fragments exhibit different petrographic features (various texture, vesicularity, alteration and composition) indicating that they derived from different lava flows. The majority of the volcanogenic clasts are the irregular, highly vesicular altered glass shards showing strongly cuspate margins formed by the curved interior surfaces of the vesicles. The alteration products are mostly carbonate minerals and limonite, and less chlorite-nontronite. The presence of preserved opaque rims within the clasts indicate the originally vesicular structure *(Fig. 11, 12)*. Alteration of volcanogenic clasts may have taken place in two stages: soon after the initial eruption on the submarine surface and after transportation in the calcareous sediments. The chlorite, chlorite-nontronite and limonite assemblages may indicate the first phase of alteration, while the second stage is represented by carbonate minerals (FLOYD, 1986).

Most of the volcanic fragments being larger than 1 cm in diameter are volcanics with higher crystallization degree. They are characterized by various textures and more or less alteration degree. Olivin and pyroxene are present only occasionally, but generally in the form of carbonate or chlorite pseudomorph. Pyroxene phenocrysts are more common than olivine and in some parts they occur with plagioclase phenocrysts forming cummuloporphyritic groups. Fresh pyroxene are common in the larger (ranging from 5 to 15cm) clasts only. Their optical characters suggest augitic composition.

Plagioclase phenocrysts (0.5—20 mm) are more common than the mafic constituents. They are fresh or medium altered. In the limestone matrix some calcite clasts can be observed, which enclose fresh plagioclase phenocrysts *(Fig. 13)*. Their origin cannot be explained unambiguously because of their small sizes (max. 3 mm)

and the lack of similar samples in the volcanic sequence of the Mecsek Mts. The composition of plagioclase phenocrysts was determined by using an universal stage. On the basis of their optical characters they have a composition of An_{50-60}. Plagioclase laths in the groundmass are more acidic, they are andesine-oligoclase, in some part albite in composition.

The originally glassy groundmass altered to chlorite-nontronite or montmorillonite, limonite or carbonate minerals. Tiny magnetite grains and ilmenite-leucoxene needles are very common in it, in some parts they appear densely. In the spilitic basalt clasts fine grained quartz occur quite often.

The great proportion of amygdales in the volcanic clasts are remarkable. Genetically two types of amygdales can be separated: vesicles infilled subsequently by secondary minerals and so-called pseudo-amygdales (RÖSLER, 1960; BILIK, 1979). These latter are remains of the magmatic incorporation of carbonate material. Steps of the incorporation of carbonate mud can be seen in the mixed rock too, suggested that some of the volcanic clasts were semi-solid in the time of embedding into the calcareous sediment. Some volcanic fragments enclose unaltered calpionellid limestone „amygdales" *(Fig. 14)*, bag-like swallowing of the carbonate matrix is also common at the margin of the volcanics.

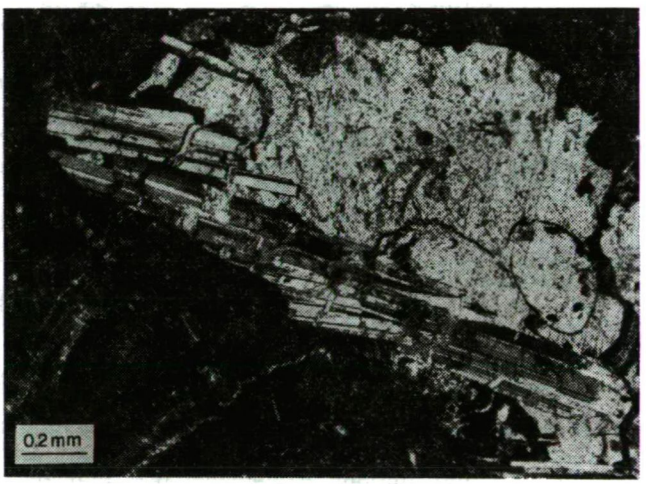

Fig. 13. Clacite clast encloses fresh plagioclase phenocrysts embedded in limestone matrix (Síngödör tributary).

(2) Sedimentary clasts

The two outcrops are different to one another considering the sedimentary clasts. At Singödör side-valley locality younger — Tithonian and Berriasian — rocks dominated (calpionellid limestone), while in the Márévár valley the age of the rocks is predominantly Kimmeridgian and Oxfordian (siliceous limestone) (NAGY pers, comm.). On the basis of embedding, the sedimentary fragments can be divided into two groups: (a) lithified and (b) semi-lithified clasts and fragments embedded in mud-state (see also NAGY, 1986). The contact between the latter ones and the carbonate matrix is indistinct *(Fig. 11)*. The clasts are more or less rounded, some of them

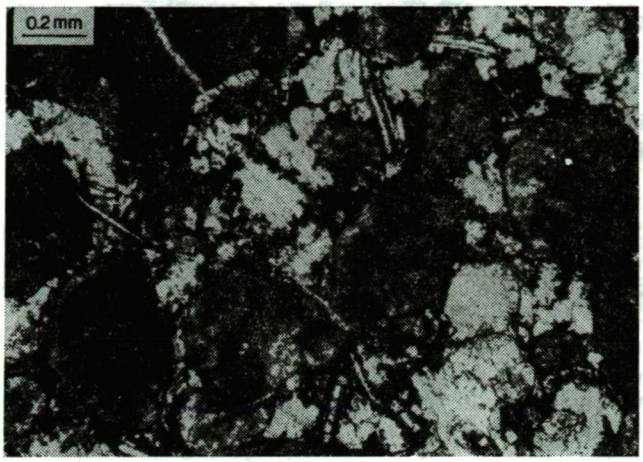

Fig. 14. Calpionellid limestone amygdales in basalt clast embedded in limestone matrix (Márévár valley).

lenticular, but the strongly siliceous limestone, chert and radiolarite fragments are angular. They are free of volcanic material and the limonitic impregnation characteristic for the the matrix, cannot be observable in them.

(3) Crystal clasts

Crystal fragments amount to the minor part of the volcanoclastic mixed rock. In the Singödör tributary the majority of them are plagioclase phenocrysts while in the Márévár valley pyroxene crystals dominate. The plagioclase crystal clasts are predominantly fresh, ranging from 0.02 to 0.5 mm. Their composition is similar to the phenocrysts of volcanic clasts, they are andesine-labradorite. Around some pyroxene crystal fragments compaction features can be observed. They are more or less altered, ranging from 0.5 to 4.5 mm and based on their optical properties their compositions are augitic. In the limestone matrix calcite and chlorite pseudomorphs appear frequently as well. Rounded quartz crystal clasts occur rarely.

(4) Matrix

The matrix of the redeposited volcanoclastic mixed rock is limestone, clayey limestone being coloured by limonite in the parts of the volcanoclastic field. The limestone is micritic, but calcite crystal clasts (0.01—1.3 mm) frequently appear. Generally the matrix itself is mixed, fossils and calcareous materials of different ages build it up mixing chaotically or arranged in bands (NAGY, 1986). The microfossils were identified by NAGY, according to him the matrix of the rock in the Márévár valley is predominantly Lower Kimmeridgian, partly enclosing Upper Oxfordian fossils. Some younger (Tithonian-Berriasian) microfossils can be found in uncertain preservation in the amygdales of a volcanic fragment. At the Singödör tributary and the borehole Hosszúhetény XX. the rock can be characterized by more mixed microfossil assemblage (Lower Kimmeridgian-Berriasian).

FORMATION OF THE REDEPOSITED VOLCANOCLASTIC LIMESTONE

According to the deep sea researches (Deep Sea Drilling Project) it is obvious that in marine environment where volcanic activity occurs, volcanic clasts can be embedded in sediments due to transportation by mass flows (at the flanks of seamounts and at the deep-sea trenches; LONSDALE and SPIESS, 1979; MURDMAA and AVDEIKO, 1980; MOBERLY and SCHLANGER *et al.*, 1986) or pyroclastic eruptions (VALLIER *et al.*, 1977; ROETHE and KOCH, 1976).

The volcano-sedimentary mixed rocks of the Dillenburger Schichten and Langenaubacher Breccia in Lahn-Dill area (FRG) were formed by reef-splitting due to the volcanic activity and the accompanying tectonic movements. Mixed sediments composed of volcanic and sedimentary clasts were accumulated at the flanks of the reef in the basin (LIPPERT *et al.*, 1970).

KOVÁCS, (1988) explained the origin of olistostromes of Uppony Mts., NE-Hungary by earthquakes accompanied by subaqueous basic volcanic activity, which resulted incorporation of the underlying carbonate sediments into the downslope moving lava flow.

A common feature of the Mecsek redeposited mixed rock and the other similar formation (Uppony Mts., Lahn-Dill, Eastern Carpathians) is their connections with submarine continental rift-type basaltic volcanism. The tectonic movements initiated by the rifting made a rough basin topography, smaller and larger seamounts were formed and the differences of bottom levels made possible resedimentation processes.

The age of the redeposited volcanoclastic limestone is not clear. According to the micropalaeontological investigations of NAGY, the oldest constituents of the rock are Upper Oxfordian, the youngest are Berriasian. NAGY, (1986) established a mixing of materials of different ages in Upper Jurassic-Lower Cretaceous limestones and stressed that the lime-mud may have been preserved as long as 30 Ma in unconsolidated state. The lasting lime-mud state is not rare in the recent marine environment: the DSDP Sites-sections expose even Eocene and Cretaceous — mud-state sediments, composed of mixed microfossil assemblages in some parts (eg. Eocene to recent; MURDMAA and AVDEIKO, 1980).

The resedimentation model (NAGY, 1986) can be applied to the interpretation of the formation of the redeposited volcanoclastic limestone. The Late Jurassic-Berriasian sequence of Mecsek Mts. was deposited in a bathyal environment (rich plankton, absence of benthos), but rarely neritic facies occured as well. The complex basin topography and the delayed lithification of carbonate sediments after Oxfordian age made possible the resedimentation and mixing of lime muds of different ages. Initiation of the basaltic volcanism associated with earthquakes and submarine eruptions (formation of pillow lava, lava breccia and hyaloclastite) accelerated this process. Solid and semi-solid volcanic clasts formed large slumps together with limestone blocks, soft carbonate mud and were embedded in carbonate mud in the deepest parts of the basin. Later these local mixed debris flow-sediments were covered by basaltic lava-breccia and hyaloclastite produced by the paroxysm of the volcanic activity.

ACKNOWLEDGEMENTS

Thanks are due to I. NAGY, Cs. SZABÓ and I. BILIK for the discussions of the Upper Jurassic-Lower Cretaceous sedimentation and volcanism of Mecsek. I would like to thank I. NAGY for the identification of microfossiles of the mixed rock. I appreciate the helpful comments on our manuscript offered by I. BILIK, Cs. SZABÓ, M. KÁZMÉR and S. KOVÁCS.

REFERENCES

BILIK, I. (1979): A Mecsek hg. alsókréta tengeralatti vulkáni képződményei. (The Lower Cretaceous volcanic rocks of submarine origin from the Eastern Mecsek Mts.) M. Sc. Thesis. Loránd Eötvös University, Budapest.

BÓNA J., KOVÁCS E., SZILÁGYI T. (1983): Vulkáni-törmelékes képződmények a Váralja 11. sz. fúrásban. (Volcanoclastic rocks in the borehole Varalja-11.) — Földt. Kut. **26** (2—3), 87—94.

FLOYD, P. A. (1986): Glassy and basaltic fragments within graded volcaniclastic sediments. East Marina Basin, DSDP Leg. 89 — Init. Repts. DSDP **89**, Washington (U. S. Govt. Printing Office), 433—446.

HARANGI, SZ. (1987): Volcano-sedimentary carbonate rocks in the Mecsek Mts. In: KÁZMÉR, M. (ed.): Field Workshop on Mesozoic Sediments in the Mecsek and Villány Mts. of Hungary, Guidebook. Department of Paleontology, Eötvös University, Budapest. 37—42.

HENTSCHEL, H., THEWS, J. D. (1979): Erlauterungen zur Geologischen Karte von Hessen 1:25 000. Blatt Nr. 5514, Hadamar. — Wiesbaden.

KOVÁCS, S. (1988): Devonian olistostrome with limestone olistoliths and volcanic matrix from Strazsa hill, Uppony Mts., Northeastern Hungary. (in Press.)

LEHMANN, E. (1941): Eruptivgesteine und Eisenerze in Mittel- und Oberdevon der Lahnmulde. — Wetzlar.

LIPPERT, H. J., HENTSCHEL, H., RABIEN, A. (1970): Erlauterungen zur Geologischen Karte von Hessen 1:25 000. Blatt Nr. 5215, Dillenburg. — Wiesbaden.

LONSDALE, P., SPIESS, F. N. (1979): A pair of young cratered volcanoes on the East Pacific Rise. — J. Geol. **87**, 157—173.

MOBERLY, R., SCHLANGER, S. O. *et al.* (1986): Initial Repts. DSDP **89**. — Washington (U. S. Govt. Printing Office).

MURDMAA, I., Avdeiko, G. P. (1980): Volcanoclastic constituents in Leg 55 sediments. — Initial Repts. DSDP 55. — Washington (U. S. Govt. Printing Office), 503—505.

NAGY, I. (1967): A felsőjura képződmények és a kréta vulkanitok viszonya a Mecsekben. (Sur le rapport entre le Jurassique Superieur et les roches volcaniques Cretacees dans la Montagne Mecsek) — Ann. Rep. of Hung. Geol. Survey from 1965., 149—168.

NÁGY, I. (1986): A reverz reszedimentáció és a mésziszap-állapot tartósságának bizonyitékai a mecseki felsőjura-alsókréta mélytengeri mészkövekben. (Evidence of reverse resedimentation and lasting lime mud state in the Upper Jurassic-Lower Cretaceous bathyal limestones of the Mecsek Mts. — Ann. Rep. of Hung. Geol. Survey from 1984., 591—609.

PESTY, L. (1985): Kőzetüveg minták kísérleti-kőzettani vizsgálata. (Experimental-petrological investigation of volcanic glass samples). Mineralogical-Geochemical Selections. MTESZ Szeged, 112—136.

ROETHE, P., KOCH, R. (1976): Miocene volcanic glass from DSDP Sites 368, 369 and 370. — Initial Repts. DSDP **41**. —Washington (U. S. Govt. Printing Office).

RÖSLER, H. J. (1960): Zur Petrographie, Geochemie und Genese der Magmatik und Lagerstatten des Oberdevons und Unterkarbons in Ostthuringen. — Freib. Forsch. **H. 92**, 1—275.

RUSSO-SANDULESCU, D., UDRESCU, C., MEDESAN, A. (1979): Petrochemical characteristics of the Mesosoic ophiolites of the Rarau—Haghimas marginal Syncline. — D. S. Inst. Geol. Geofiz. **66.**, 153—185.

SANDULESCU, M., KRAUTNER, H. G., BALINTONI, I., RUSSO-SANDULESCU, D., MICU, M. (1981): The structure of the East Carpathians (Moldavia—Maramures area.) — Guidebook to Excursion B1. Carpatho—Balkan Geol. Ass. XII. Congr. Bucharest 1981., 18—21.

VALLIER, T. L., BOHRER, D., MORELAND, G., MCKEE, E. E. (1977): Origin of basalt microlapilli in Lower Miocene pelagic sediment, northeastern Pacific Ocean. — Geol. Soc. Amer. Bull. **88,** 787—796.

Manuscript received, 27 May, 1988

Acta Mineralogica-Petrographica, Szeged, XXIX, 95—106, 1987—1988

GENERAL GEOLOGICAL SETTING AND CHARACTER OF TURKISH SEPIOLITE DEPOSITS

TANER IRKEÇ

General Directorate of Mineral Research and Exploration of Türkey (MTA)

ABSTRACT

Field exploration work and analytic research on the Konya-Yunak sepiolite clearly revealed that the occurence was a result of the replacement of magnesite by sepiolite mineral in the magnesite pebbles and fragments derived from the surrounding magnesite deposits, and transported to the Miocene sedimentary basin. The replacement process developed under alcaline conditions bearing sufficient silica. Along with the pebbles composed wholly of magnesite or sepiolite, there also occur pebbles composed of both minerals in a crystalline mixture. But even sepiolitic concretions still preserve more or less the primary physical properties of magnesite. Serpentine minerals, dolomite and calcite have not entered into the formation reactions. Excess silica has precipitated as nodules or veinlets. On the other hand, matrix of the meerschaum consists mostly of the mineral palygorskite, which generate under almost the same contitions, except of a higher Al^{3+} ion concentration.

INTRODUCTION

Natural ore deposits of economic significance, composed principally of the mineral "sepiolite" may occur as sedimentary type bedded deposits or as concretional type meerschaum (in Turkish "lütetasi") deposits. While the first type occurs as small or relatively large scale deposits in various countries, the occurence of meerschaum is recorded only at a number of districts (e.g. in Tanzania and the USA), the most outstanding of which are located in Turkey. Turkish meerschaum is unique from the point of view of several mineralogic and physical properties demanded in the world markets, such as pureness, softness, whiteness, etc. Considering these phenomena, the geologic features and genesis of Turkish meerschaum will be brought principally as the subject of discussion in this paper, and will be completed by giving some brief information on the sedimentary, bedded type occurrences in the vicinity of Eskişehir Province in Central Turkey, with a table of comparison of various geological and physical properties of both types.

Turkish sepiolite (meerschaum type) mining activity is based mainly on the deposits in Eskisehir Province. In recent years, however, meerschaum deposits of similar physicochemical properties have been discovered in the Kony Province in Central Turkey, about 150 km southeast of Eskişehir *(Fig. 1)*.

Academic investigation on meerschaum have been concentrated mainly on these deposits (YENIYOL, 1982; YENIYOL and ÖZTUNALI, 1985), and correlation to those in Eskişehir has been realized, resulting in the establishment of many common geological features. Analytic data concerning XRD, DTA and TG investigation of Konya sepiolite exhibit an exact similarity of the two occurences.

Geological features and genesis of the above-mentioned two meerschaum occurrences will be described hereunder.

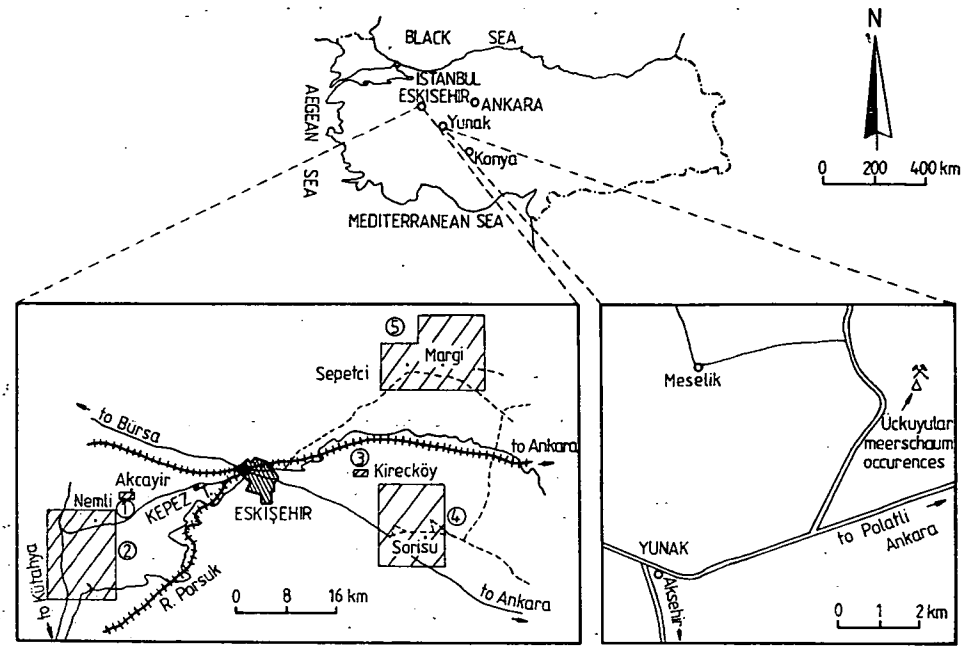

Fig. 1. Location map of the meerschaum deposits around Eskeşehir and Konya provinces, Central Turkey.

BRIEF HISTORY OF SEPIOLITE PRODUCTION IN ANATOLIA

Occurrence of sepiolite in Anatolia has been known since the Roman Epoch, and records on this are met in many historical documents. The first record on production and beneficiation date, however, is as late as the last decades of the 15th century (ÖNCEL and DENIZCI, 1982).

Sepiolite based industrial activity in Europa began to develop in the first half of the 18th century. Pipes and other ornametal goods were manufactured in Austria, Belgium and France, utilizing essentially the Turkish meerschaum. However, not long after, Vienna became the real and unique center of the world sepiolite trade. This situation continued until 1950, when goods made of meerschaum started to be manufactured in the Eskişehir Province.

Large-scale meerschaum mining activity in the vicinity of Eskişehir started around 1850's, in order to supply raw material to the European sepiolite industry. Production, which reached the peak with 12 000 boxes (1 box=app. 25 kg. of dry sepiolite) at the end of 19th century ceased in 1912, due to the political developments in Europe and Turkey. In the war years between 1913 and 1922, a small amount of procudtion was realized, and marketed together with the present stocks at a rate of about 200 boxes p.a. Since 1923, sepiolite production and mining activity have continued in an unstable way by traditional simple mining methods, with the production amount ranging from 41 to 3691 boxes p.a.

BRIEF INFORMATION ABOUT SEPIOLITE

Meerschaum, which is the concretional concentration of sepiolite, is mineralogically a hydrated magnesium silicate. Typical color of meerschaum is white to light gray. The mineral has a hardness of 2 to 2,5, with conchoidal to irregular fracturing. Specific gravity varies with porosity from about 2 to less than 1 (INDUSTRIAL MINERALS and ROCKS, 1975). Crystallographic structure may be monoclinal or pseudo-rhombohedra, while its chemical composition being stated in different forms by several investigators. BRAUNER and PREISINGER (1956) stated the chemical formula of meerschaum as $2MgO.3SiO_2.nH_2O$, while CAILÉRE and HÉNIN (1961) suggested a formula as $(Si_{12})(Mg_9)O_{30}(OH_6)(OH_2)_4.6H_2O$, based on X-ray determination of crystal structure. YENIYOL and ÖZTUNALI (1985), give the structural formula for the dehydrated half unit cell of the Konya sépiolite, on the basis of the chemical analysis carried out on specimens previously ignited at 1000 °C, as $Si_{12}/Al_{0.04}\ Fe_{0.09}\ Mg_{7.87}/O_{32}\ Ca_{0.01}$.

The mineral sepiolite contains zeolitic water, bound water, and constitution water in its structure, and dehydration occurs in four steps (NAGATA *et al.*, 1974; BAILEY, 1980).

Predominant occurence of crystalline fibers, which merge into sheetlike forms in a complex, interwined mass is characteristic at the scanning electron microscope (SEM) photographs of a Turkish meerschaum specimen (INDUSTRIAL MINERALS and ROCKS, 1975; p. 834). Structure of some sepiolites resemble to that of attapulgite and these have been named as "-sepiolite" or para-sepiolite (AKINÇI, 1967). The principal difference between fibrous attapulgite and sepiolite is that magnesium is replaced to some extend by aluminum in the former. Randomly distributed flaky type sepiolite, on the other hand, is termed as "β-sepiolite" (AKINÇI, 1967).

According to BRAUNER and PRESINGER (1956), no structural change occurs in meerschaum at igniting up to 350 °C, thus providing good absorption capability for iodine, mercury, oil and alcohol, which make the mineral utilizable in filtration and in the chemical industry, besides its traditional usage in ornamentation.

Genesis of sepiolite has been explained by diversing theories. In some of these, sepiolite occurence is suggested to be in direct relation to magnesite formation, while in some others direct generation, from serpentine being proposed (PARRY and REEVES, 1968; MILLOT, 1970; POST, 1978). Recent field and laboratory investigations on the Konya—Yunak sepiolite in central Turkey has shown clearly that the sepiolite formation took place in the detritic magnesite pebbles, which must have been derived from the surrounding magnesite deposits, and the co-existence of equi-dimensional rock fragments may support that the formation took place in diagenetic stage (YENIYOL, 1982; YENIYOL and ÖZTUNALI, 1985). The occurrence of pebbles with variable sepiolite to magnesite ratio point to the formation of sepiolite replacing magnesite. Quartz and dolomite minerals occuring as primary constituents of magnesite, on the other hand, have not taken place in the sepiolite formation process.

The mineral palygorskite, the main constituent of the matrix, is also a product of the "alkaline media rich in silica". In this case, however, the Al:Si ratio is higher. Existence of serpentinite, dolomite and calcite in the matrix show that these minerals have not entered into the sepiolite formation process (YENIYOL and ÖZTUNALI, 1985).

SEPIOLITE DEPOSITS IN TURKEY

Sedimentary, bedded type and concretional meerschaum type sepiolite occur in a number of districts in Turkey, but deposits of economic interest are located only in the vicinity of Eskişehir Province in central Turkey. On the other hand, field investi-

gations supported by analytical results have been concentrated on the occurrences around the Yunak town, which is located about 8 km. NE of Konya in central Turkey. Province of Konya is located about 150 km SE of Eskişehir *(Fig. 1)*. Similar geological setting of the two districts make the correlation of the data possible. These two deposits will be described under this heading.

Sepiolite deposits in Konya Province (Central Turkey)

These deposits are located at the Ückuyular district, close to the Yunak town in Konya Province *(Fig. 1)*. Magnesite deposits occur in the close vicinity. The deposits are not exploited at present.

General geology. The Yunak sepiolite occurrence is located in the Neogene conglomeratic sequence. It represents a lense 3 to 4 m. thick with 500 m of extension, gently dipping south concordant to the general trend of the sequence. The conglomeratic sequence, composed of large but generally rounded pebbles, is cemented by a light creamy matrix of dolomite, serpentinite, silicified serpentinite, recrystallized limestone, magnesite fragments and grains. Variable matrix type and pebbles, and degree of cementation are common throughout the sequence. Horizons of clay, sand and tuffs of alkaline volcanism may be observed occasionally (YENIYOL and ÖZTUNALI, 1985).

Massive, vein type and Blumenkhol type magnesite deposits occur within the surrounding serpentinized rocks, belonging to the ophiolitic assamblage. Pebbles of the conglomerate, whose diameters occasionally reach 25 to 30 cm, include magnesite and sepiolite in various ratios, preserving the composition and physical properties of the initial magnesite. Fractures of drying in the pebbles of sepiolitic composition, which are light creamy colored and slippery when wet, are filled with a sandy or silty material, and they partly bear very thin silica veinlets. Gradual change from magnesite to sepiolite may even be observed in a single pebble, and beside pebbles of total magnesite or sepiolite composition, those with sepiolitic magnesitic composition in various degrees may be found too. (YENIYOL and ÖZTUNALI, 1985).

Mineralogical composition. YENIYOL and ÖZTUNALI (1985) have studied the mineralogy and chemistry of the Yunak (Konya) sepiolite by using XRD, DTA, TG and chemical analysis techniques. For this purpose, specimens of sepiolite-magnesite and sepiolite composition, and highly altered serpentinite pebbles were chosen. The results will be summarized here.

The mineral sepiolite could be determined only in the pebbles of magnesitic appearance. The most intensive reflection of the sepiolite is from the (110) plane at 12,34 Å. Other reflections, their intensities and correlation to those of Eskişehir sepiolite are given in Table 1.

According to the mineralogical investigations, sepiolite is found together with magnesite in a crystal-mixture in the pebbles. The pebbles may contain quartz and dolomite. Sepiolite is not observed in serpentinite pebbles or in the "serpentinite matrix" (YENIYOL and ÖZTUNALI, 1985). XRD investigations reveal that the matrix composes completely of palygorskite, with very low amounts of serpentine mineral (essentially antigorite), dolomite and calcite.

The thermal behaviour of Konya and Eskişehir sepiolites may be followed from the DTA and TG patterns in *(Fig. 2)*. Endothermic reaction peaks at 100 °C, 320 °C an 490 °C are due to the release of zeolitic water and bound water, in two stages. With the release of water in the last two stages, "unhydrous sepiolite" forms, and a twining in mineral structure occurs (NAGATA *et al.*, 1974; SERNA *et al.*, 1975).

TABLE 1

X-ray powder diffraction data of Eskişehir and Konya sepiolites (after YENIYOL *and* ÖZTUNALI, *1985)*

hkl	Eskişehir		Konya	
	d(observed)	I	d(observed)	I
110	12.36	100	12.34	100
130	7.6	9	7.6	10
200, 040	6.7	5 b	6.8	7 b
150	5.0	5 b	5.0	8 b
060	4.51	35	4.50	30
131	4.32	25	4.30	35
260	3.74	20	3.73	25
080	3.36		3.36	
420	2.28	25 i, b	3.30	25 i, b
331	3.18		3.18	
261	3.05		3.05	
0.10.0, 510, 002, 441, 281, 530, 022, 112, 371, 191, 2.10.0, 390	2.67	40 i	2.68	40 i
132	2.49		2.49	
202, 042, 550, 1.11.0	2.45	20 i, b	2.45	15 i, b
222	2.40		2.37	
062, 312, 2.10.1	2.26	20 i	2.26	15 i
082	2.07	8 b	2.06	9 b
	1.88	4 b	1.88	5 b
			1.72	6 b
	1.69	6 b	1.69	8 b
	1.59	5 b	1.59	10 b
	1.55	6	1.55	10 b
	1.51	11	1.52	12

i=indistinguished, b=broad

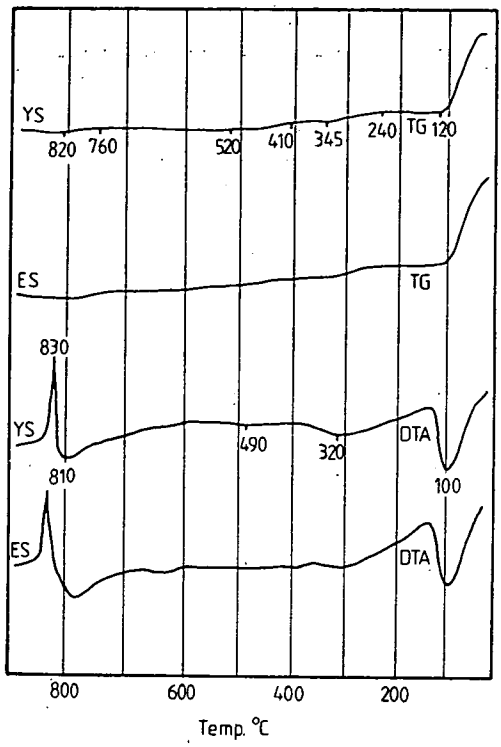

Fig. 2. TG and DTA patterns of Konya and Eskişehir sepiolites. YS=Yunak (Konya) sepiolite, ES=Eskişehir sepiolite.

The exothermic reaction at 810 °C reflects the transformation of sepiolite to a new mineral. the enstatite. As seen in *(Fig. 2)*, thermal characteristics of Konya and Eskişehir sepiolites show great similarity, except for some insignificant deviations.

Total release of water for the Konya sepiolite at 1000 °C is determined to be 21,63% (YENIYOL and ÖZTUNALI, 1985). Chemical composition is given in Table 2.

TABLE 2

Chemical composition of the Konya sepiolite. after YENIYOL *and* ÖZTUNALI *(1985)*

	wt %
SiO_2	53.02
Al_2O_3	0.19
Fe_2O_3	0.51
MgO	23.13
CaO	0.06
K_2O	0.02
Na_2O	0.02
Total H_2O	21.63
	99.58

According to these data, sepiolite formula calculated for dehydrated half unit cell is:

$$Si_{12}/Al_{0.04}Fe^{3}_{0.09}Mg_{7.87}/O_{32}Ca_{0.01}$$

Genesis. Konya sepiolite shows an exact similarity to that of Eskişehir, from the point of view of the sedimentary sequence in which it occurs, and the surrounding lithologic units. Occurrence of magnesite deposits around the sepiolite-bearing horizons and the close relation between the magnesite and sepiolite pebbles in the sedimentary sequence suggest a close genetic relation of sepiolite formation to magnesite. Even pebbles, composed of only sepiolite bear the imprint of all the physical properties of magnesite pebbles. These all lead to the conclusion that the sepiolite was formed in the diagenetic stage of conglomerates by in situ replacement of magnesite mineral, replacement being realized in several degrees (YENIYOL and ÖZTUNALI, 1985).

Quartz and dolomite minerals of the primary magnesite composition are preserved even in the wholly sepiolitized pebbles, i.e. these minerals have not interferred with the sepiolite formation reactions. On the other hand, absence of sepiolite formation in serpentinite may be considered as a distinct proof for the genetice relation of sepiolite to magnesite.

In consequence with the mode of occurence given above, it is not possible to relate directly the sepiolite formation to any rock member of the ophiolitic assemblage. Sepiolite formation is the result of a multi-stage alteration process of magnesium rich basic and ultrabasic rocks of the ophiolitic association. The alteration progressed from the serpentinization of the stated rocks through the magnesite formation under available physicochemical conditions, the transport of fragments to the sedimentary basin, and formation of nodules of magnesite in the sediments, with finally origin of sepiolite by the in situ replacement of magnesite under the influence of alkaline media rich in silica.

The mineral palygorskite, which is the main constituent of the matrix, is also formed under alkaline media rich in silica, like the sepiolite. However, the Al:Si ratio of these solutions must be higher (app. 3:1). For the formation of this mineral, beside Mg^{2+}, the presence of Al^{3+} ion in the media is necessary. This factor is responsible for the formation of palygorskite, consuming small magnesite grains which offer a much greater specific surface in the matrix, while sepiolite is forming by replacing magnesite in the pebbles. Presence of serpentinite, dolomite and calcite minerals in the matrix prove that these minerals have not entered into the formation process (YENIYOL and ÖZTUNALI, 1985). Palygorskite formation may be explained by "neoformation" from the solutions carrying Mg^{2+}, Si^{4+} ions, derived from the magnesian rocks in the vicinity, but needs support on the basis of detailed and laboratory investigation data.

Sepiolite deposits in Eskişehir Province (Central Turkey)

Although Konya—Yunak sepiolites are those on which scientific researches aiming to solve the mineralogy and genesis problems of sepiolite have been concentrated, deposits with economic reserves and on which mining activity is being carried out today are located in the Eskişehir Province. So far that the weerschaum type sepiolite is sometimes referred as "Eskişehir tasi" (Eskişehir stone) domestically. Meerschaum, which is produced by traditional simple mining methods in general, is beneficiated in the workshops in Eskişehir, after which the manufactured goods, mostly pipes and boul inserts, are offered to international and domestic markets.

Sepiolite occurrences in the Eskişehir Province are located at about 30 to 40 km. east and west of Eskişehir town center, and may be examined in 5 groups close to each other. These districts are shown in *(Fig. 1)*.

General geology. The meerschaum type sepiolite occurs in Neogene formations in the Eskişehir region

Lithologic units of pre-Neogene are schists, gneiss, greywacke, marble and granite of Palaeozoic, and ophiolitic rocks of Mesozoic.

Rocks of the ophiolitic assemblage are harzburgite and dunite type peridotites, pyroxenite, gabbro, radiolarian chert, serpentinite and silica-carbonate alteration products of the stated rocks. These rocks are exposed in wide areas in the west, northeast and southeast of Eskişehir.

Peridotites are located mostly in the central parts of the ophiolite areas. Those of dunitic composition are the host rocks for chromite, and chrysotile asbestos deposits, in minor.

In the northeast occur tectonite harzburgites. In the serpentinized sections, chrysotile and antigorite occur together with small magnetite grains, Stockwork, Blumenkhol and vein type magnesite deposits compose important reserves in the area.

In the northeast, around Margi and Sepetci villages *(Fig. 1)*, dunite is widely exposed. Along the Neogene contacts, wholly dolomitzed peridotites, undergone carbonate alteration are exposed.

Silica-carbonate alteration products are composed of chalcedony, microcrystalline quartz and limonite infiltrations. They carry small magnesite nodules in the west, around the Nemli village *(Fig. 1)*.

Gabbroic rocks crop out in the northeast and west of Eskişehir. These are composed of saussuritized plagioclase and augite, uralitized pyroxene, and rarely magnetite. Various schists and radiolarian cherts partly impart the assemblage. Mostly albite-epidot-chlorite schists crop out in the northeast. Neogene formations around Eskişehir overlie the Mesozoic formations unconformably, and are composed of Upper Miocene and Pliocene rocks. The widespread lithologic units of Neogene sediments are important for their being the host rocks for meerschaum and sedimentary, bedded type sepiolite occurences.

Upper Miocene in the Eskişehir region is represented by terrestrial conglomerate, composed of reddish-brown, angular ophiolitic rock fragments, schists and marble pebbles. The matrix is dolomite, and the economically important nodular sepiolite horizons occur in this unit. Thickness of the conglomerate varies from 160 m to 250 m. In some parts, concordant rhyolitic tuff horizons are observed (ÖNCEL and DENIZCI, 1982).

Pliocene consists of sandstone, dolomite, magnesite, sepiolitic clay, sedimentary sepiolite and limestone. Horizontal gradual change into rhyolitic tuff is observed occasionally. These lithologic units are exposed in a wide area in the east and west of Eskişehir. Thickness of the Pliocene sequence varies from 500 m to 800 m. The serie carries the sedimentary magnesite and sepiolite deposits. Sedimentary magnesite overlies the dolomite, 5 to 10 m thick, with ultrabasic rock fragments. The thickness of the generally compact magnesite horizon locally reaches up to 10 m. Sepiolite beds occur as 0.3 to 3.0 m thick, redish to greenish colored clayey horizons. This type of sepiolite is soft, easily grindable, and it disintegrates upon wetting. The horizons frequently carry silica-chert veinlets. A geological profile of the Pliocene sedimentary sequence with sepiolite, from Kepeztepe (W Eskişehir) is given in *(Fig. 3)*.

A massive, detritic, generally white colored limestone overlies the Pliocene sequence. This unit generally includes silica veinlets and nodules.

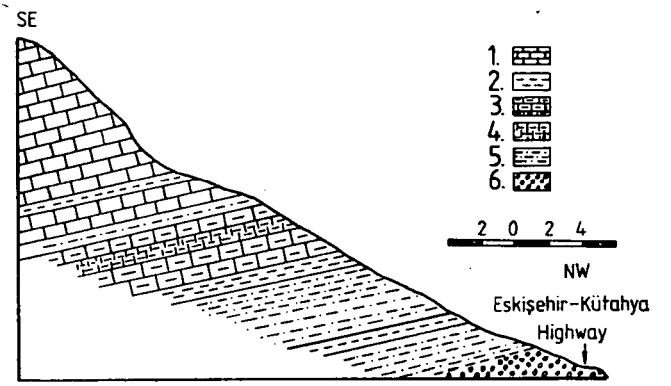

Fig. 3. Geological profile from the Kepeztepe bedded sepiolet occurrence, Western Eskişehir. (1) white massive-detritic limestone, (2) yellowish-white clayey marl, (3) yellowish marly limestone, (4) bedded sepiolite (meerschaum type), (5) brown, sandy sepiolitic clay, (6) conglomerate, partly containing sepiolite nodules or concretions.

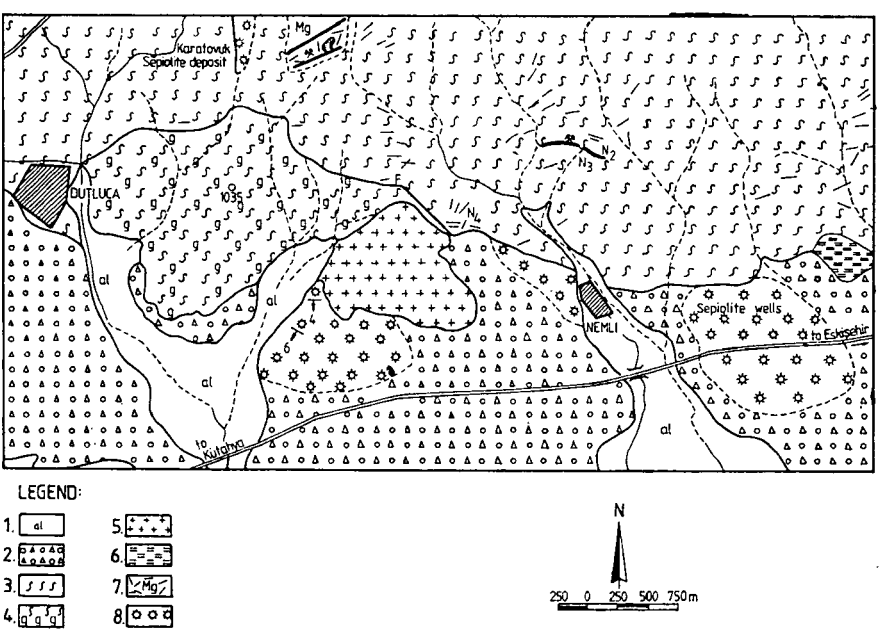

Fig. 4. Geological map of a section of the magnesite-sepiolite bearing area, around the Nemli and Dutluca villages, Western Eskişehir. (1) alluvium, (2) Neogene dolomite-cemented conglomerate, (3) Mesozoic serpentinized peridotite, (4) Mesozoic Gabbro (saussuritized, uralitized), (5) Paleozoic granite, (6) Paleozoic schist, (7) Magnesite veins, (8) sepiolite wells. After ÖNCEL and DENIZCI (1982).

Influence of region tectonism is seen in Pre-Neogene lithologies. In Palaeozoic units dominant strike trend is NW, dipping 70°—80° NE. Volcanism is mostly of alkaline character, and is effective in Neogene.

A simplified geologic map, partly covering the area in Bo. 2 in *(Fig. 1)*, bearing magnesite and meerschaum deposits in the west of Eskişehir is given in *(Fig. 4)*.

Modes of occurrence of sepiolite ground Eskişehir. Meerschaum and sedimentary type sepiolite deposits, as stated previously, occur in the Neogene formations in Eskişehir Province. The first type occurs in the Upper Miocene conglomerate, and the second type is generally in Pliocene.

A. *Meerschaum type sepiolite:* Distribution of the Upper Miocene conglomerate-bearing meerschaum is shown in *(Fig. 1)*, in 5 groups.

Genesis of the Eskişehir meerschaum is similar to that of Konya. Both the individual magnesite and sepiolite pebbles, and concretions made up of a crystal mixture of the two minerals occur in the conglomerate. By analogy, it may be concluded that the sepiolite concretions were formed by the replacement to several degrees of the magnesite in alkaline media rich in silica. Due to this feature, no direct relation to any ophiolitic rock unit can ever be established.

No occurence of sepiolite in serpentinized rocks of the ophiolitic assemblage has ever been recorded from Eskişehir region. Serpentinite, dolomite and quartz have not entered into the formation reactions, but their compounds being dissolved by alkaline solutions have been partly concentrated as nodules or thin films of silica under the meerschaum bearing horizon. Thus, it is clear that the theory about meerschaum formation, directly from the magnesium and silica-bearing solutions as a neoformation is not suitable for the Eskişehir deposits, although being proposed formerly and accepted for long (YENIYOL and ÖZTUNALI, 1985).

Chemical composition of a typical meerschaum specimen from No. 5 in *(Fig. 1)*, in the Eskisehir Province is given in Table 3, as A.

TABLE 3

Chemical composition of a meerschaum (A) and a sedimentary sepiolite (B) specimen from Eskişehir.
(A — after ÖNCEL *and* DENIZCI, *1982., B — after* AKINÇI, *1967)*

	A (%)	B (%)	
SiO_2	54.49	58.65	
Fe_2O_3	0.44	2.86	
Al_2O_3	0.50	4.14	(including TiO_2)
CaO	3.52	2.93	
MgO	26.61	18.14	
LOI	14.53	13.14	
	100.10	99.86	

B. *Sedimentary, bedded type sepiolite:* Sepiolite deposits of sedimentary formation are found within the Pliocene lacustrine sequence, which is exposed in the east, northeast and west of Eskişehir. Sepiolite generally occurs between two dolomitic beds, and sometimes in alternation with magnesite and dolomite.

Kepeztepe sedimentary sepiolite occurence, whose vertical geological profile is given in *(Fig. 3)*, is located about 15 km west of Eskişehir. Here, the Pliocene sequence has been deposited from basement to top in the order: brown-sandy sepiolitic clay, overlying the Upper Miocene conglomerate, greenish-white clayey marl, bedded sepiolite-yellowish marly limestone alternation, brown-sandy sepiolitic clay, and the

overlying white-massive, detritic limestone. The thickness of the bedded sepiolite horizon is approximately 1.5 m.

Sedimentary sepiolite does not resemble the meerschaum by its appearance. It is brown colored when moisty, but turns beige-dirty white upon drying. The contained amount of impurity is much higher than in meerschaum, and in economic aspect, its quality could never be compared to that of the latter.

Chemical analysis of a sedimentary sepiolite specimen from Kepeztepe is given in Table 3 as B.

X-ray diffraction investigations of sedimentary sepiolite yielded that the main constituent was poorly crystalline sepiolite with some gypsum (AKINÇI, 1967).

Comparison of various geological and physical properties of meerschaum and sedimentary sepiolite from Eskişehir area is given in Table 4.

TABLE 4

Comparison of several features of meerschaum and sedimentary sepiolite from Eskişehir area (partly after AKINÇI, *1967)*

Feature	*Meerschaum*	*Sedimentary sepiolite*
host rock	comglomerate, composed mostly of serpentinite garvels, and cemented by dolomite	dolomite or detritic marly, lacustrine limestone
geologic age	Miocene	Pliocene
color and shape	snow-white concretions	chocolate-colored layers
dry color	snow-white	light-beige, dirty white
dry surface property	very thin fractures	relatively deep fractures
processability when dry	processable upon moistening	disintegrates when moistened
cavities, foreign particles, veinlets	very rare	generally present
specific gravity	0.508 g/cm³	0.894 g/cm³
crystal lenth in electron microscope photo	1.5—2 μ	0.5—1 μ
shape of fibers	acicular, slightly cylindrical	acicular

CONCLUSIONS

In this paper, it has been tried to approach the genesis and geological features of the meerschaum type sepiolite occuring around Eskişehir and Konya, both of the provinces being located in central Turkey.

Eskişehir meerschaum carries the same geologic and mineralogic properties with that of Konya, with the exception that the main constituent of the matrix is dolomite.

Around the meerschaum bearing Neogene basins, there occur abundant magnesite deposits, both in Konya and in Eskişehir. Within the Neogene units, interlayering of volcanic material, mainly rhyolitic tuffs which liberate silica and alkalies, is seen frequently.

SAMPSON (1975) gives a detailed description of the Tanzanian meerschaum deposits, and contributes to their genesis problem. He mentions the occurence of irregular masses, veins and films of meerschaum along faults, fracture zones and bedding planes in dolomitic limestone and in the overlying unit of sepiolitic mudstone. In his pro-

posed mode of occurence, sepiolite is derived from the overlying sepiolitic mudstone, and carried into cavities of limestone by percolating water. Thus the process is simple deposition in a sedimentary basin, which later was affected by structural movements, and a redeposition took place.

From the description above, it may be seen that the modes of occurence of Turkish and Tanzanian meerschaum are quite different. Obviously, this is a factor controlling the quality.

Occurrence as concretions in Neogene conlomerate makes the exploration of meerschaum deposits extremely difficult. Drilling is only useful to determine the base level, and it may just cut the sepiolite concretions by chance.

Due to the difficulties involved, until today, only the meerschaum horizons above the ground water level have been exploited in Turkey. The ground water level extends at depths form 28 m to 63 m.

It is almost impossible to calculate proven reserves for meerschaum occurences in Turkey. Only the probable reserve for some deposits may be estimated. Reserves for sepiolite are given in boxes and each box contains 12 kg of dry sepiolite. For Eskişehir region, probable reserve of about 1.4 million boxes of meerschaum has been estimated (ÖNCEL and DENIZCI, 1982).

What may be concluded at this point is that Turkey will carry on holding the world monopoly in high quality meerschaum production, although a stable trend is difficult to achieve, with the production figures ranging from a few hundred boxes to several thousands p.a., since long years.

This paper is a contribution to the IGCP Project No. 197, "Metallogeny of ophiolites".

REFERENCES

AKINÇI, Ö., 1967, "Eskişehir I 24-cl Paftasinin Jeolojisi ve Tabakali Lületaşi Zuhurlari", Maden Tetkik ve Arama Enst. Derg. (Bull. of Min. Res. Exp. Inst. of Turkey) **V. 67**, Ankara. 82—97.

BAILEY, S. W., 1980, "Structures of Layer Silicates, Crystal Structures of Clay Minerals and Their X-Ray Identification", G. W. BRINDLEY—G. BROWN (ed.) Mineralogical Society, London 125—195.

BRAUNER, K. and PREISINGER, A., 1956, "Struktur und Enstehung des Sepoiliths", Tschermaks Min. Petr. Mitt. **6**, 120—140.

CAILLÉRE, S. and HÉNNIN, S., 1961, "Sepiloite", The X-ray Identification and Crystal Structures of Clay Minerals Mineralogical Society, Clay Minerals Group, London, 325—342.

Industrial Minerals and Rocks, 1975, S. J. LEFOND (ed.), Amer. Soc. of Pet. Geol. New York. 833—836.

MILLOT, G., 1970, "Geology of Clays". Springer Verlag, New York.

NAGATA, H., SHIMODA, S. and SUDO, T., 1974, "On Dehydration of Bound Water of Sepiolite", Clays and Clay Minerals. **22**, 285—293.

ÖNCEL, Z. and DENIZCI, F., 1982, "Eskişehir Bölgesi Lületaşi ve Magnezit Etüdleri Raporu", Rep. of Min. Res. Exp. Inst. of Turkey (MTA). No. **7181**, Ankara. 3 V.

PARRY, W. T. and REEVES, C. C. JR., 1968, "Sepiolite from Pluvial Mound Lake, Lynn and Terry Counties, Texas". Amer. Mineral. **53**, 984—993.

POST, J. L., 1978, "Sepiolite Deposits of the Las Vegas, Nevada Area", Clays and Clay Minerals. **26**, 58—64.

SAMPSON, D. N., 1975, "Sinya Meerschaum Mine, Northern Tanzania" in Industrial Minerals and Rocks (S. J. Lefond, ed.), p. 834.

SERNA, C., AHLRICHS, J. L. and SERRATOSA, J. M., 1975, "Folding in Sepiolite Crystals", Clays and Clay Minerals **23**, 452—457.

YENIYOL, M., 1982, "Yunak (Konya) Magnezitlerinin Oluşum Sorunlari, Degerlendirilmeleri ve Yöre Kayaçlarinin Petrojenezi", Istambul Yerbilimleri Derg. (Bull. of Earthsciences, Istanbul) **3**, 21—51.

YENIYOL, M. and ÖZTUNALI, Ö., 1985, "Yunak Sepiyolitinin Mineralojisi ve Oluşumu", Proc. of the 2nd National Clay Symp., Univ. of Hacettepe, Ankara 171—186.

Manuscript received, 6 June, 1988

Acta Mineralogica-Petrographica, Szeged, XXIX, 107—118, 1987—1988

METHODS FOR MEASURING THE MATURITY OF ORGANIC MATTER IN DIAGENESIS STAGE

M. HETÉNYI

Department of Mineralogy, Geochemistry and Petrography,
Attila József University

ABSTRACT

Several methods are used for measuring maturity of the organic matter. However, the degree of efficiency varies at different stages of the thermal maturity. During diagenesis and the beginning of catagenesis the fluorescence and O/C atomic ratio are considered to be the best indicators for characterizing the level of maturation. On the other hand, the techniques requiring long sample-preparation time can not be utilized as routine tools.

The aim of this paper is to propose a new applicability of a parameter measured by a generally accepted method. This parameter is the oxygen index determined by Rock Eval pyrolysis.

According to the results presented in this report the OI linearly decreases with the maturation level during the diagenesis and early catagenesis.

The correlation between oxygen index and maturity was experimentally demonstrated by laboratory thermal degradation of kerogen type I. Furthermore, the oxygen index has been proved to be an efficient indicator of coal rank from lignites to high vol. bitumenous coals. Applicability of the paramteres was checked on sedimentary organic materials of two boreholes.

The oxygen index decreased linearly in function of advanced diagenesis during both artificial and natural evolution. The correlation between the OI and the depth or between the OI and the temperature of thermal degradation is satisfactory ($r^2=0{,}81$—$0{,}99$). The connection seems to be valid independently of the type of organic matter. On the basis of our present results, however, the parameter can only be used in the case of coals and sedimentary organic matter of high organic carbon content. Preferred evolution interval of its application ranges from about $R_0=0{,}2$—$0{,}3$ per cent to $R_0=0{,}7$—$0{,}8$ per cent.

Keywords: coals, kerogen, maturity parameters, oxygen index, Rock Eval pyrolysis, early catagenesis.

INTRODUCTION

Several chemical and physical properties of the organic matter are used as indicators for its maturation. During the thermal evolution hydrocarbons, resins and asphaltenes have been formed with increase in depth and temperature. At the same time, the kerogen structure and as a consequence its properties also change. A great variety of analytical methods have been developed to determine the level of maturation. A lot of techniques are based on the properties of kerogen. Other parameters are proposed to measure the amount and quality of degradation products: bitumen, oil or gas.

Principal methods used for characterizing the rank of evolution can be summarized as follows: chemical indicators of maturity based on bitumen or crude oil, physicochemical methods based on kerogen, as well as optical microscopy and pyrolysis methods (TISSOT and WELTE, 1984).

Numerous procedures have been developed to measure the amount and the chemical composition of degradation products. The abundance of bitumen or hyd-

H—6701 Szeged. P.O. Box: 651 Hungary.

rocarbons and the composition of hydrocarbons are well-known maturity indicators. The quantity and composition of light hydrocarbons (LEYTHAEUSER *et al*, 1979a, b; DURAND and ESPITALIÉ, 1972; PHILIPPI, 1975; SCHAEFER *et al.*, 1983; THOMSON, 1979), as well as the Carbon Preference Index (BRAY and EVANS, 1961; TISSOT *et al.*, 1977) and the different ratios of biological marker hydrocarbons (BRASSELL *et al.*, 1983; MACKENZIE *et al.*, 1980, 1981, 1982; SEIFERT and MOLDOWAN, 1979, 1981) are also useful as maturation indices.

Various chemical and physical parameters of the kerogen also give good informations about its maturity stage. Oxygen and hydrogen content of kerogen and its evolution path have to be considered one of the principal chemical methods used for characterization the type and maturity of the source rocks and coals, too (van KREVELEN, 1961; TISSOT *et al.*, 1974). Some physical techniques measuring the rank of evolution are electron spin resonance (DURAND *et al.*, 1977; BAKR *et al.*, 1988), infrared spectrophotometry, thermal analysis etc.

Optical examination is widely accepted method for measuring the maturity of organic matter. Several scales of maturation based on color and structure alteration of palynomorphs have developed (STAPLIN, 1969). Fluorescence of liptinite macerals decreases during the diagenesis and partly during catagenesis (ALPERN *et al.*, 1972; TEICHMÜLLER and DURAND, 1983). The classical maturation index is the vitrinite reflectance. It is the best and well known parameter characterizing both the coalification stage and the maturity of source rock (DOW, 1977; TEICHMÜLLER, 1982; TISSOT and WELTE, 1984).

The pyrolysis conducted under an inert atmosphere is a rapid and efficient method to determine maturity. GRANSCH and EISMA (1970) used the CR/CT ratio as an indicator of state of maturity. In 1977 ESPITALIÉ *et al.* developed a new standard pyrolysis method of source rock characterization and evaluation. The temperature (T_{max}) corresponding to the maximum of hydrocarbon generation increases progressively with the thermal evolution during the assay. There is a very good relationship between T_{max} and vitrinite reflectance (BERTRAND, 1984; ESPITALIÉ *et al.*, 1985, 1986). Therefore this method is particularly valuable in the case of marine or lacustrine kerogen (types I and II) where vitrinite is often scarce or absent (TISSOT and WELTE, 1984). NEVERTHELESS T_{max} can be used as a rank parameter for coals, too (BERTRAND, 1984; JOHNS *et al.*, 1984; LEPLAT and PAULET, 1985; MONTHIOUX *et al.*, 1985; PETERS, 1986; TEICHMÜLLER and DURAND, 1983; VERHEYEN *et al.*, 1984).

The efficiency of methods mentioned above is very different. Almost all of them can be used for determining the boundaries between diagenesis, catagenesis and metagenesis. On the other hand, the sensitivity of various maturation indicators to individual evolution zone is not the same.

Some of them is particularly valuable in the catagenesis and metagenesis (for example vitrinite reflectance, aromatic compounds of oil and bitumen, T_{max} measured by Rock Eval pyrolysis etc.). Only a few parameters can be considered as a good index for evaluating maturity within the diagenesis stage (for example fluorescence of liptinites, ESR, elemental analysis of kerogen). Furthermore, many of these techniques are known more as research rather than routine tools due to the time and care needed in their application (TISSOT and WELTE, 1984).

Concerning the immature coals the O/C atomic ratio was found to be the best qualification parameter (BERTRAND, 1984). However, the elemental analysis is not a routine method because the kerogen has to be isolated previously. On the other hand there is a good correlation between the O/C atomic ratio and the oxygen index measured by Rock Eval method.

In this work an attempt was made to utilize the oxygen index (OI) as an indicator for maturation. It is thought to be an efficient maturity indicator in the diagenesis zone, which is considered as "the zone of oxygen".

EXPERIMENTS

The total organic carbon content (TOC) was measured at 1000 °C under intense oxygen flow by combusting in a Carmbograph—8 equipment. Kerogen was isolated by physical method (HETÉNYI and VARSÁNYI, 1976). Experimental evolution was carried out from 300 °C to 500 °C under nitrogen atmosphere in a Heraeus-type temperature-programme furnace. Products were collected in cooled traps, residues were extracted by chloroform and by benzene-acetone-methanol mixture of 70:15:15 ratio. Coals, kerogens, as well as the residue of thermal degradation ("unconverted kerogen") were characterized by Rock Eval pyrolysis (ESPITALIÉ *et al.*, 1977). The CR/CT ratio was measured on the basis of ASTM standard (CUMMINS *et al.*, 1972).

RESULTS

1. *Change of maturity indices during the artificial evolution with special regard to diagenesis stage.*

Experimental assay of thermal evolution was carried out on an immature kerogen to study the efficiency of maturity indicators measured by Rock Eval pyrolysis. The kerogen type I reached the boundary of diagenesis and catagenesis at higher temperature than the other ones. Thus, kerogen type I seems to be the most suitable raw material to study in detail the diagenesis. The artificial evolution was performed on kerogen isolated from a maar-type oil shale (Pula, Hungary). This kerogen belongs to type I; its H/C atomic ratio is 1,7; CR/CT ratio is less than 0.1; hydrogen index is 890 mgHC/gTOC; oxygen index is 42 $mgCO_2$/gTOC.

The organic matter was thermally degraded at 8 different temperatures during 5 hours under nitrogen atmosphere (HETÉNYI, 1983). After extracting the bitumen the residue (so called "unconverted kerogen") was characterized by Rock Eval pyrolysis (Table 1).

According to the total organic carbon contents, the hydrogen indices and the PC/TOC ratios the boundary of the diagenesis and catagenesis is between 375—400 °C. Comparing the results of thermal degradations performed at these two temperatures the change of the TOC is 21 per cent, the change of HI is 39 per cent and the change of PC/TOC is 36 per cent. At lower temperature these parameters are nearly constant. For example the hydrogen index of the unheated kerogen is 890 mgHC/gTOC and the residue after thermal degradation at 375 °C is 868 mgHC/gTOC, e.g. the change is only 2 per cent (Table 1).

The T_{max} is considered to be the most reliable indicator — among those measured by pyrolysis — for characterizing thermal evolution. However, the T_{max} is influenced by the type of organic matter during the diagenetic stage and at the beginning of catagenesis (TISSOT and WELTE, 1984). As we can see in Table 1, the T_{max} values are unchanged during the zone of evolution mentioned above, therefore it is not proved to be a properly sensitive index to characterize the maturity stage of an immature kerogen type I.

TABLE 1

Thermal degradation of the kerogen type I.
Characterization of the unconverted kerogen by Rock Eval pyrolysis
(degradation period = 5 hours)

Temperature °C	TOC %	PC/TOC %	HI	OI	T_{max} °C	S2/S3
Unheated kerogen	74.0	77	890	42	443	25.70
200	72.8	74	890	29	443	31.28
300	73.6	74	885	23	445	38.16
325	73.8	74	888	21	447	41.79
350	75.0	73	873	19	447	44.04
375	75.5	72	868	16	451	54.72
400	59.8	44	521	17	447	26.20
450	37.4	10	120	29	454	4.08
500	34.2	4	33	27	454	0.77

HI = mgHC/gTOC
OI = $mgCO_2$/gTOC

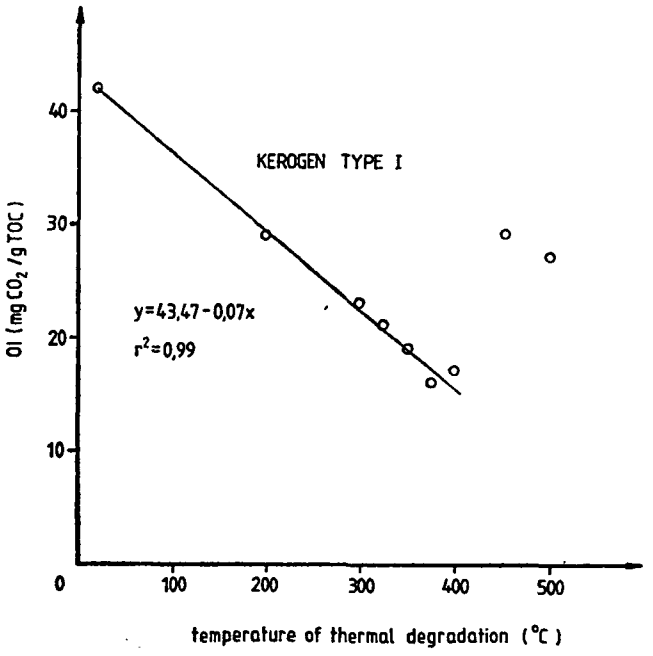

Fig. 1. Change of oxygen index in function of temperature of thermal degradation.

At the same time the oxygen index decreased progressively in function of the increasing degradation temperature *(Fig. 1.)* The excellent correlation ($r^2=0.99$) between the oxygen index and degradation temperature suggests that the oxygen index is a valuable indicator for characterizing the maturity of organic matter within the first zone of the evolution process.

2. *Oxygen index as a possible indicator of coal rank*

The vitrinite reflectance is to be considered the best tool for determining the coal rank. According to TEICHMÜLLER *et al.* (1982), however, the efficiency of this parameter depends on the maturation level. Concerning to its applicability there are three sections:

a) $R_0 > 1.1$: efficiency is good

b) $0.5 < R_0 < 1.1$: efficiency is low

c) $R_0 < 0.5$: the indicator is not properly sensitive.

TABLE 2

Rank parameters of a series of Hungarian coals measured by ROCK EVAL *pyrolysis and their vitrinite reflectance*

Samples	R_0 %	PC/TOC %	HI mgHC/gTOC	OI $mgCO_2$/gTOC	T_{max} $_oC$	S2/S3
Lignite	0.30	5.7	59	50	402	1.16
Lignite	0.34	5.7	64	45	407	1.41
Sub-Bit. C	0.42	3.3	38	40	417	0.94
Sub-Bit. C	0.43	7.4	85	38	421	2.23
Sub-Bit. A	0.48	7.1	81	37	428	2.16
High vol. Bit. A	0.82	6.9	76	5	446	12.77
High vol. Bit. A	0.87	8.9	105	7	448	13.77
High vol. Bit. A	0.95	10.2	120	5	453	20.28

Some Hungarian coals of low vitrinite reflectance were examined by Rock Eval pyrolysis. The value of R_0 ranges from 0.30 per cent to 0.95 per cent. Within the mentioned part of the coalification scale vitrinite reflectance is only weakly effective. It would be useful to develop another method to characterize the evolution level of lignites and subbituminous coals. Therefore T_{max} values and oxygen indices were studied as maturity indicator (Table 2).

As we can see in *Figs. 2* and *3* both parameters are linearly correlated to coal rank. But there is an essential difference between the change of OI and T_{max}. Oxygen index decreases linearly from an immature lignite ($R_0 = 0.30\%$) to high vol. bituminous coals (R_0=about 0.80%) reaching finally a minimum value. As from high vol. bit. coals oxygen indices are so low that their change is also insignificant. Consequently the OI proved to be an excellent maturity indicator but only in the diagenesis and at the beginning of the catagenesis. At the same time T_{max} changes linearly during the diagenesis and catagenesis, too. The rises of the curves are very different in these two zones as a consequence of various chemical processes.

On the basis of the present results the data measured by Rock Eval pyrolysis — both the T_{max} and OI — seem to be useful supplements to other parameters for

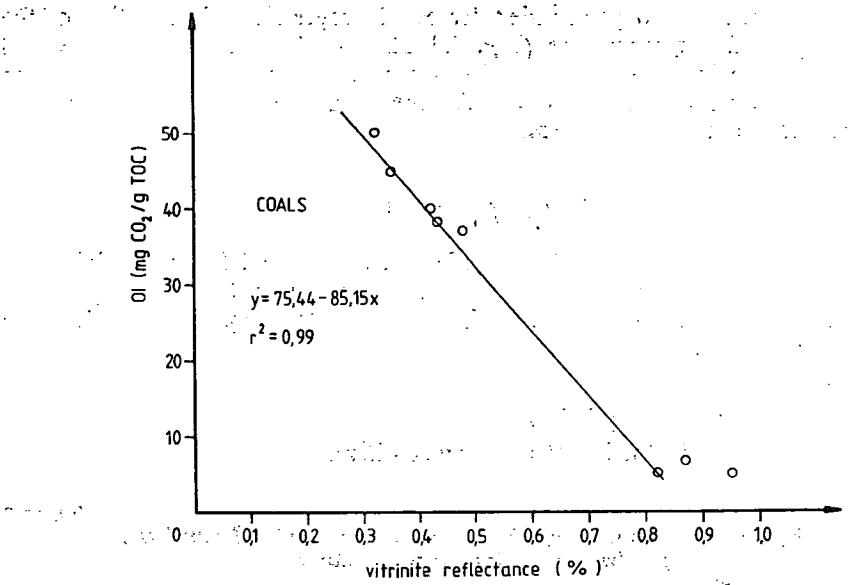

Fig. 2. Comparison of oxygen index from Rock Eval pyrolysis and vitrinite reflectance in coals

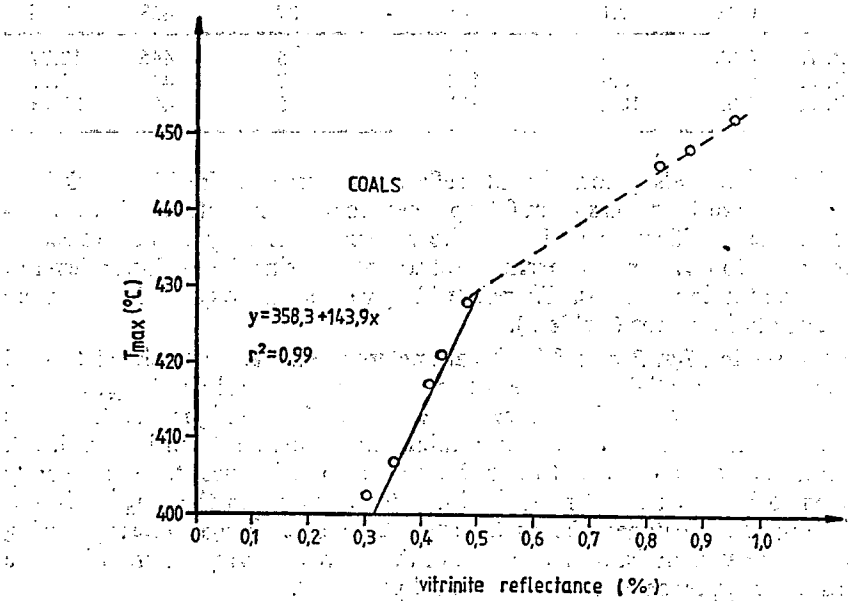

Fig. 3. Comparison of T_{max} from Rock Eval pyrolysis and vitrinite reflectance in coals (in diagenesis zone: full line, in catagenesis zone: dashed line).

characterizing coal rank. One of the most valuable methods to determine the evolution level of lignites and subbituminous coals would be the simultaneous use of these parameters. Particularly, because they can be measured by a single Rock Eval pyrolysis.

3. *Change of oxygen index in function of depth*

Applicability of maturation parameters studied in this paper was checked on sedimentary organic materials. Core samples from Tpk-I borehole (Hungary) and cuttings from Makó-3 borehole (Hungary) were investigated by Rock Eval pyrolysis.

TABLE 3

Characterization of core samples from Tpk-I borehole (Hungary) by ROCK EVAL *pyrolysis*

Depth (m)	TOC %	HI mgHC/gTOC	OI $mgCO_2/gTOC$	T_{max} °C	S2/S3	Hydrocarbon potential kgHC/ton of rock
294.6	43.39	167	80	397	2.09	90.95
361.0	47.38	159	76	387	2.08	95.74
391.0	50.51	142	70	382	2.01	88.68
429.3	43.57	116	75	391	1.55	58.58
684.9	45.08	131	63	402	2.09	64.71
714.4	46.39	95	65	404	1.45	47.73
865.8	48.99	92	61	503	1.51	47.89
919.0	43.51	129	56	403	2.29	61.85
1212.2	49.48	129	38	408	3.37	67.99
1328.2	54.36	138	29	407	4.75	78.88
1466.0	62.94	156	19	409	8.05	10 32
1575,3	22.30	175	21	416	8.22	4 22
1586.0	62.56	188	18	411	10.35	123.56

13 core samples containing high quantity of organic carbon were investigated from Tpk borehole. The total organic carbon content changes from 22.3 per cent to 62.9 per cent, average value is 47.7 per cent (Table 3). These samples are considered to be lignites or coals. In *Figs. 4* and *5* T_{max} and oxygen can be seen plotting against depth. Both parameters change linearly in function of depth. Relationship, however between the oxygen index and depth seems to be better ($r^2=0.97$) than that between the T_{max} and depth ($r^2=0.78$).

Large number of samples from Makó-3 borehole were analysed. From 1010 m to 2090 m cuttings in every 20 m were measured by Rock Eval pyrolysis (Table 4). The quantity of organic carbon is very changeable. It ranges from 7 per cent to 56 per cent. Some of the cuttings are coals and the others contain kerogen type III (HI = = 100—170 mgHC/gTOC). The high value of hydrocarbon potential (8—56 kgHC/ton of rock) is due to the significant organic carbon content. The T_{max} seems to be an unreliable maturity parameter in these samples. Values change between 402 °C and 422 °C independently of depth (Table 4). At the same time oxygen index linearly decreases with depth *(Fig. 6)*. There is a fair correlation ($r^2=0.81$) between the OI and depth.

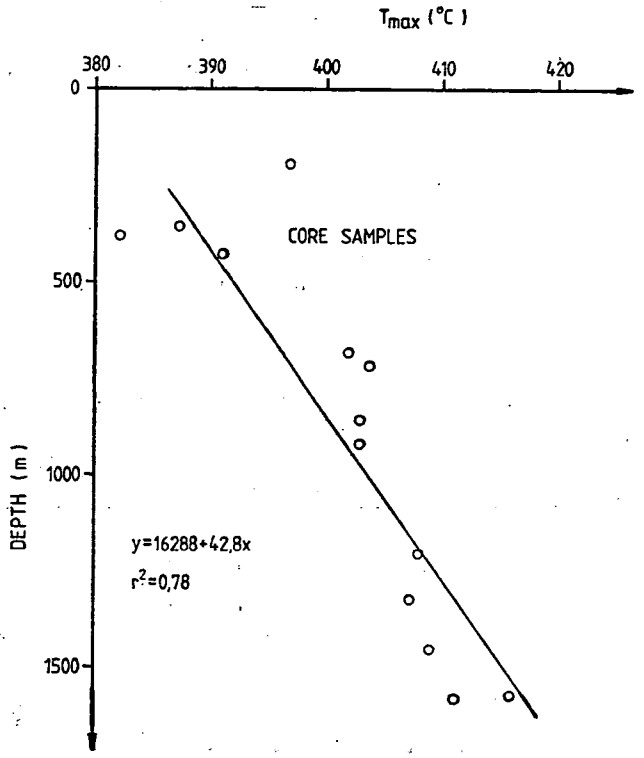

Fig. 4. Change of T_{max} measured on core samples in function of depth.

CONCLUSION

1. On the basis of results presented in this paper the oxygen index seems to be a useful supplement to other parameters for characterizing the maturity of different organic materials.

2. The oxygen index is a particularly effective maturation indicator during the diagenesis and at the beginning of the catagenesis.

3. Its applicability was checked among both artificial and natural conditions of the diagenesis. The OI decreased linearly in function of advanced evolution. A good relationship was found between the OI and the depth, as well as between the OI and the degradation temperature of experimental evolution. The correlation coefficient was excellent in the case of thermal degradation of a kerogen type I and in the case of core samples (r^2=0.97—0.99). A fair correlation coefficient (r^2=0.81) was determined by Rock Eval pyrolysis of cuttings.

4. In according to our results this parameter can only be used to measure the maturity of coals and sedimentary organic matter of high organic carbon content. Further examinations are necessary to apply this indicator for samples containing a small quantity of organic carbon.

5. Simultaneous use of OI and T_{max} has proved to be a valuable method to determine the coal rank from lignites to high vol. bituminous coals.

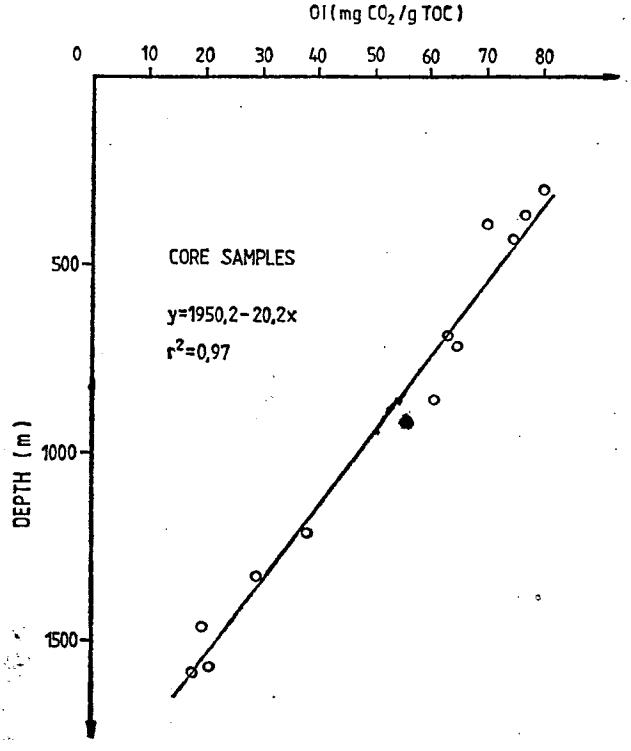

Fig. 5. Change of oxygen index measured on core samples in function of depth.

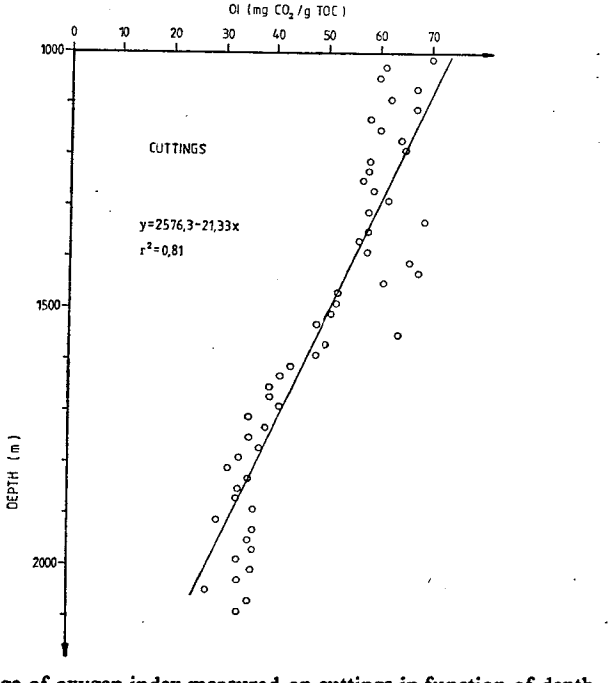

Fig. 6. Change of oxygen index measured on cuttings in function of depth.

TABLE 4

Characterization of cutting samples from Makó-3 borehole (Hungary) by ROCK EVAL *pyrolysis*

Depth m	TOC %	HI mgHC/gTOC	OI $mgCO_2$/gTOC	T_{max} °C	S2/S3	Hydrocarbon potential kgHC/ton of rock
1010	7.44	106	70	417	1.50	8.41
1030	14.23	112	61	415	1.83	16.95
1050	14.62	113	60	422	1.87	17.39
1070	12.55	114	47	414	1.70	15.28
1090	23.49	128	62	415	2.04	31.65
1110	22.92	133	67	413	1.96	32.07
1130	32.99	141	58	415	2.42	49.09
1150	18.08	126	60	419	2.10	24.21
1170	15.40	122	64	418	1.90	19.83
1190	28.04	120	65	415	1.82	35.42
1210	32.20	139	58	413	2.37	46.88
1230	38.35	136	58	413	2.31	54.77
1250	30.18	115	57	414	2.03	36.36
1270	22.71	119	59	416	1.98	28.21
1290	17.16	123	62	416	1.96	22.13
1310	9.81	108	58	418	1.85	11.10
1330	11.20	112	69	421	1.62	13.19
1350	18.59	130	58	414	2.22	25.26
1370	36.20	150	51	414	2.92	56.42
1390	13.89	114	58	417	1.97	16.64
1410	5.90	102	66	416	1.52	6.32
1430	13.93	127	68	414	1.86	18.69
1450	7.02	96	56	420	1.68	7.06
1470	18.17	124	47	413	2.62	23.50
1490	21.91	128	47	418	2.71	29.24
1510	14.26	132	51	421	2.17	19.79
1530	37.06	120	48	414	2.48	47.44
1550	9.89	123	64	418	1.90	12.82
1570	19.66	122	50	417	2.43	24.93
1590	14.28	139	48	418	2.87	20.76
1610	27.47	129	43	418	2.96	37.07
1630	24.94	121	41	421	2.93	31.64
1650	48.87	121	39	410	3.09	62.35
1670	22.51	136	39	416	3.46	32.54
1690	47.58	134	41	417	3.26	66.83
1710	40.41	141	35	414	4.02	59.69
1730	9.23	126	38	420	3.27	12.12
1750	55.99	155	35	414	4.37	92.46
1770	24.58	154	37	421	4.12	39.85
1790	21.37	162	33	421	4.90	35.82
1810	32.26	168	31	412	5.34	57.16
1830	55.67	133	35	409	3.79	78,53
1850	45.65	164	28	416	5.76	78.58
1870	33.14	162	28	413	5.66	56.27
1890	50.53	138	31	417	4.41	72.98
1910	28.87	128	29	418	4.43	38.43
1930	18.01	144	36	419	3.91	27.03
1950	11.38	148	35	419	4.12	17.40
1970	8.74	137	36	422	3.72	12.42
1990	8.68	108	33	417	3.27	9.85
2010	27.27	154	38	417	3.98	43.50
2030	12.39	157	33	421	4.67	19.94
2050	20.07	172	27	419	6.36	35.76
2070	14.65	156	35	417	4.41	23.83
2090	16.68	148	33	418	4.41	25.66

ACKNOWLEDGEMENT

The author expresses her gratitude to Á. JÁMBOR and Á. SZALAY making available for her the samples investigated.

REFERENCES

ALPERN, B. DURAND, B. ESPITALIÉ, J., TISSOT, B. (1972): Localisation, caractérisation et classification petrographiques des substances organiques sédimentaires fossiles. In: Advances in Organic Geochemistry, 1971. ed. by von GAERTNER, H. R. and WEHNER, H., Oxford-Braunschweig: Pergamon Press, 1—28.

BAKR, M., AKIYAMA, M., SANADA, Y. and YOKONI, T. (1988): Radical concentration of kerogen as a maturation parameter. Org. Geochem. **12/1,** 29—32.

BERTRAND, P. (1984): Geochemical and petrographic characterization of humic coals considered as possible oil source rocks. Advances in Organic Geochemistry, 1983, Pergamon Press, 481—488.

BRASSELL, S. C. and EGLINTON, G. (1983): Steroids and triterpenoids in deep sea sediments as environmental and diagenetic indicators. In: Advances in Organic Geochemistry, 1981. ed by BJORØY M. *et al.*, 684—697.

BRAY, E. E. and EVANS, E. D. (1961): Distribution of n-paraffins as a clue to recognition of source beds. Geochim. Cosmochim. Acta. **22,** 2—15.

CUMMINGS, J. J. and ROBINSON, W. E. (1972): Thermal degradation of Green River kerogen at 150° to 350 °C U. S. Bur. Mines. Rep. Invest. **7620,** 15.

GRANSCH, J. A. and EISMA, E. (1970): Characterization of the insoluble organic matter of sediments by pyrolysis. In: Advances in the Organic Geochemistry 1966, ed. by HOBSON, G. D., SPEERS, G. C., Pergamon Press, 407—426.

HETÉNYI, M. and VARSÁNYI, I. (1976): Contribution to the isolation of the kerogen in Hungarian oil shales. Acta Miner. Petr., Szeged, **XXII/2,** 231—239.

JOHNS, R. B., CHAFFEE, A. L. and VERHEYEN, T. V. (1984): Chemcial variation as a function of lithotype and depth in Victorian basin coal. In: The chemistry of low-rank coals. Ed. by H. H. SCHOBERT, ACS Sympsium Series. Am. Chem. Soc., 109—132.

KVALHEIM, O. M., CHRISTY, A. A., TELNAES, N. and BJØRSETH, A. (1987): Maturity determination of organic matter in coals using the methylphenantrene distribution. Geochim, et Cosmochim Acta, V. **51,** 1883—1888.

KREVELEN, D. W. VAN (1984): Coal, 3rd ed., Elsevier.

LEPLAT, P. and PAULET, J. (1985): Study of diagenesis, catagenesis and metagenesis of coals and dispersed organic matter with high-temperature modified Rock Eval. Petroleum Geochemistry in Exploration of the Norvegian Shelf, **28,** 319—326.

LEYTHAEUSER, D., SCHAEFER, R. G. and WEINER, B. (1979/a): Generation of low molecular weight hydrocarbons from organic matter in source beds as a function of temperature and facies. Chemical Geology, **25,** 95—108.

LEYTHAEUSER, D., SCHAEFER, R. G., CORNFORD, C., WEINER, B., (1979/b): Generation and migration of light hydrocarbons (C_2—C_7) in sedimentary basins. Org. Geochem., **1,** 191—204.

MACKENZIE, A. S., PATIENCE, R. L., MAXWELL, J. R., VANDERBROUCKE, M. and DURAND, B. (1980): Molecular parameters of maturation in the Toarcian shales, Paris Basin, France-III. Changes in aromatic steroid hydrocarbon. Geochim. Cosmochim. Acta, **45,** 1345—1355.

MACKENZIE, A. S., BRASSELL, S. C., EGLINTON, G. and MAXWELL, J. R. (1982): Chemical fossils: the geological fate of steroids. Science, **217,** 491—504.

MONTHIOUX, M., LANDAIS, P. and MONIN, J. CL. (1985): Comparison between natural and artificial maturation series of humic coals of the Mahakam delta, Indonesia. Org. Geochem., **8/4,** 275—292.

PETERS, K. E. (1986): Guidelines for evaluating petroleum source rock using programmed pyrolysis. AAPG Bull., **70,** 318—329.

PHILIPPI, G. T. (1975): The deep sub-surface temperature controlled origin of the gaseous and gasoline-range hydrocarbons of petroleum. Geochim. Cosmochim. Acta, **39,** 1353—1373.

SAJGÓ, CS., MACKENZIE, A. S. and MAXWELL, J. R. (1983): Changes in the biological marker distribution Within a deep borehole in a superthick Neogene sequence in South-East Hungary and in adjacent oil pools. Org. Geochem., **5/2,** 65—73.

SCHAEFER, R. G. and LEYTHAEUSER, D. (1983): Generation and migration of low-molecular weight hydrocarbons and sediments from Site 511 of DSDP/IPOD Leg 71, Falkland Plateau, South Atlantic. In: Advances in Organic Geochemistry, 1981, ed. by BJORØY, M. *et al.*, 164—174.

SEIFERT, W. K. and MOLDOWAN, J. M. (1979): The effect of biodegradation on steranes and terpanes in crude oils. Geochim. Cosmochim. Acta, **43**, 111—126.
SEIFERT, W. K. and MOLDOWAN, J. M. (1981): Paleoreconstruction by biological markers. Geochim. Cosmochim. Acta, **45**, 783—794.
STAPLIN, F. L. (1969): Sedimentary organic matter, organic metamorphism and oil and gas occurrence. Can. Petr. Geol. Bull., **17**, 47—66.
TEICHMÜLLER, M. (1982): The importance of coal petrology in prospecting for oil and natural gas. In: Textbook of Coal Petrology (3rd ed.) ed. by STACH et al., Gibr. Bornstraeger, Berlin—Stuttgart, 399—412.
TEICHMÜLLER, M. and DURAND, B. (1983): Fluorescence microscopical rank studies on liptinites and vitrinites in peat and coals, and comparison with the results of the Rock Eval pyrolysis. Int. J. Coal Geol., **2**, 197—230.
THOMPSON, K. F. M. (1979): Light hydrocarbons in subsurface sediments. Geochim. Cosmochim. Acta, **43**, 657—672.
TISSOT, B. DURAND, B., ESPITALIÉ, J. and COMBAZ, A. (1974): Influence of nature and diagenesis of organic matter in formation of petroleum. Am. Assoc. Petr. Geol. Bull. **58/3**, 499—506.
TISSOT, B., PELET, R., ROUCACHÉ, J., COMBAZ, A. (1977): Utilisation des alcanes comme fossiles géochimiques indicateurs des environments géologique. In: Advances in Organic Geochemistry, 1975, ed. by CAMPOS, R., GONI, J., Madrid, 117—154.
TISSOT, B. P. and WELTE, D. H. (1984): Petroleum formation and occurrence. 2nd ed., Springer-Verlag.
VERHEYEN, T. V., JOHNS, R. B., and ESPITALTÉ, J. (1984): An evaluation of Rock Eval pyrolysis for the study of Australian coals including their kerogen and humic acid fractions. Geochim. Cosmochim. Acta, **48**, 63—71.

Manuscript received, 1 June, 1988

Acta Mineralogica-Petrographica, Szeged, XXIX, 119—130, 1987—1988

CHARACTERIZING CRUDE OILS AND SOLUBLE DISPERSE ORGANIC MATTERS BY HIGH PRESSURE LIQUID CHROMATOGRAPHY

P. TÓTH, G. PESTI

Hungarian Hydrocarbon Institute, Section for Geochemistry

ABSTRACT

The analysis and the comparative examination of hydrocarbon samples are very important from gcochemical aspects. To determine correlations for rock to rock, rock to disperse organic matter, oil to oil is one of the task of geochemistry.

On the basis of the below introduced and presented method it is possible to analyse quikly significant number of oil samples of relatively small quantities. By so doing comparison and classification of a kind of crudes from different locations and depths can be made. From the experimental results the identity of production site or a migration route may be concluded.

The analysis comprises (i) the samples preparation to HPLC, (ii) the HPLC analysis (iii) the computer processing.

During the analytical process of sample preparation for HPLC the crude oil or the chloroform soluble disperse organic matter were separated on a pre-column packed with silica gel for fractions eluated or non-eluated by *n*-hexane.

The fraction eluated by *n*-hexane containing the *n*-hexane-eluated aromatic components was used for HPLC which are specials and characteristics of different oils so the chromatograms of the crudes and the disperse organic matters are suitable for comparative analysis (finger print).

The computerized comparative analysis involves the determination of the location and heigth of peaks and the cluster analysis. The computer gives a plot of "dendrogram" showing the correlation of different types of crude oils and organic matters.

INTRODUCTION

Using high pressure liquid chromatography (HPLC) many workers investigated the analysis of hydrocarbons.

STEVENSON (1971), SUATONI and SWAB (1975), DARK *et al.*, (1977) determined the group composition of hydrocarbons (saturate, aromatic, heterocyclic aromatic) and obtained valuable informations on the composition, or comparability of oils.

GRIMALT and ALBAIGÉS (1982) pointed out that the polycyclic aromatic hydrocarbons in the crude have structural characteristics which are suitable for identification.

MILAN POPL and co-workers (1978) made a comparative analysis of the rock extracts and arrived at the same conclusions.

The liquid chromatograms of aromatics in the hydrocarbons represent a fingerprint of a given crude therefore are suitable to decide identity, similarity or difference of the samples examined.

H—8801 Nagykanizsa, Vár utca 8. Hungary.

PRINCIPLES OF METHOD

The crude or the disperse organic matter soluble in chloroform was separated in a pre-column packed with silica gel to fractions that can be eluated by normal hexane and that cannot be eluated by *n*-hexane.

The part eluated by *n*-hexane was HPLC analysed. The chromatograms were recorded on a microprocessored data logger and were classified by a computer using cluster analysis technique.

PREPARING SAMPLES FOR HPLC ANALYSIS

The samples examined were crude oils and disperse organic matters soluble in chloroform. In the analitics of disperse organic matters soluble in chloroform (hereinafter bitumens) one of the problems was the small (10 to 20 mg) sample weight. Bitumens are obtained by extracting core samples in a SOXHLET extractor with chloroform, then the chloroform is evaporated in a nitrogen stream.

Max. amount of bitumens compared to the rock is . 25 weight percent, and generally from . 01 to . 07 w%. Only a part of the extracted bitumen samples can be used for chromatographic examinations since the residues can provide — through other analytical methods — further informations that are important from geochemistry's point of view.

It is a well known fact in literature that the liquid chromatographic measuring of crudes and oil-products is preceded by a proper preparation of the samples to be examined. The asphaltenes should be released from the crude since the precipitated asphaltenes damage the HPLC column. The exception is the field of gel chromatography (GPC) where BOMBAUGH and co-workers (1968) demonstrated that chromatograms can also be made from crudes.

Our sample preparation consisted of a simple and relatively quick examination. The oils or bitumens were separated in a glass column 4 mm inside diam. and 120 mm long, through an absorbent Kieselgel 60 of .063 to .2 mm particle composition using normal hexane as solvent, to two fractions: part that can be eluated with normal hexane and part that cannot be.

For the actual HPLC examination fraction eluated with normal hexane was used. The components not eluated with normal hexane were unneeded for the measurements so were left in the column, containing the polarized heterocyclic compounds and the asphaltenes "undesirable" for HPLC measuring. Time for preparatory examination was half an hour.

Preparing the samples took place under identical conditons. Amount of silica gel (Kieselgel 60) was always 2 gs. The silica gel used was activated for an hour at 120 °C by an argonic fluidization. The eluate was the Merck *n*-hexane made for chromatographic purposes and also used for HPLC measuring, and the sample amount was 10 to 20 mg. The sample had been dissolved in normal hexane and was transferred to the column previously wetted with *n*-hexane. The eluation volume was 100 ml, and the eluation rate was 3 ml/min.

It was examined to what extent the amount of hydrocarbons eluated changes with an increase in the volume of the eluate. By using obviously a larger column and a higher amount of sample (.1 to .2 g) it was shown that eluating with 800 ml of *n*-hexane 100 percent of the eluatable amount can be obtained. When increasing the eluation volume no change was observed either in the shape of HPLC chromato-

grams (amount of heterocyclic aromatics) or in the sample weight obtained after evaporating the normal hexane. Separation from this same sample was repeated using an amount of 20 mgs and an eluation volume of 100 mls. The two chromatograms were completely identical.

HPLC ANALYSIS

The chromatograph countained the following units: pump, type WATERS 6000A, a sample injector, type WATERS U6K, detector PERKIN ELMER LC—55, recorder type MICROGRAPH BD—5 and a column 250 mm long and 4.6 mm inside diameter, packed with 5 μ Lichrosorb Si—60.

The solvent was Merck *n*-hexane manufactured for liquid chromatographic purposes, with a water content below. 005 percent.

The *n*-hexane was protected from the moisture content of the air using a calcium chloride tube.

The measuring conditions were as follows: flow rate of the eluate was 2.2 ml/min, pressure drop was 700 psi, paper speed was 10 mm/min, sensitivity was 2.0 mV. The detector was operated at a wavelength of 254 nm in the UV range. Measuring time was 10 minutes.

For the HPLC measurement a hydrocarbon blend obtained during sample preparation and eluated with *n*-hexane was used. This fraction contained the saturated and normal hexane-eluated aromatic components of the oil or bitumen examined (the heterocyclic aromatics cannot be eluated from the pre-column in case of 100 ml eluation volume).

The UV detector is insensitive to saturated hydrocarbons at the 254 nm wavelenght, but the light absorbtion by the aromatics is very high, thus a chromatogram of the suitable quality can be made also of a small concentration (10 mg/100 ml) solution *(Fig. 1a)*.

Chromatograms (finger-prints) for identical types of oils are the same *(Fig. 1a* and *1b)* since they consist of aromatic components of the same composition. On the other hand that of different types of oils is significantly different due to differences in the aromatic compositions *(Fig. 1a) (Fig. 1c)*. Chromatograms in *Fig. 1a* and *Fig. 1b are* almost completely identical. Both oils are from the Szilvágy area, Hungary, but from two different wells. Therefore the significant difference of chromatogram in Figure 1c from the two chromatograms above is surprising since this sample is also from Szilvágy.

Based on the chromatograms it is obvious that samples marked Szilvágy 41 and Szilvágy 33 *(Fig. 1a* and *1b)* are crudes of the same type and age, while sample Szilvágy 24 is totally different from them *(Fig. 1c)*.

Chromatograms in *Fig. 1c* and *1d* also suggest the same origin, but in this case two oil wells at some kilometer distance from each other are involved (the Szilvágy 24 and Barabásszeg 15).

Chromatograms of chloroform-soluble disperse organic matters (most important samples of geochemical survey) also allow the above comparison to be made. Bitumens from Bulgaria were used for the examination.

From chromatograms in *Fig. 2a, 2b,* and *2c* similarity and difference of the bitumens can easily be observed.

To check selectivity of the HPLC column and to process chromatograms using a computer a calibration blend containing aromatics was made. Composition of the calibration blend in the order of eluation was: benzene, naphthalene, phenantrene,

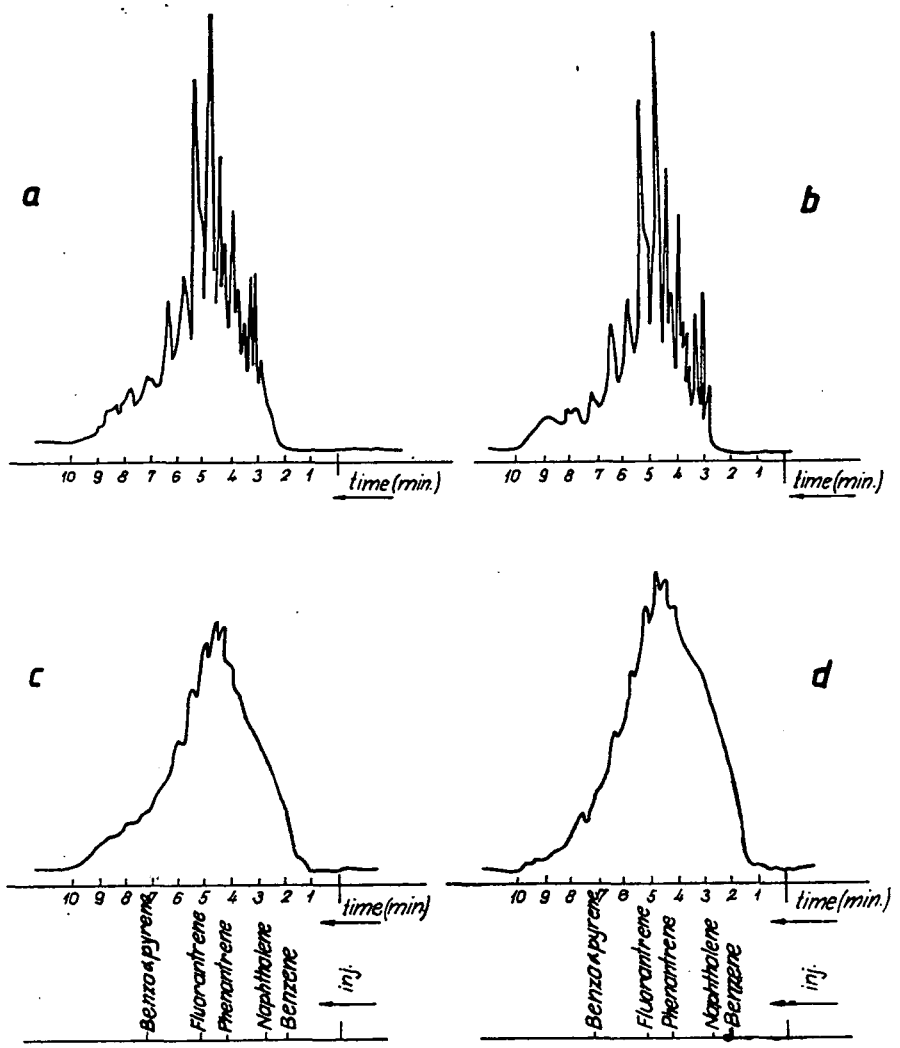

Fig. 1. Chromatograms of oil samples a: Chromatogram of oil sample marked Szilvágy-41 b: Chromatogram of oil sample marked Szilvágy-33 c: Chromatogram of oil sample marked Szilvágy-24 d: Chromatogram of oil sample marked Barabásszeg-15

fluoranthene and benzo-alpha-pyrene *(Fig. 3)*. The HPLC method was adsorption (liquid to solid) chromatography. The column was packed with porous silica gel. This system is very sensitive to traces of water and strong adsorbent substances (e.g. heterocyclic aromatics, resins, asphaltenes). In case these compounds are fed to the column, its selectivity decreases, the shape of the chromatograms changes and thus a comparison between the chromatograms cannot be made.

Therefore after every 10 sample measurements the column was checked using the above mentioned blend for calibration, and correction of errors due to possible

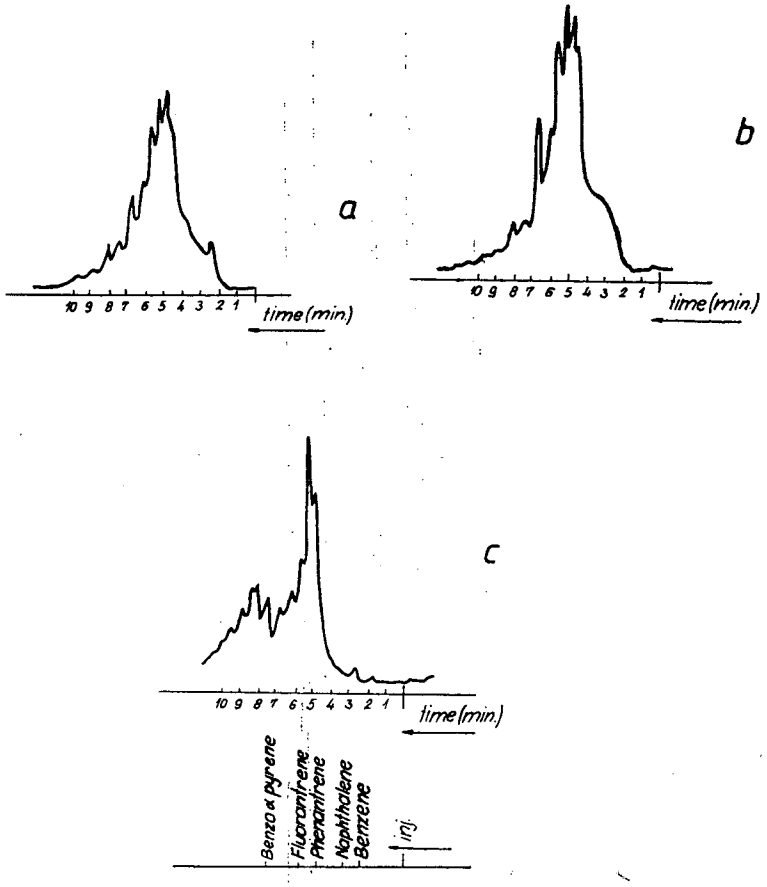

Fig. 2. Chromatograms of bitumen samples. a: Chromatogram of bitumen marked P—427 b: Chromatogram of bitumen marked P—428 c: Chromatogram of bitumen marked M—705

shifts in retention time allowed by means of the computer program. Occasionally hydrocarbon samples were injected into the column together with the calibration blend and thus identifying location of peaks became more reliable *(Fig. 4)*.

Based on chromatograms of the calibrating blend the qualitative examination of the samples was also allowed namely whether the di-, tri- or polycyclic aromatics are dominant in a given hydrocarbon.

COMPUTERIZED COMPARATIVE ANALYSIS OF CHROMATOGRAMS

The computerized processing involved input of the chromatograms into the computer, pre-processing the data, determining location and high of peaks and eventually making the cluster analysis.

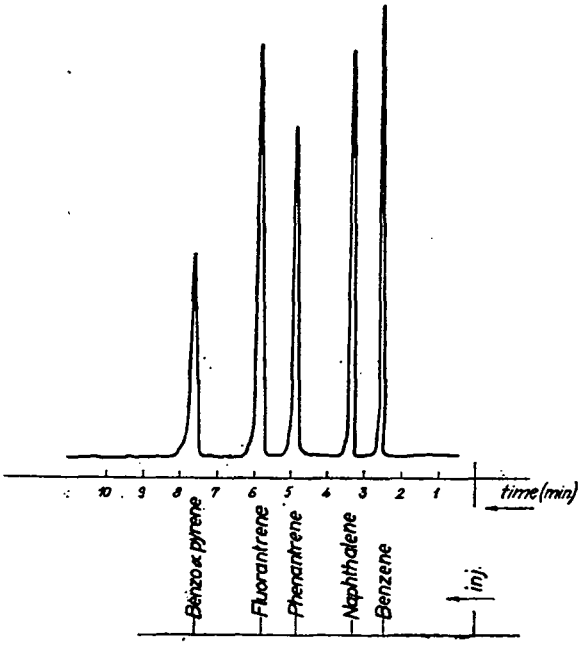

Fig. 3. Chromatogram of calibrating blend

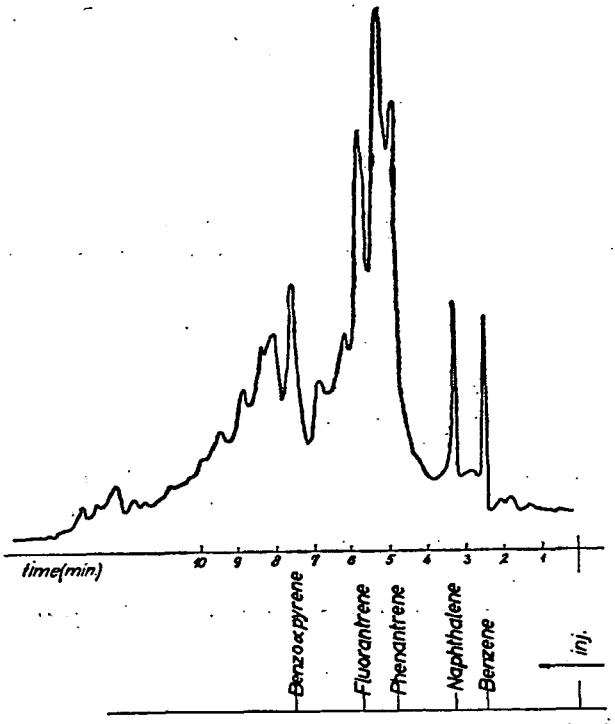

Fig. 4. Chromatogram of bitumen marked M—705 plus calibrating blend

Recording the chromatographic data took place using a casette data logger supported by an i8080 micro processor. The 10 minute measuring time was associated with a .1 sampling time thus a single chromatogram was represented by 6000 points. Data were loaded into the background storage of Computer TPA 1140 by means of the RS232C interface for the data logger.

The high number of points representing the chromatographic data and the noise interfering the data (partly generated during measuring and partly digital noise originated from the caracteristics of the data recorder and computer) required a preliminary data processing. During pre-processing the chromatograms were transformed to the same scale, were smoothed then the number of representing points were reduced to one fith *(Fig. 5)*.

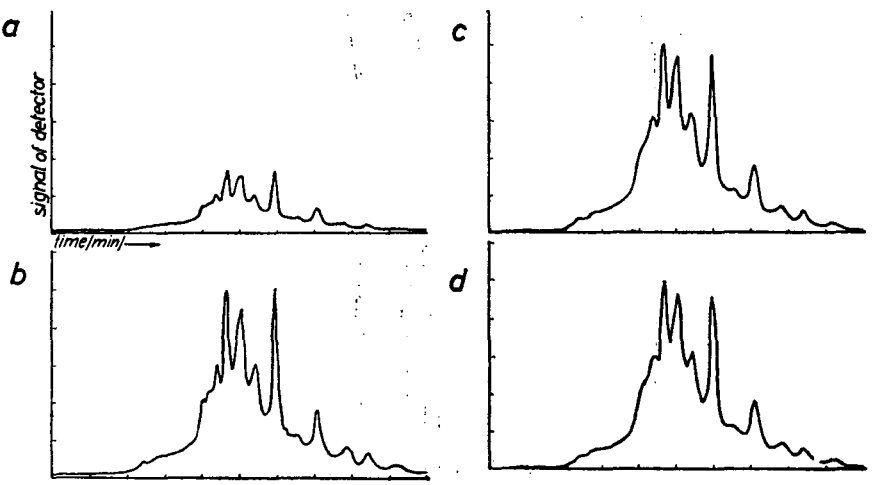

Fig. 5. Chromatogram pre-processing. a: Chromatogram input to machine b: Chromatogram transformed c; Chromatogram smoothed d: Chromatogram reduced

To determine the location of peaks two independent criteria were used in the program system. First, as per the definition in the classical analysis a peak was assumed at every point where the first derivate changes from positive to negative. Secondly, the spot with a minimal negative curve between two inflection points was considered as a peak *(Fig. 6)*. Using this second criterion near peaks not separated can be found, however the technique is very sensitive to noise and the points obtained must be selected. Identifying the peaks was made comparing the expected retention times obtained by processing the chromatogram of the calibrating blend, to the retention time of a given peak. The program corrected the expected retention times through knowing the spot of the newly found peaks. Basis for further processing was formed by the vectors derived from the values of peaks. These so called basic vectors were groupped by cluster analysis.

A primary task was to define the distance between the basic vectors. Out of the established distance concepts the Euclidean distance and the distance formed from

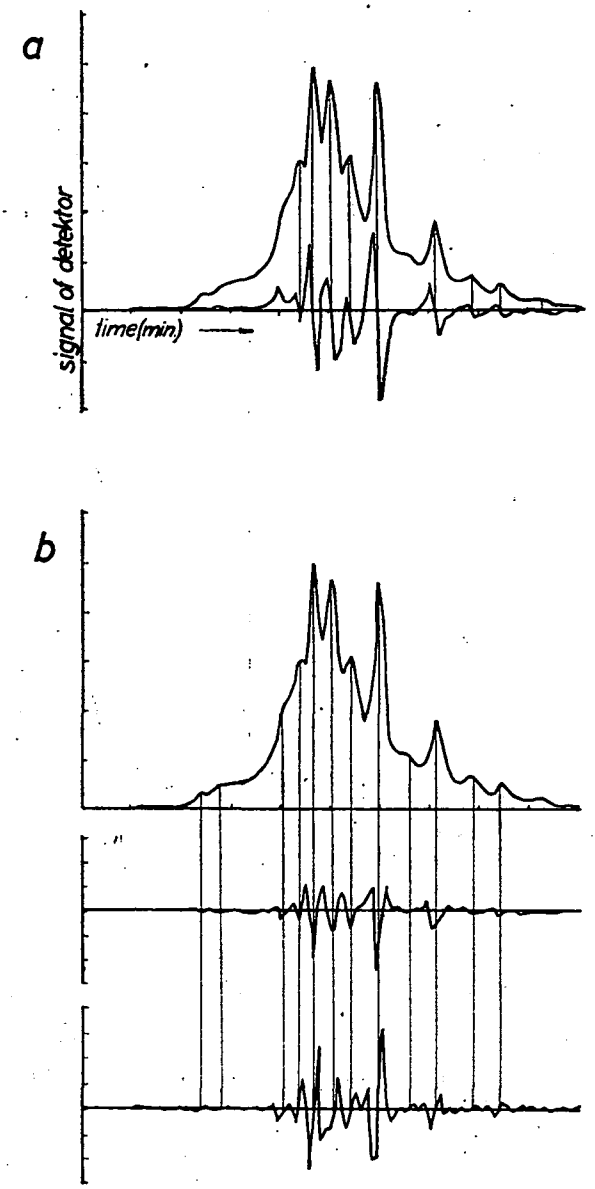

Fig. 6: Determining location of chromatographic peaks. a: As per first criterion first derivate. b: As per second criterion second derivate, third derivate

the correlation proved to be useful. The first one excelled through its simplicity and fastness, the later through its good coincidence with the everyday concept of similarity.

$$D_E(\bar{X}, \bar{Y}) = \sqrt{\sum_{i=1}^{N} (X_i - Y_i)^2}$$

$$D_r(\bar{X}, \bar{Y}) = \frac{1}{r(\bar{X}, \bar{Y}) + 1} - 0{,}5$$

$$r(\bar{X}, \bar{Y}) = \frac{\sum_{i=1}^{N} \left(X_i - \frac{1}{N} \sum_{j=1}^{N} X_j\right)\left(Y_i - \frac{1}{N} \sum_{j=1}^{N} Y_j\right)}{\sqrt{\sum_{i=1}^{N} \left(X_i - \frac{1}{N} \sum_{j=1}^{N} X_j\right)^2 \sum_{i=1}^{N} \left(Y_i - \frac{1}{N} \sum_{j=1}^{N} Y_j\right)^2}}$$

X, Y	basic vectors
Xi, Yi	components of basic vectors
N	dimension of basic vectors
D_E	Euclidean distance
D_r	generalized distance formed from the correlation
r	correlation coefficient from experience

Out of the possible algorhythms for clustering two were carried out.

1. The first one is a Kruskal algorhythm described by ANDERBERG (1973) which is a realization of the smallest spanning tree method. The clusters obtained by this technique correspond to the classes obtained by the nearest neighbour technique. Basic vectors "A" and "B" belong to the same group when there exist a finite series of the basic vectors the first element of which is "A" and the last one is "B", and the distance of any two neighbouring basic vectors is below a given threshold. According to DUDA and HART (1973) this technique is advantageous if the basic vectors form well distinquished groups. It is disadvantageous in case the basic vectors to be groupped can be attached to loosely connected chains *(Fig. 7)*.

2. The second one is the method of the furthest neighbour. Basic vector "A" belong to a given group alpha if its distance from all basic vectors in the group is below a given threshold. This technique is disadvantageous if the groups of basic vectors are of different size. With loosely connected chains they are out up so that elements groupped to a class show great similarity (7.8). This classification is worth carrying out as an addition to the previous one. If the two results obtained are different, detecting the reasons requires a detailed analysis. It is debatable whether the chains obtained by the first method represent a real progressing series, or only the samples difficult to group and interpolated between groups formed by the second method cause the formation of chains mentioned.

MEASURING RESULTS AND CONCLUSIONS

The computer recorded the results of analysis on a "dendrogram". In *(Fig. 8)* "dendrogram" of a given geological area's oils are shown, while in Fig 9 that of the Bulgarian disperse organic matters. The length of the horizontal lines up to the vertical ones indicates the similarity of the hydrocarbons.

In *(Fig. 8)* it can be seen that the computer distinguishes two main groups.

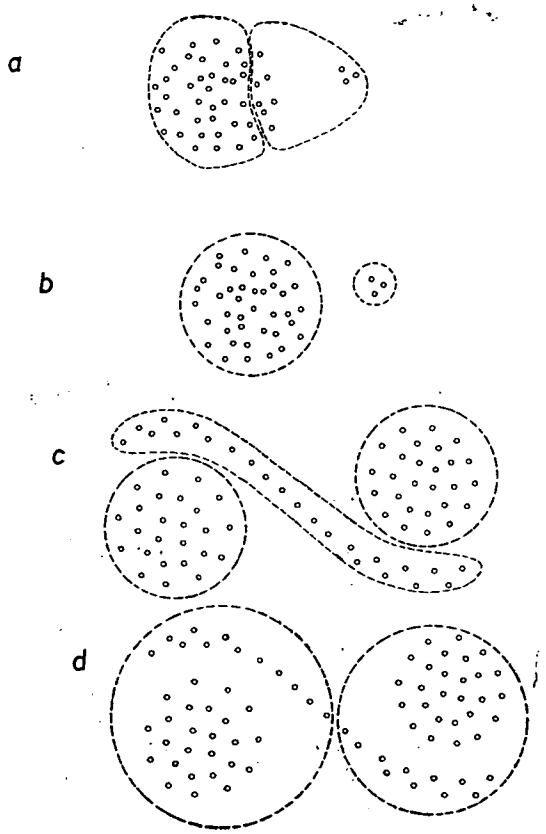

Fig. 7. Cluster analysis for basic vectors of two dimensions. a: Furthest neighbour method — disadvantageous. b: Nearest neighbour method for well distinquished groups — advantageous. c: Nearest neighbour method for loosely connected chains. d: Furthest neighbour method for loosely connected chains.

The first group is terminated at the sample marked Pusztaapáti 4, while the second one starts with sample Szilvágy 24. Further separation of the samples within the groups is shown in *Fig. 8.*

It is obvious that for example within the same group oil marked Szilvágy 41 is much more similar to Szilvágy 33 than sample marked Szentgyörgyvölgy 1 to Csesztreg 1. However oil Csesztreg I. does not belong to any group.

In "dendrogram" of Bulgarian bitumens *(Fig. 9)* a similar grouping can be observed.

The method is fast, requires a low demand for sample and can be rutinly applied in the fields of geochemical survey (great number of samples to be analysed) and in all fields where the objective is to identity hydrocarbons or their derivatives (e.g. detecting sources of trace amounts of oily contaminations).

The computerized evaluation allows establishing a data bank by means of which identification of oil samples with an unknown origin is also possible.

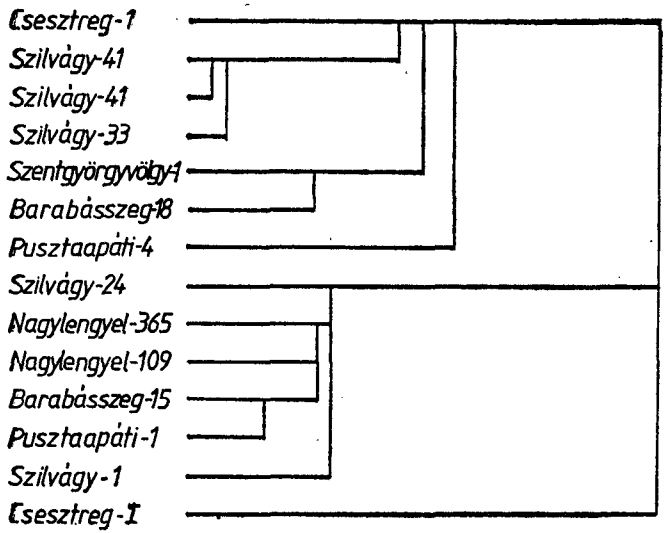

Fig. 8. Result of cluster analysis for oils

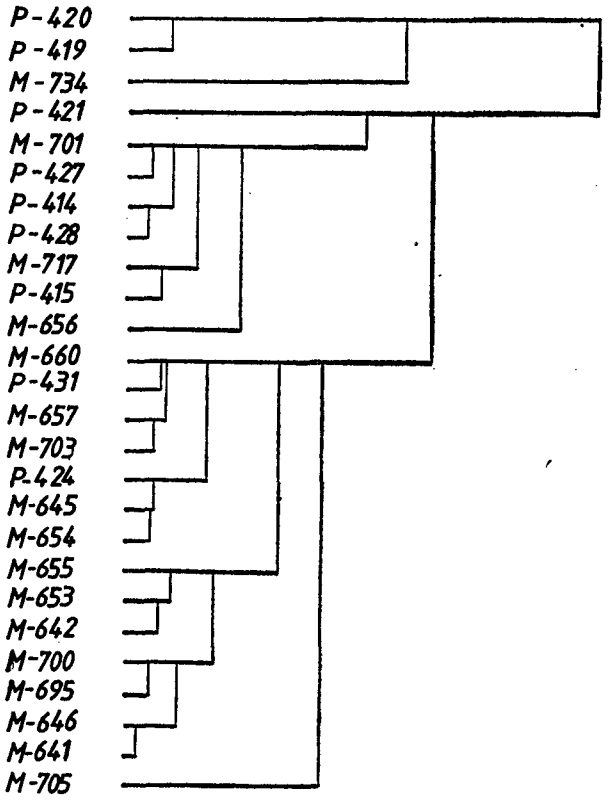

Fig. 9. Result of cluster analysis for bitumens.

REFERENCES

1. STEVENSON, R. (1971): Rapid Separation of Petroleum Fuels by Hydrocarbon Type, — Journal of Chromatographic Science. **9**, 257—262.
2. SUATONI, J. C. and SWAB, R. E. (1975): Rapid Hydrocarbon Group — Type Analysis by High Performance Liquid Chromatography, — Journal of Chromatographic Science. **13**, 361—366.
3. DARK, W. A., MCFADDEN, W. H., and BRADFORD, D. L. (1977): Fractionation of Coal Liquids by HPLC with Structural Characterization by LC-MS, — Journal of Chromatographic Science. **15**, 454—460.
4. GRIMALT, J. and ALBAIGÉS, J. (1982): Oil Spill Identification by High-Speed HPLC, — Journal of High Resolution Chromatography and Chromatography Communications. **5**, 255—260.
5. MILAN POPL, VLADIMIR DOLANSKY, GUSTAV SEBORT and MICHAL STEJSKALT (1978): Hydrocarbons and porphyrins in rock extracts, — FUEL. **57**, 565—570.
6. BOMBAUGH, K. J., DARK, W. A. and LEVANGIE, R. F. (1968): Application of Gel Chromatography to Small Molecules. II, — Separation Science. **3(4)** 375—392.
7. ANDERBERG, M. R. (1973): Cluster Analysis for Applications. — Academic Press, New York and London 131—155.
8. DUDA, R. O. and HART, R. E. (1973): Pattern Classification and Scene Analysis, — Stanford Research Institute, Menlo Park, California 228—237.

Manuscript received, 23 February, 1988

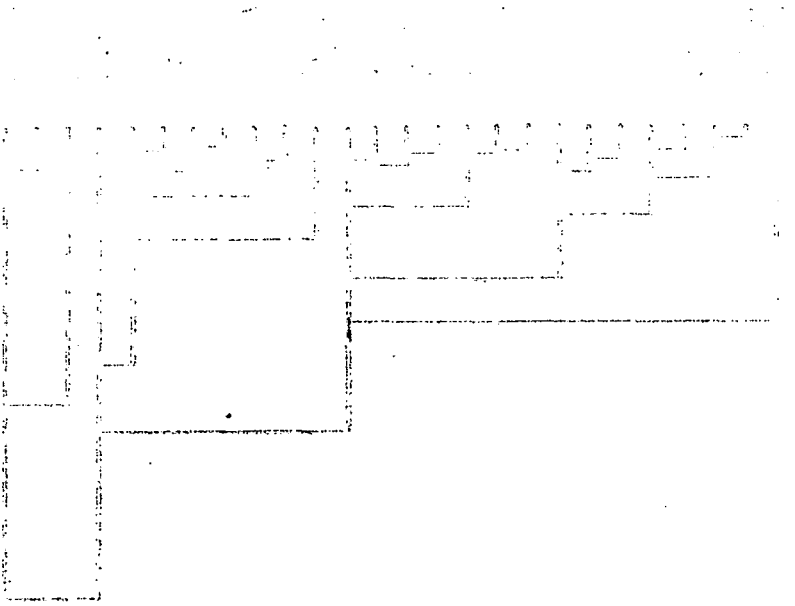

Acta Mineralogica-Petrographica, Szeged, XXIX, 131—137, 1987—1988

QUALITY REDUCING PROPERTIES OF HUNGARIAN BROWN COALS

L. PÁPAY*

Department of Mineralogy, Geochemistry and Petrography
Atilla József University

ABSTRACT

Hungarian brown coals of different ages and from different mines were examined. On the basis of elementary analysis it can be established that the maturity of Hungarian brown coals is lower and their total sulfur content is higher than that of foreign coals. A part of the total sulfur is included in pyrite form but it is very likely that the larger part of the sulfur content is organic sulfur. During combustion of these coals the largest part of the organic sulfur and a part of the pyrite sulfur gets into atmosphere as combastible sulfur. For reasons of environmental protection the experiments should be contained to reduce the amount of the sulfur dioxide getting into the atmosphere to minimum value.

INTRODUCTION

On the basis of archival documents the coal mining was started in Hungary in the April of 1759 from the coal bed could be found in the neighbourhood of Wansdorf village (today is Brennbergbánya) was attached to Sopron (BÁN, 1936). Since that time Jurassic black coal, Eocene-Oligocene and Miocene brown coal and Pliocene lignite have been being mined. In the first place the exploited coals are used up as the source of energy. Therefore from the point of view of environment protection the sulfur content of mineral coals is an important information.

The total sulfur content is usually combined from inorganic and organic sulfur. The sources of inorganic sulfur content is the elemental sulfur occurring in little quantities, the frequent pyrite or marcasite, melnikovite, pyrrhotine some rarely occurring sulfid minerals (chalcopyrite, arsenopyrite, etc.).

The sulfate sulfur content is originated mainly from gypsum and anhydrite. The organic sulfur can be determined as the difference between the total sulfur and the sum of pyritic-, metallic-sulfid and sulfate sulfur content.

According to previous views concerning the sulfur content of mineral coals, it is mainly originated from the proteins (cystein, cystine, methionine) and from other organic compounds. Recently the researchers' opinion it that the sulfur content in the fossil organic matter is predominantly of secondary origin. Namely, is has come from the sulfates through the reduction performed by *Desulfovibrio desulfuricans* bacteria under anaerobic circumstances. Organic material of sediments is oxidised by the bacteria using up oxygen of the sulfates to the reaction while sulfates are being reduced into hydrogen sulfide.

H—6701 Szeged, P.O. Box: 651 Hungary.

In the presence of iron pyrite has been formed. Without iron hydrogen sulfide in practice other sulfuric compounds, even elemental sulfur have been formed (KLESMENT *et al.*, 1985).

The common paludal microflora does not proliferate in the acid water of swamps so most of the "normal" mineral coals do not contain much sulfur. The paludal bacteria have been proliferated only in alkaline waters. The water of the swamps can be turned into alkaline in three different ways:

1. The reaction of the water of deeper sapropelic swamps is usually more alkaline because of the lower humus content (jüttja pH=6—7, sapropel pH=8—8.5);
2. Acidity of marshes effected on by the saline water is lost because of the sea water (pH=8);
3. The water of swamps turns to alkaline in consequence of dissolution of the carbonate content of surrounding limestones.

In Hungary this third case is the most important. It is effective on several areas. The peat or coals surrounded by limestone usually contain organic sulfur in large quantity (SZÁDECZKY-KARDOSS, 1952).

In laboratory investigations catalytic effect of carbonates on petroleum and sulfur reaction wered determined (VALITOV, 1978).

It was established on the basis of oil shales' elementary analysis (KLEMENT, 1985) that the organic material contained much sulfur if the mineral component of the oil shale was carbonate, and the sulfur content could be found in the form of pyrite if the mineral component were argillaceous. The sulfur content of the fossil matter is influenced by the rock-type and even by its iron content which is only 0.5% or lower in the carbonate rocks, while 6.5% (Fe_2O_3+FeO) in the argillaceous rocks (VOYTKEVITSH *et al.*, 1977).

More than half part of the total sulfur content of brown coals consists of organic sulfur. Its distribution is shown in Table 1 in case of American and Australian brown coals (SMITH and BATTS, 1974; SCHOBERT, 1984).

TABLE 1

Forms of sulfur in Texas lignites and Australian brown coals

	Total sulfur (%)	Pyritic sulfur (%)	Sulfate sulfur (%)	Organic sulfur (%)	Description
Texas USA					
Wilcox mean	0.9	0.26	0.02	0.62	
Jackson east	1.29	0.40	0.02	0.87	
Yegus east	0.99	0.50	0.02	0.47	
Gippsland Basin	7.9	0.07	0.44	7.41	Brown coals
Victoria Australia	6.5	0.09	0.42	6.01	with high
	6.8	0.01	0.17	6.65	organic sul-
	7.2	0.12	1.83	5.23	for contents
Yallourn	0.2	0.00	0.01	0.19	Coals with
	1.2	0.09	0.42	0.65	low sulfur contents

In addition to brown coals measurements on soils and peats also were performed, and two forms of organic sulfur were reported:

1. A carbon-bounded sulfur such as in amino acids and heterocyclics; and

2. A carbon-oxygen bounded sulfur as in choline sulfate or sulfated polysaccharides.

The latter sulfur form is referred to as estersulfate and in many cases accounts for over half of the organic sulfur (TABATABAI and BREMNER, 1972).

The fact that the organic sulfur content in different peats is higher than it is could be expected from original vegetable matter, and that only less than 40% of organic sulfur content is originated from amino acids called researchers' attention to clear up how the sulfur built into the organic fraction of peat and what is the source of the main part of the organic sulfur (CASAGRANDE *et al.*, 1979). It was established on the basis of experiments with elemental sulfur (^{35}S) and $H_2^{35}S$ that the elemental sulfur and the sulfur of hydrogen sulfid built into the organic material. Hydrogen sulfide has already able to react with peat at room-temeperature and the largest part of the organic sulfur can be found in humin and humic acids.

There are in the peat swamps elemental sulfur and hydrogen sulfid which may be originated microbiologically, i.e. the laboratory experiments can be carried out in the nature, too.

The intricacy of the processes proceeding in the nature is shown by the fact that different sulfur compounds were produced from sulfur-free amino acids with the aid of elemental sulfur (MARTIN and HODGSON, 1973). In addition, carbohydrates react with hydrogen sulfid at low temperature (100—200 °C) yielding variety of organosulfur compounds including thinphenes, thiols, sulfids and sulfones (MANGO, 1983), finally sulfate ions oxidize the methyl group to carboxyl in the presence of hydrogen sulfide (TOLAND, 1960).

SAMPLES AND ANALYTICAL METHODS

57 coal samples from different mines *(Fig. 1)* were examined. The determination of carbon was carried out by Carmhograph 8 (Wösthoff) in oxygen flow at 1000 °C.

The hydrogen content was determined by CHN—1 analysator.

The nitrogen determination was carried out by the Kjeldahl-method. Measurements were carried out after destruction in concentrated sulfuric acid in form of ammonium ion, using ion-selective electrodes in an equipment of OP—264 type.

The determination of the total sulfur was carried out with Eschka-mixture (2 parts by weight MgO and 1 part by weight anhydrous Na_2CO_3) at 800 °C. The sulfate precipitated with barium chloride was determined by gravimetric analysis as $BaSO_4$.

RESULTS

Data of some Hungarian brown coals analysed by us are shown in Table 2. In Table 3 the total sulfur content data of some Hungarian brown coals are summarized in chronological succession on the basis of published data and our measurements. The name of analyst or informator is marked.

For comparison some total sulfur content data of measured brown coal occurrences of the world are presented in Table 4.

TABLE 2

Elementary analyses of Hungarian brown coals

Coal fields	Mines	Number of samples	Age	C	H	N	S	O dif.	Dry, ash-free basis C	H	N	S	O dif.
				(wt %)					(wt %)				
Tatabánya	Nagyegyháza	8	Eocene	59.0	4.7	0.2	5.3	30.8	72.1	5.7	0.3	6.5	15.4
basin	Csordakút	6		54.0	4.4	0.7	4.0	36.9	70.6	5.7	0.9	5.3	17.5
Veszprém	Balinka	5	Eocene	50.0	3.9	0.3	5.7	40.1	70.9	5.6	0.4	8.3	14.8
area	Dudar	8		48.7	4.1	0.2	5.3	41.7	69.2	5.8	0.3	7.7	17.0
Dorog	Lencsehegy	11	Eocene	55.7	4.9	0.1	5.3	34.0	70.9	6.3	0.2	6.3	16.3
basin	Mogyorósbánya	3	Oligocene	56.3	4.5	0.2	3.8	35.2	70.9	5.6	0.3	4.8	18.4
Borsod	Kurityán	5	Miocene	48.9	4.3	0.3	3.0	43.5	69.0	6.0	0.5	4.3	20.2
basin	Putnok	11		51.1	4.2	0.3	2.4	42.0	70.6	5.8	0.4	3.1	20.1

TABLE 3

The total sulfur content data of some Hungarian brown coals summarized in chronological succession on the basis of published data and our measurements

Coal fields	Mines	GRITTNER S(%) 1906	VARGA—NYÚL S⁺(%) 1937	KÁPLÁR S(%) 1968)	BALÁZS—JUHÁSZ S(%) 1969	MOLNÁR S(%) 1970	MOLNÁR S(%) 1981	PÁPAY S(%) 1985—86	PÁPAY S⁺(%) 1985—86
Borsod basin		3.51			0.5—3.5 mean2.6			2.6	3.4
Veszprém area	Balinka			4.0		5.1	5.04	5.7	8.3
	Dudar			3.2		4.4	5.00	5.3	7.5
Tatabánya basin		3.74	4.5	3.3		4.5	4.20	4.7	6.0
Dorog basin		1.10—3.41	4.8	3.5		3.7		4.9	6.0

⁺ dry, ash-free basis

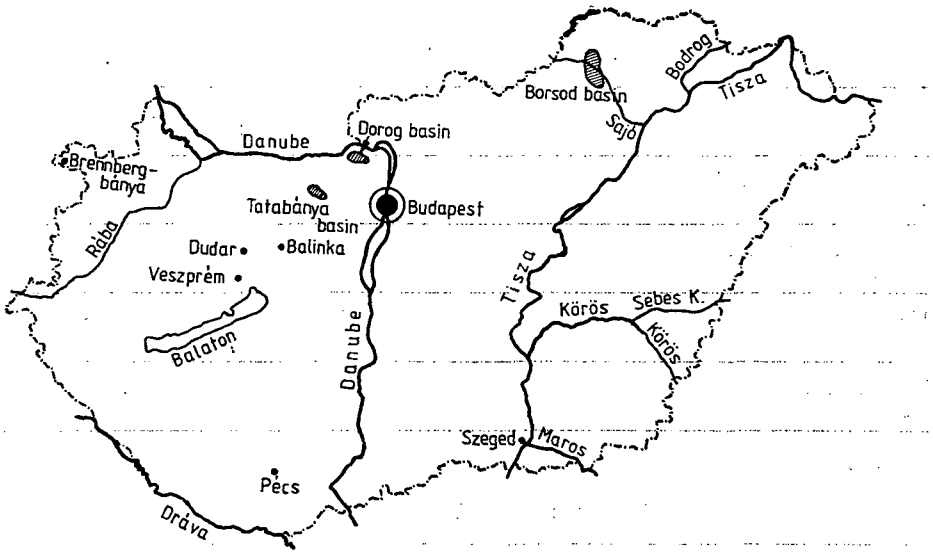

Fig. 1. Geographical setting of the studied region.

CONCLUSIONS

The average carbon content of Hungarian brown coals studied is 10—15% lower than that in foreign coals. On the other hand, the total sulfur content is higher than those. The total sulfur content of 57 brown coal samples was found to be 4.4%. (On dry, ash-free basis: 5.7%.)

According to our own measurements the total sulfur content of Miocene brown coals of Borsod basin is the lowest among the Hungarian occurrences. Examining chronologically the sulfur data of some brown coals exploited in different mining districts, on increasing tendency can be established with a certainly oscillation during the last 80 years.

If the qualitative distribution of total sulfur content is examined — on the basis of published data and the available pyritic sulfur data of informing character — the conclusion can be drawn that the pyritic sulfur content is low in the Eocene brown coals of Lencsehegy and Dudar. The pyritic sulfur content is 10% or higher in the coals from Nagyegyháza, Csordakút, Balinka and partly in the course of Oligocene age from Mogyorósbánya, respectively. The major part of Miocene coals of Borsod basin is characterized by low pyritic sulfur content, nevertheless, the pyritic sulfur content of the brown coal mined out from Putnok is higher than the average.

Presuming that the sulfate sulfur is not a significant quantity in Hungarian coals, it can be made probable that the sulfur is bounded in organic compounds in the samples of low pyritic sulfur content.

During combustion of these coals the major part of sulfur bounded in organic compounds and partly the pyritic sulfur get into the atmosphere as combustible sulfur. The sulfur content data of different Hungarian brown coals are published in Table 5 (TARJÁN, 1981; FEJÉR—OSWALD, 1988).

On the basis of above mentioned establishments the sulfur content of brown coals must be decreased to minimum value in one of the possible manners — before

TABLE 4

Some total sulfur content data of major brown coal occurrences of the world

Coal fields	S (wt %)	Moisture ash free or dmif (wt %)
Victorian brown coal Australia		0.14—5.36
Rhenish brown coal Germany	0.25+	
Norther Great Plains lignites USA	0.6—0.8 mean 0.7	0.9—1.1 mean 1.0
Texas lignite USA	0.9—1.29 mean 1.05	1.35—2.25 mean 1.79

+ S(org)

TABLE 5

Forms of sulfur in Hungarian brown coals

Mines	Total sulfur (wt %)	Pyritic sulfur (wt %)	Combustible sulfur (wt %)
Lencsehegy II	6.5	0.8	5.0
Nagyegyháza	4.4	1.1	3.7
Balinka	4.6	1.1	3.6
Dudar	4.7	0.8	3.4
Borsod	2.5		1.8

combustion, during combustion or from flue gas — before using up in thermal power-station in order to reduce the amount of air polluting sulfur dioxide. Or course, the ideal solution of this question would be giving up the combustion of coals in thermal power-station.

In Hungary experiments have been continued for years to reduce the amount of sulfur dioxide in order to satisfy our international engagement i.e. by 1993 the quantity of sulfur dioxide emitted into the atmosphere will have been decreased by 30%.

REFERENCES

BALÁZS, Z. and A. JUHÁSZ (1969): A borsodi barnaszenek kéntartalmának vizsgálata (Investigation of the sulfur content of Borsod brown coal) (in Hungarian). — BKL Bányászat **102. 6,** 408—415.

BÁN, I. (1936): A brennbergi kőszénbányászat története 1759-től 1792-ig (Geschichte des Brennberger Steinkohlenbergbaues 1759—1792). (in Hungarian). Bányászati és Kohászati Lapok. **LXIX. 4,** 80—87. **LXIX. 5,** 103—113. **LXIX. 6,** 130—135. **LXIX. 7,** 154—158.

CASAGRANDE, D. L., G. IDOWU, A. FRIEDMAN, P. RICKERT, K. SIEFERT and D. SCHLENZ (1979): H_2S incorporation in coal precursors: origins of organic sulphur in coal. — Nature. **282,** 599—600.

CASAGRANDE, D. J. and NG. LILY (1979): Incorporation of elemental sulphur in coal as organic sulphur. — Nature. **282,** p. 598—599.

FEJÉR, L. and GY. OSWALD (1988): Relationship between coal use and sulphur content of the air (in Hungarian with English, German, Russian abstract). — Föld. Kut. **XXXI. 2,** 13—18.

GRITTNER, A. (1906): Szénelemzések (Coal analyses). Budapest. — In: VITÁLIS, I. (1939): Magyarország szénelőfordulásai (Occurrence of coals in Hungary) (in Hungarian). Sopron.

KÁPLÁR, Zs. (1968): Energiahordozók elméleti és tüzelési értékmérője (Theoretical and firing parameters of sources of energy) (in Hungarian). — BKL Bányászat. **101. 4,** 182—189.
KLESMENT, I. R. and K. E. UROV (1985): Sulfur genesis in oil shales (in Russian). — Oil Shale. **2/2,** 139—148.
MANGO, F. D. (1983): The diagenesis of carbohydrates by hydrogen sulfide. — Geochim. Cosmochim. Acta. **47,** 1433—1441.
MARTIN, T. H. and G. W. HODGSON (1973): Geochemical origin of organic sulfur compounds: reaction of phenylalanine with elemental sulfur. — Chem. Geol. **12,** 189—208.
MOLNÁR, J. (1983): Szeneink ésszerűbb tüzeléstechnikai felhasználása (On more rational utilization of our coals firing technology) (in Hungarian). — BKL Bányászat. **116. 7,** 477—479.
SCHOBERT, H. H. (1984): The chemistry of low-rank coals. American Chemical Society, Washington.
SMITH, J. W. and B. D. BATTS (1974): The distribution and isotopic composition of sulfur in coal. — Geochim. Cosmochim. Acta. **38,** 121—133.
SZÁDECZKY-KARDOSS, E. (1952): Szénkőzettan (Coal petrology) (in Hungarian). Akadémiai Kiadó, Budapest.
TABATABAI, M. A. and BRENNER, J. M. (1972): Forms of sulfur carbon, nitrogen and sulfur relationships in Iowa soils. — Soil Sci. **114. 5,** 380—386.
TARJÁN, G. (1981): Adalékok az eocénprogram vertikumához (Contribution to the Eocene Program) (in Hungarian) — BKL Bányászat. **114. 1,** 9—16.
TOLAND, W. G. (1960): Oxidation of organic compounds with aqueous sulfate. — J. Amer. Chem. Soc. **82,** 1911—1916.
VALITOV, H. B. and R. B. VALITOV (1978): Rol karbonatnih porod v formirovanii sernistih neftey i kataghennogo serovodoroda (Role of carbonate rocks in the formation of sulfurian oil and catagenetic hydrogen sulfide (in Russian), — Geokhimiya. **6,** 950—955.
VARGA, J. and GY. NYÚL (1937): A magyar tüzelőszeripar (The Hungarian fuel industry). Technika. Budapest, 1937. évf., 1. sz. — In: VITÁLIS, I. (1939): Magyarország szénelőfordulásai (Occurrence of coals in Hungary) (in Hungarian). Sopron.
VOYTKEVITSH, G. V., A. E. MIRSHNIKOV, A. S. POVARENNIKH and V. G. PROHOROV (1977): Kratki spavotshnik po gheokhimii (Brief guide to geochemistry) (in Russian). Nedra, Moszkva. 80, 83

Manuscript received, 30 May, 1988

Acta Mineralogica-Petrographica, Szeged, XXIX, 139—143, 1987—1988

Reminiscent of an old book

"Critical Review of Minerals from Transylvania" by A. KOCH, Kolozsvár, 1885

PROOFS FOR THE EXISTENCE OF ANORTHITE-SPINEL-GARNET PERIDOTITE SERIES OF INCLUSIONS IN BASALTS OF THE PERSÁNYI MOUNTAINS TRANSYLVANIA, ROUMANIA.

SZ. BÉRCZI

Department of General Technics, Eötvös Loránd University

ABSTRACT

On the basis of the correct descriptions of mineral componensts of different geological finding sites in the book: „Erdély ásványainak kritikai átnézete" (Critical review of minerals from Transylvania) by ANTAL KOCH, Kolozsvár (1885) it has been possible to identify the basalts of the Persányi Mountains as host rocks of different mafic and ultramafic xenolith inclusions.

INTRODUCTION

There are about 200 places all over the world where alkalic basalt volcanism has delivered peridotites and other related mafic derivates as xenolith inclusions from the upper mantle and lower crust regions to the surface of the Earth. (FORBES, KUNO, 1967.) The mineral assemblages of peridotites are not in equilibrium with the host basalts in which they are embedded. During the last three decades the peridotite xenolith inclusions containing basalts became important sources for mantle petrology because these are the most widely distributed test places where mantle rocks can be detected. (GREEN, RINGWOOD, 1967). In measuring mantle-crust processes inclusions from any new finding sites may have individual features over the general similarities of peridotites and their derivates.

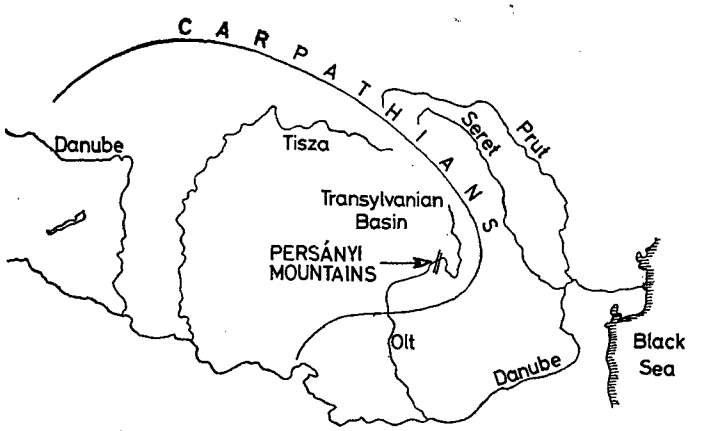

Fig. 1. The location of the Persányi Mountains in Transylvania, Roumania.

H—1088 Budapest, Rákóczi út 5, Hungary.

Due to the old traditions in mining since medieval ages and because of wealthy and variable rocks and tectonic setting, the Hungarian geology was among the most developed surveys in Europe during the Austro—Hungarian Monarchy. The most outstanding scientific achievement of XVIIIth centurian Hungarian geology was the discovery of the tellur, in the Transylvanian gold-tellur ore minerals. On the level of the geology of the world every important informations have been collected and published in the last century. On the basis of one of these collections which has been made about the minerals of a historical region of Hungary I should like to call the attention of interested geologists to a probable source region of peridotite inclusions and some derivates in Transylvania. These peridotite containing basalts can be found in the Persányi Mountains, 50 km northwest from Brassó (Brasov). The collection which has preserved informations about these sources is the book by ANTAL KOCH (at that time the professor of the Kolozsvár University); the title of the book: Erdély ásványainak kritikai átnézete (Critical Review of Minerals from Transylvania), Kolozsvár 1885. (Clausenburg, today Cluj-Napoca, Roumania).

MINERALS OF PERIDOTITES IN KOCH'S BOOK

Koch's book has been based on disciplinary works and descriptions of minerals finding places known 100 years ago. The book specifies the known important minerals of its age alphabetically with their finding places, characteristics and rocks which contain them. All mineral names are followed by the name of the investigator who has introduced it. The text of the book is written in Hungarian language.

At minerals the different finding sites are specified. There not only the local characteristics of minerals are described, but their mineral environments, too. Reading over the book the finding sites of the minerals which are the major constituents of peridotites (e.g. at olivine, pyroxene, spinel and garnet) some finding sites were repeated. These finding sites — e.g. Hidegkút, Hévíz, Kőhalom, Alsó-Rákos (their names recently in Roumanian: Fintina, Hoghiz, Rupea, Racos, respectively) — all were groupped in a local neighbourhood: on the basaltic region of Persányi Mountains. The cross references at mineral components of peridotites and other supposed inclusions (anorthite, bronzite, diallag, pyrope, and the earlier mentioned components) have made it clear for me, that in the basalts of the Persányi Mountains the so called "olivine bombs" were peridotite inclusions — may be of different types from different depths. I exhibit here the most characteristic places of the book in English translation in order to confirm my suggestions.

p. 14. AMPHIBOLE. HAÜY
Black, so called volcanic amphibole.

Kőhalom. From the hill named Turzon (Freythum) ACKNER also mentions thin nice amphibole crystals but more recently M. SCHUSTER described a size of a fist inclusion which was covered with a melted crust and it consisted exclusively of massive brown-black basaltic amphibole. But when he broke to pieces an inclusion consisting of ashy augite he found some nice crystals, too.

p. 52. BRONZITE, KARSTEN

Alsó-Rákos. In the break-through of the Olt river according to TSCHERMAK a dark, white-dotted, tough rock consisted of olivine, clearly splitting large, oil-green-brown diallag and bronzite leaves to which yet white anorthite grains contributed.

Hidegkút. According to M. SCHUSTER the olivine bombs lying in the basalt-lapilli of the la Gruju Hill consist of the mixture of olivine, grass-green augite, black-conchoidal augite, black spinel and a little bronzite which last mineral is intergrown inside the grass-green augite and its colour is also green but turning to brown.

Kőhalom. M. SCHUSTER has found the most amount and the most beautiful bronzites in the olivine-bombs scattered in the basaltlapilli of the hillside named Turzon. These minerals occurred in brown-green grains with one well splitting direction and with an other one which forms 87° 54′ angle with that of the earlier direction. In very thin splinters it melted into a dim green-like email, a larger piece of it became a sphere only after a longer heating. Nevertheless it became melted with more difficulty than the grass-green augite mixed with it and more easily than the typical bronzite from Kraubath. Therefore it is near to the hypersthenite.

p. 87. DIALLAG, HAÜY

Alsó-Rákos. According to TSCHERMAK the olivine-gabbro from this place half consists of olivine and besides this component diallag, bronzite and a little anorthite are the constituents of the rock. The diallags form small grains, which are in fresh state and are oil-onion-green, they can be completely splitted in the direction of transversal face and less in the direction of the longer face of minerals.

p. 95. GARNET, ALBERTUS MAGNUS

Hidegkút. On the hill named Gruju in the basalt-lapilli in a size of a fist volcanic bomb which consisted of the mixture of olivine + little bronzite + grass-green augite + + black conchoidal spinel there were 4—10 mm-s in diameter sized pell-mell cracked garnet balls with beautiful dark rose-red color and half transparent. With borax it gives the reaction of the chrome, that is why I had considered it earlier to heve been a pyrope, but it did not show the characteristical blood-red color of this mineral.

p. 137—138. OLIVINE, WERNER

The most olivines occur in the basalts of the Persányi Mountains (Alsó-Rákos, Bogáth, Hévíz, Hidegkút, Komána), there are far less in the basalts of Volkány and Detunata.

Hidegkút. On the hill named Gruju in the opened basalt-lapilli abundantly lie smaller-larger olivine-bombs. Besides of olivine they consist of black conchoidal and grass-green augite, little bronzite, black conchoidal spinel and rarely dark rose-red chromegarnet grains.

PYROXEN, HAÜY

p. 149—150. (a) AUGITE, WERNER

The augite versions occurring in the olivine-bombs of the basalts are very interesting.

(a) *Hidegkút and Hévíz.* Between the two villages on the La Gruju hill there are pitch-black, well conchoidal-breaking augites in nut sized thick pieces in the basalt-lapilli or in the massive basalt itself. (Spec. grav. = 3.25)

(b) Grass-green slightly splitting augite (non omphacite!) occurs as an important constituent of olivine-bombs but occurs in the basalt itself also as inclusion in nut-sized pieces to which the ashy-basalt is strongly stuck. (Spec. grav. = 3.5)

Hidegkút. In the olivine-bombs from the basalt-tuff and lapilli of the Gruju Hill, which turn up frequently, M. SCHUSTER has showed a formless black spinel which might have been a variant of the pleonaste and near to picotite. This spinel in the form of pea-size grains with pitch-black, very bright, conchoidal and splinter-like breaking, rigid and very hard characteristics, with olivine, green augite and very thin bronzite leaves constitutes the (above mentioned) olivine-bombs which are sometimes head sized in diameter.

CONCLUSIONS

The identification of peridotite and related mafic inclusions in the basalts of the Persányi Mountains from the 100 years old literature could became a recognition only on the basis of the achievements of mantle petrology in the last three decades. (KUSHIRO, KUNO, 1963; FORBES, KUNO, 1967; GREEN, RINGWOOD, 1967, 1970; EMBEY-ISZTIN, 1976, 1978). On the basis of this background and the shown description of mineral assemblages of inclusions in basalts of the Persányi Mountains the following characteristics can be summarized from the KOCH's book

(1) The amount of constituting minerals in the order of decreasing

$$Ol \gg Cpx > Opx > Sp > Ga$$

(2) Peridotites from different mantle regions may be expected on the basis of the anorthite, spinel and spinel+garnet accompanying phases of inclusions which characterize mantle composition at increasing depths.

On the basis of these descriptions of KOCH, numerous peridotite inclusions have been collected by the author on the La Grújú hill at Hidegkút (Fintina). Their detailed description will be given in the next volume of Acta Mineralogica-Petrographica.

NOTE ADDED IN PROOF

In the recent works (PATRULIUS *et al.*, 1968; MARINESCU *et al.*, 1981; POPESCU *et al.*, 1976; POPESCU *et al.*, 1970; RADULESCU *et al.*, 1981; VASILESCU *et al.*, 1968;) no references of the results of this book and the signs of investigations on inclusions from basalts of Persányi Mts. has been occured. In the light of the wide interest on the petrology of mantle rocks I felt it important to appreciate these almost forgotten data in order to activate research to explore this promising source region.

REFERENCES

EMBEY-ISZTIN, A. (1976): Felsőköpeny eredetű lherzolitzárványok a magyarországi alkáli olivin-bazaltos bazanitos vulkanizmus kőzeteiben (Lherzolite nodules of upper mantle origin in the alkali olivine basaltic, basanitic rocks of Hungary.) Földtani Közl. **106,** 42—51.

EMBEY-ISZTIN, A. (1978): On the petrology of spinel lherzolite nodules in basaltic rocks from Hungary and Auvergne, France. Annls. Hist.-nat. Mus. Nat. Hung. **70,** 27—44.

EMBEY-ISZTIN, A., PELTZ, S., PÓKA, T. (1985): Petrochemistry of the Neogene and Quaternary basaltic volcanism in the Carpathian Basin Fragmenta Mineralogica et Palaeontologica. **12,** 5—18.

FORBES, B., KUNO, H. (1967): Peridotite inclusions and basaltic host rocks. In: Ultramafic and related rocks (Ed. P. J. WYLLIE). Wiley, New York.

GREEN, D. H., RINGWOOD, A. E. (1967): The genesis of basaltic magmas. Contrib. Mineral. Petrol. 15, 103—190.
GREEN, D. H., RINGWOOD, A. E. (1970): Mineralogy of peridotitic compositions under upper mantle conditions. Phys. Earth Planet Interiors. 3, 359—371.
KOCH, A. (1885): Erdély ásványainak kritikai átnézete (Critical review of minerals from Transylvania). Kolozsvár.
KUSHIRO, I., KUNO, H. (1963): Origin of primary basalt magmas and classification of basaltic rocks. J. Petrology. 4, 75—89.
MARINESCU, F., GHENEA, C., PAPAIANOPOL, I. (1981): Stratigraphy of the Neogene and the Pleistocene boundary. Guide to Exc. A6. XIIth Congress of Carpatho-Baklan Geol. Ass. Bucharest.
PATRULIUS, D., DIMITRESCU, R., GHERASI, N. (1968): Geological Map of S. R. Romania scale 1:200 000, sheet and book Brasov (28). Institute of Geology, Bucharest.
POPESCU, I., MIHAILA, N., PELTZ, S., TICLEANU, N., ANDREESCU, I. (1976) Geological Map of S. R. Romania scale 1:50 000, sheet Racos (78/d). Institute of Geology, Bucharest.
POPESCU, I., PATRULIUS, D., POPA, E., CODARCEA-DESSILA, M., DRAGULESCU, A., BORCOS, M., VASILESCU, A. (1970): Geological Map of S. R. Romania scale 1:50 000, sheet Persani (94/b). Institute of Geology, Bucharest.
RADULESCU, D., BORCOS, M., PELTZ, S., ISTRATE, G. (1981): Subduction magmatism in Romanian Carpathians. Guide to Exc. A2. XIIth Congress of Carpatho-Balkan Geol. Ass. Bucharest.
VASILESCU, A., MURESAN, M., POPESCU, I., SANDULESCU, J., POPESCU, A., BANDRABUR, T. (1968): Geological Map of S. R. Romania scale 1:200 000. sheet and book Oderhei (20). Institute of Geology, Bucharest.

Manuscript received, 29 June, 1988

88-3748 — Szegedi Nyomda
Felelős vezető: Surányi Tibor igazgató

Illustrations

Figures should be used only where they are essential to elucidate the text.

The illustrations should be numbered according to their sequence in the text, and in the text references should be made to each figure.

All illustrations should be given separately, not stuck on sheets and not folded. The number of the figure and the authors name schould be noted on the reverse side of the photographs and on the lower frontside of drawings, indicating at the same time the top of the figure where it is necessary.

Captions for all figures should be given typewritten on a separate list at the end of the manuscript. Drawn text in the figures should be kept to a minimum.

Drawings should be made on tracing paper by Indian ink. The thickness of the lines and the size of the lettering should be big enough to allow a necessary reduction.

Photographs of good contract and intensity on glossy paper are only acceptable. Colour photographs or drawings cannot be accepted.

Use bar scale on all illustrations instead of numerical scales that must be changed if reduction is necessary.

References

All references to publications made in the text should be made by quoting the author's name (without initials) and year of publication in parenthesis.

The list of references at the end of the manuscript should be arranged alphabetically by author's names and chronologically per author.

If the referred publications are written by more than two authors, in the text only the name of the first author should be indicated, the other co-authors are denoted by "et al.", however, in the list of references the names of authors and all co-authors should be mentioned.

In the list of references all references should be written, e.g. Balogh, K., A. Barabás (1972): The Carboniferous and Permian of Hungary. Acta Miner. Petr., Szeged, XX/2, 191—207.

At references to books beside the author's name, year of publication, title and the publishing house should also be mentioned.

In the case of references for symposium volumes, special issues or multi-authors books, the following system should be used: Roser, B. P. ,C. W. Childs, and G. P. Glasby (1980); Manganese in New Zealand. In: I. M. Varentsov and Gy. Grasselly (Editors): Geology and Geochemistry of Manganese, Vol. II Akadémiai Kiadó, Budapest, 199—211.

Manuscript that are not adequately prepared will be returned to the author(s).